

May 2022

Looking Through Glass: Phytoplankton Players in Freshwater Silicon Cycles

Allison Marie Driskill
University of Wisconsin-Milwaukee

Follow this and additional works at: <https://dc.uwm.edu/etd>



Part of the [Biogeochemistry Commons](#), [Fresh Water Studies Commons](#), and the [Microbiology Commons](#)

Recommended Citation

Driskill, Allison Marie, "Looking Through Glass: Phytoplankton Players in Freshwater Silicon Cycles" (2022). *Theses and Dissertations*. 2993.
<https://dc.uwm.edu/etd/2993>

This Thesis is brought to you for free and open access by UWM Digital Commons. It has been accepted for inclusion in Theses and Dissertations by an authorized administrator of UWM Digital Commons. For more information, please contact scholarlycommunicationteam-group@uwm.edu.

LOOKING THROUGH GLASS: PHYTOPLANKTON PLAYERS
IN FRESHWATER SILICON CYCLES

by

Allison M. Driskill

A Thesis Submitted in
Partial Fulfillment of the
Requirements for the Degree of

Master of Science
in Biological Sciences

at

The University of Wisconsin – Milwaukee

May 2022

ABSTRACT

LOOKING THROUGH GLASS: PHYTOPLANKTON PLAYERS IN FRESHWATER SILICON CYCLES

by
Allison M. Driskill

The University of Wisconsin – Milwaukee, 2022
Under the Supervision of Professor Erica B. Young

Spring dissolved Si (dSi) concentrations in Lake Michigan doubled from 1983 to 2016. Most recent budgets for Si were done in the 1980s, when Lake Michigan was much more eutrophic and prior to invasions by dreissenid mussels. To investigate possible causes of recent dSi increases, I investigated a wide range of phytoplankton taxa for dSi utilization and examined the rate of dSi release from diatoms in freshwater. These laboratory experiments were coupled with frequent nearshore and infrequent offshore sampling for dSi fluctuations over two years. The phytoplankton utilization experiments found only taxa known for creating biosiliceous structures were affected by Si limitation and were inhibited by the addition of GeO_2 (a SiO_2 analog) in a Si-replete growth medium. Only these taxa accumulated significant biogenic Si (bSi), examined by chemical digestion and using Si localization with scanning electron microscopy. To examine possible rates of dissolution of bSi into the dSi pool, jars of Lake Michigan sterile or filtered Lake Michigan water were inoculated with either killed diatoms or

cleaned frustules. Jars were inverted to mix frequently. I tested the rate of dSi release from freshwater pennate diatom *Synedra sp.* at temperatures representing the Lake Michigan hypolimnion (4 °C) and summer epilimnion (18 °C). The dissolution of bSi was faster at 18 °C, but both temperatures showed almost 100% dissolution by day 176. In a second experiment, two different species, a pennate and a centric diatom, were examined for dissolution over a shorter period of 76 days at 4 °C. In this experiment, ~50% dissolution was observed for both diatom species. There was a significant difference in dissolution rates between species, with smaller, centric diatoms dissolving faster than a larger pennate, indicating that bSi dissolution in Lake Michigan is likely to be affected by the diatom species composition. With only siliceous species using dSi, the Si cycle is likely to be influenced by the growth of diatoms in Lake Michigan. Dissolution could also occur faster in the warmer nearshore regions where benthic beds of *Cladophora* with diatom epiphytes could foster bacterial communities efficient at dSi recycling.

In memory

of

Jackson

TABLE OF CONTENTS

Abstract.....	ii
Table of Contents.....	v
List of Figures.....	ix
List of Tables	x
Acknowledgements.....	xi
Chapter 1: Introduction.....	1
Diatoms and the freshwater Si cycle	2
Si uptake in diatoms and other phytoplankton.....	4
The influences of benthic, filamentous <i>Cladophora</i> on the nearshore Si cycle.....	6
A changing Si cycle in Lake Michigan	7
Chapter 2: A survey of freshwater phytoplankton silicon utilization.....	13
Introduction.....	13
Materials and Methods	16
Cultures.....	16
Growth Rates	18
Dissolved and biogenic Si determination	19
Cell imaging and microscopy	20
Statistical analyses	22
Results.....	22
Growth rates	22
bSi content	22
Depletion of dSi from medium	24
Discussion.....	25
Si growth requirements and accumulation	25
Depletion of Si(OH) ₄ in medium.....	28
Effects of GeO ₂	30
Si imaging	30
Lake Michigan Si cycling	32

Chapter 3: Dissolution of freshwater diatom frustules with natural bacterial assemblages.....	46
Introduction.....	46
Materials and methods.....	50
Experiment I: Temperature comparison.....	51
Experiment II: Diatom species comparison.....	56
Statistical analyses and rate calculations.....	59
Scanning Electron Microscopy.....	62
Results.....	64
Experiment I: Effect of temperature.....	64
Experiment II: Effect of diatom species.....	67
Discussion.....	71
Dissolution rates and effect of temperature.....	71
Dissolution rates from different diatom species.....	74
Bacterial mediation of dissolution in freshwater.....	76
Ecological context.....	78
References.....	92
Appendix A: Role of nearshore benthic algae in Lake Michigan silica cycle.....	107
Appendix B: Riverine and nearshore Lake Michigan.....	127
Appendix C: DY-V recipe.....	134

LIST OF FIGURES

Figure 1.1	Overview of diatom silicification and dissolution.....	4
Figure 1.2	<i>Cladophora</i> and epiphytes	6
Figure 1.3	Lake Michigan dSi concentrations	7
Figure 2.1	Representative growth curves	39
Figure 2.2	Bulk bSi content of cultures	40
Figure 2.3	Cellular Si content	41
Figure 2.4	Cellular Si content of DY-V and Si-free cultures.....	42
Figure 2.5	SEM and EDS imaging.....	43
Figure 2.6	PDMPO fluorescence microscopy.....	44
Figure 2.7	Depletion of dSi in DY-V media.....	45
Figure 3.1	Experiment I raw dSi values.....	82
Figure 3.2	Experiment I change in dSi by jar.....	83
Figure 3.3	Experiment I dissolution rates	84
Figure 3.4	Experiment I depletion of bSi over time	85
Figure 3.5	Light micrographs of <i>Synedra</i> sp. and <i>Cyclotella</i> sp.	86
Figure 3.6	Experiment II raw dSi values.....	87
Figure 3.7	Experiment II change in dSi by jar.....	88
Figure 3.8	Experiment II dissolution rates	89
Figure 3.9	Experiment II depletion of bSi over time.....	90
Figure 3.10	SEM images of dissolution.....	91

LIST OF TABLES

Table 2.1	Silicification of marine and freshwater diatoms	35
Table 2.2	Sources of cultures used in Ch. 2 experiments	37
Table 2.3	Growth rates in plastic and glass vessels of cultures	38
Table 3.1	Dissolution experimental design.....	81

ACKNOWLEDGEMENTS

I am very grateful for the help of my advisor, Dr. Erica Young, who has made sure I kept on track and always provided thorough feedback to help me be a better scientist. I am grateful for the encouragement, understanding, and the opportunity to pursue this research. Thanks for helping me find the right words. I am also thankful for my committee members. Dr. John Berges for helping me collect boat samples, helping me find better ways to analyze data, and using stories to explain concepts. Dr. Harvey Bootsma for letting me tag along on the boat with his students, connecting me with people who could help me, and providing feedback on my experiments. Dr. Mark Brzezinski for helping fill my gaps in knowledge and giving me new directions I could take. Dr. Heather Owen for helping me with the SEM, even late at night when I just had to see what was in that hole even if it took an entire hour to angle and focus it. I am grateful for my lab members, who let me bounce ideas off of them and blow off steam, as well as the other friends I have made in graduate school. I appreciate the help of the staff in biological sciences and freshwater sciences for keeping me afloat and helping make sure everything was filled out in time. This research was funded by the Wisconsin SeaGrant, and I received scholarships from the Clifford Mortimer and Ruth R. Walker funds as well as the Chancellor's award.

CHAPTER 1: INTRODUCTION

The silicon cycle in freshwater ecosystems is heavily influenced by algae. Silicon availability can shape lower food webs and has long been recognized as important in aquatic ecosystem function. Despite this importance, Si is not a required nutrient for autotrophic growth, which has meant that it has received less study than other macronutrients such as phosphorus and nitrogen (e.g. Falkowski et al. 1998; Elser et al. 2007; Galloway et al. 2013; McCarthy et al. 2016). Silicon is the second most abundant element on earth, residing primarily in mineral forms that are biologically inaccessible to most aquatic organisms (Reynolds 1986). Silicon is often found bound to oxygen, forming an amorphous silicon dioxide (silica or silicate, SiO_2), or the aqueous silicic acid (H_4SiO_4) which forms in water at a neutral pH (Iler 1979). Silicic acid is the form most commonly utilized by aquatic organisms (Martin-Jézéquel et al. 2000). Some bacteria can degrade mineral silicon (such as feldspars), likely in pursuit of the other elements bound within the mineral (Vandevivere et al. 1994; Ehrlich 1996; Bennett et al. 2001). In aquatic sciences, free silicic acid in the water is termed dissolved Si (dSi) to differentiate it from silica in rocks and minerals (lithogenic silica), or biologically incorporated silica (biogenic silica, bSi). Most aquatic Si research focuses on the cycling of silicon between dSi and bSi pools, most extensively within diatoms (e.g. Baines et al. 2010; Tréguer and De La Rocha 2013; Hildebrand et al. 2018). However, Si can also be taken up by non-diatom species so our understanding of the silicon cycle needs to include their potential

contribution. Chapter 2 of this thesis surveys both freshwater diatoms and other relevant freshwater phytoplankton species for Si utilization to better understand the role of phytoplankton in freshwater Si cycles.

Diatoms and the freshwater Si cycle

Diatoms are prevalent in both marine and freshwater ecosystems, contributing ~10% of global primary production of carbon (Tréguer et al. 2021). They make a cell wall, called a frustule, out of bSi (Tilman 1981; Ragueneau et al. 1994; Nelson et al. 1995; Tréguer and De La Rocha 2013; Panizzo et al. 2017; Tréguer et al. 2018). For this reason, they are the predominant and often the only group of phytoplankton to be considered in aquatic Si budgets and cycles (Schelske 1988; Ragueneau et al. 1994; Pauer et al. 2008). Diatom silicification is so tightly coupled to the cell division cycle that cells will not complete cell division when the external concentration of silicic acid is below a minimum threshold, making Si a limiting nutrient for diatom growth (Darley and Volcani 1969; Hildebrand et al. 2018 and references within). Among diatoms, the degree of frustule silicification can vary among species (Ryves et al. 2001; Hoffmann et al. 2007; Tréguer et al. 2018) as well as within a single species in response to nutrient stress (Brzezinski 1985; Hutchins and Bruland 1998; Baines et al. 2010; Wilken et al. 2011) or grazing pressure (Pondaven et al. 2007).

Diatoms are capable of depleting the dSi in freshwater environments to levels that are limiting for further diatom growth (Schelske and Stoermer 1972; Gibson et al.

2000; Carrick and Lowe 2007). This depletion can be counteracted by the dissolution of bSi from the frustules of dead diatoms, which is examined in Chapter 3 of this thesis, and external riverine inputs, examined in Appendix B. Dissolution of Si is very important in both marine and freshwater ecosystems (DeMaster 1981; Tréguer et al. 1995; Brzezinski et al. 2003b; Opfergelt et al. 2011). The recycling of bSi in the photic zone is especially important in supporting marine diatom growth, with dissolution rates exceeding net bSi production in some areas (Tréguer and De La Rocha 2013).

Currently, most of our understanding of Si use by diatoms is based on research in marine diatoms. Less research has been done on freshwater diatoms, but even this research is often done on diatom detritus (usually stripped frustules) or bSi in sediments by paleolimnologists (e.g. Reavie et al. 2017). There are many differences in freshwater and marine ecosystems that can contribute to silicification differences in the diatoms that live there. Besides osmolarity affecting the sinking rates of diatoms in freshwater vs. marine, diatoms in freshwaters can sink to relatively shallower sediments and still become later re-suspended into the photic zone (Raven and Waite 2004). In contrast, the sinking of diatoms to ocean sediments effectively removes their bSi from the Si cycle within the euphotic zone (Assmy et al. 2013; Tréguer and De La Rocha 2013; Siegel et al. 2016; Tréguer et al. 2018). Freshwater diatoms may also be more silicified than marine diatoms on average (Conley et al. 1989). With diatoms being prevalent components of both marine and freshwater ecosystems, it is important to study them in

both environments. An in-depth survey of freshwater diatoms isolated in culture as well as an examination of the silicification of diatoms in nature are both important to compare to marine studies.

Si uptake in diatoms and other phytoplankton

There are similarities in the mechanisms of bSi structure formation across several silicifying groups of algae. To make biogenic structures, dissolved silicic acid needs to be taken up by the cell (Fig. 1). The amount of Si that is taken up by algae corresponds both to ambient concentrations of dSi available and the Si requirements of a species. In marine diatoms, ambient concentrations of silicic acid above 30 μM is enough to sustain growth without any active uptake, but lower concentrations require active transport through silicon transporter proteins (SITs) (Hildebrand et al. 1997; Thamatrakoln and Hildebrand 2008). SIT genes were first identified in diatoms but have also been found in

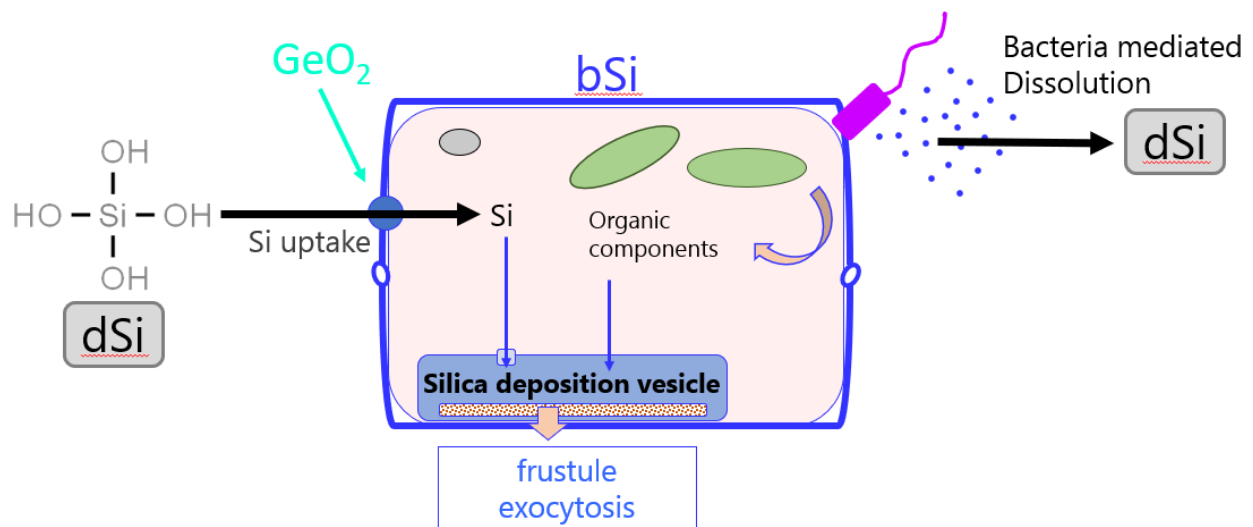


Figure 1. Diatom silicification, showing the intake of $\text{Si}(\text{OH})_4$ through a silicon transporter (SIT), polymerization within the SDV, and frustule formation. Once a diatom senesces, the bSi components can re-dissolve into the dSi fraction through bacteria mediated dissolution (Modified from Berges et al, 2022)

the genomes of silicifying Chrysophytes, the Synurophytes, as well as in Choanoflagellates, and analogs of a gene for a similar transmembrane protein (SIT-L) have been found in a variety of both siliceous and non-siliceous eukaryotes including rhizarians, tunicates, calanoid copepods, dinoflagellates, and even coccolithophores (Marron et al. 2016b). Once silicic acid has been taken up by a cell, most algae that form siliceous structures (e.g. diatoms, Chrysophytes, and choanoflagellates) will sequester it into the silica deposition vesicle (SDV) (Preisig 1994; Vrieling et al. 1999; Tesson et al. 2017; Hildebrand et al. 2018). The SDV controls the deposition of newly polymerized biogenic silica by controlling the internal pH of the SDV (Vrieling et al. 1999). The acidic nature of the SDV can be used to a biologist's advantage to visualize newly formed siliceous structures with the fluorescent dye 1-(4-pyridyl)-5-((4-(2(dimethylaminoethylamino carbamyl)-methoxy)phenyl)oxazol (PDMPO), which is pH sensitive and was originally developed to view acidic organelles (Diwu et al. 1999; Shimizu et al. 2001; Leblanc and Hutchins 2005). This dye has been used to examine silicification in actively growing cells, but the dye indication of acidic vesicles complicates its application across species that do not use an SDV for silica deposition (Shimizu et al. 2001). However, PDMPO can be a highly valuable tool to localize bSi incorporation, in addition to other methods of Si localization and uptake determination.

The influence of benthic, filamentous *Cladophora* on the nearshore Si cycle

The freshwater benthic, filamentous green alga *Cladophora sp.* hosts an abundance of diatom epiphytes (Fig. 2), and has formed large beds in the nearshore of Lake Michigan since the early 2000s (Bootsma et al. 2004; Malkin et al. 2009; Young et al. 2010). Not only are the epiphytes taking up



Fig. 2. Filaments of *Cladophora sp.* collected from Bradford Beach in Milwaukee, WI in late July 2018. Cells of tightly appressed diatoms *Cocconeis sp.* (arrows) and a group of stalked diatoms (circled) possibly *Rhoicosphenia*, can be seen attached to the *Cladophora*.

Si, but *Cladophora* itself may also use Si (Moore and Traquair 1976). In Lake Ontario, *Cladophora* assemblages (with epiphytes) had a total Si content of 3.1-5.8 mmol Si g⁻¹ biomass, compared to cultured (epiphyte-free) *Cladophora* having an average of 0.14 mmol Si g⁻¹ biomass (Malkin et al. 2009). Experimental degradation of *Cladophora* assemblages in laboratory bottles resulted in a 100-fold increase in dSi in the water over 58 days (Konjura et al. 2013, unpublished). This release of Si from *Cladophora*-diatom assemblages may indicate that *Cladophora* itself contains labile pools of Si or that dissolution of epiphytic diatoms may be increased in a *Cladophora* community, potentially due to the fostering of bacteria favorable for diatom dissolution. Freshwater

dissolution is addressed in Chapter 3 while my contribution to research on *Cladophora* influences on the nearshore Lake Michigan Si cycle is addressed in Appendix A (also published as Berges et al. 2021).

A changing Si cycle in Lake Michigan

In Lake Michigan, marked changes in pelagic dSi concentrations in the past three decades necessitate revisiting previously estimated Si budgets (Fig. 3). Measurements of

dSi in samples collected offshore (areas >50 m deep) at the same stations

showed an 18-24 μM increase from the

1988-92 period to 2007-9 (Fig. 3,

Engevold et al. 2015; Barbiero et al.

2018). This increase in pelagic dSi was

hypothesized to be a result of

decreasing diatom population

abundances, with several studies noting

a disappearance of the spring diatom

bloom, attributed to the invasion of

quagga mussels filtering the pelagic standing stock of diatoms during spring isothermal

period and reduced phosphorus loads during summer stratified period (Fahnenstiel et

al. 2010; Kerfoot et al. 2010; Vanderploeg et al. 2010; Cuhel and Aguilar 2013; Rowe et

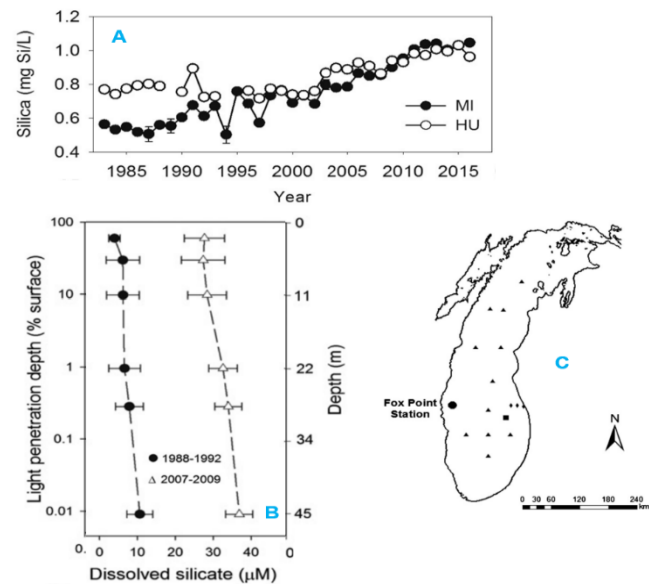


Fig. 3. Pelagic dSi concentrations in Lake Michigan show significant increases from values recorded in the 1980s. Graph **A** shows average spring dSi from GLNPO sites (triangles on map **C**, modified from Barbiero et al. 2018). Graph **B** shows summer dSi at a ~100m station, Fox Point (dot on map **C**, modified from Engevold et al. 2015). Error bars are standard deviation

al. 2017). Summer phytoplankton surveys of samples collected from southwestern Lake Michigan at the Fox Point 100 m station (Fig. 3C) in 2008 showed similar species composition to a survey with comparable methods done on the eastern side of the lake in 1985-88 (Sandgren and Lehman 1990; Simmons et al. 2016; Berges et al. 2021). Therefore, it is unlikely that the dSi increases are solely caused by decreasing diatom populations. One hypothesis is that permanent sedimentation of diatoms is decreasing, so recycling of silicate in the lake is increasing in efficiency (Barbiero et al. 2002). Though the pelagic dSi increases are well documented, we have less data on the nearshore Si fluxes in Lake Michigan. Nearshore areas are generally more productive and dynamic than offshore regions (Schelske 1985; Pothoven et al. 2016; Bockwoldt 2018). Along with the benthic algal blooms over the last 20 years (Bootsma et al. 2004; Berges et al. 2021), the nearshore Si dynamics are more influenced by riverine inputs and upwelling, which typically occur in August or September in Lake Michigan (Mortimer and Csanady 1975; Conley et al. 1993). More high frequency analysis of dSi and bSi in nearshore zones in Lake Michigan, could add new insights to Si utilization in the nearshore that could potentially help explain the offshore increases. Nearshore dynamics are explored in Appendix A and B of this thesis.

A previous budget for silica in Lake Michigan was created by Schelske (1985), and suggested that diatom production was the most important factor in silica cycling in Lake Michigan. This budget was created during a time when there was an annual diatom

bloom during the spring isothermal period, usually starting around March/April and peaking in May or June (Fahnenstiel and Scavia 1987; Schelske 1988). This spring bloom was typically of the large, centric, chain-forming diatom *Melosira sp.* (now classified as *Aulacoseira sp.*), with the diatom bloom breaking down as stratification set in and the community composition shifted to diatoms such as *Tabellaria sp.* and a greater abundance of green algae and cyanobacteria (Brooks and Torke 1977). It was estimated that out of diatom production of $89 \text{ g SiO}_2 \text{ m}^{-2} \text{ y}^{-1}$, 3.3% of that bSi would be permanently sedimented and the majority of the rest would be recycled back to the dSi fraction (Schelske 1985). So according to those estimates, around 96% of all bSi produced by diatoms during the year will be recycled back to dSi. Despite this high level of bSi recycling in Lake Michigan, in 1984-1985, Carrick and Lowe (2007) found that benthic diatom populations were still limited by Si. Si depletion in the photic zone during 1975 was suggested to cause a shift from a phytoplankton population composed of nearly 100% diatoms in early spring to ~12% diatoms in August (Conway et al. 1977).

Since Schelske created his Si budget (Schelske 1985), anthropogenic phosphorus loading has been reduced (Dolan and Chapra 2012). In 1972, the Canadian and United States environmental agencies created the Great Lakes Water Quality Agreement which mandated phosphorus loading goals and regular monitoring of all of the Laurentian Great Lakes (Burlakova et al. 2018). From 1980 to 2008, there has been a significant decrease in total phosphorus in pelagic Lake Michigan (Mida et al. 2010), and this

decline has largely been attributed to declines in particulate rather than soluble reactive phosphorus (Barbiero et al. 2018). This has also been accompanied by changes in chlorophyll concentrations as well as the community composition during the spring isothermal period to summer stratification. The early summer pelagic chlorophyll *a* concentrations decreased by 50% from the period of 1995-2000 to 2007-2010 (Pothoven and Fahnenstiel 2013). These declines were also concurrent with the increased expansion of invasive dreissenid mussels, the zebra mussels (*Dreissena polymorpha*) and quagga mussels (*Dreissena rostriformis bugensis*) (Vanderploeg et al. 2010). Concurrent with the arrival and expansion of dreissenids in Lake Michigan was increased secchi depth, a shift to smaller phytoplankton taxa, general reduction in benthic amphipods that relied on settling phytoplankton, increased benthic *Cladophora* populations, and shortening water column P residence time offshore, encapsulated in an hypothesis of a nearshore phosphorus shunt, depleting P in the offshore lake (Bootsma et al. 2004; Hecky et al. 2004; Kerfoot et al. 2010; Cuhel and Aguilar 2013; Mosley and Bootsma 2015; Engevoold et al. 2015; Madenjian et al. 2015; Barbiero et al. 2018). Mussels have been shown to selectively ingest more desirable algae and reject toxic strains of cyanobacteria in pseudofeces (Vanderploeg et al. 2001). In the more eutrophic Lake Erie, dreissenid populations collapsed in the central basin in the late 1990s which correlated with an increase in diatoms and decrease in dSi in that area – an effect that was not seen in areas of Lake Erie where mussel populations remained strong (Karatayev et al. 2018).

Clearly, the invasion of dreissenid mussels in the Great Lakes has significantly changed nutrient and phytoplankton population dynamics. The distribution of mussels in Lake Michigan could be important for Si fluxes in different parts of the lake. Since the nearshore is affected differently than the offshore, it will be important to examine and compare both regions when considering lake-wide silica dynamics. In addition, the nearshore benthic *Cladophora* plus epiphyte assemblages are affecting Si utilization and silicate recycling in the nearshore (Berges et al. 2021) but could also be affecting the flux of silica to the offshore.

There needs to be a re-examination of silica in Lake Michigan given the recent increases in dSi in the offshore regions and the ongoing effects of invasive species on the food web and nutrient cycling. Including nearshore fluxes into overall Si budgets for Lake Michigan could determine if the nearshore is experiencing similar increases as the offshore. Regular monitoring of both riverine inputs and nearshore fluxes of dSi and bSi will provide an important contrast to the offshore monitoring done by other studies (e.g. Barbiero et al. 2018). Determining realistic freshwater diatom bSi dissolution rates will give further insight into how quickly the bSi pool can be converted to dSi. In addition, examining Si utilization by phytoplankton groups other than diatoms in culture experiments could provide important information about which groups are contributing to Si cycling in Lake Michigan. Combining culture work with environmental sampling will provide better values for lake-wide phytoplankton driven Si fluxes which can be

compared to previous budgets (Schelske 1985) and can improve models of lower food web and nutrient fluxes (Pauer et al. 2008) that didn't consider any other algal groups to be contributing to the Si cycle.

CHAPTER 2: A SURVEY OF FRESHWATER PHYTOPLANKTON SILICON UTILIZATION

Introduction

In freshwater, diatoms are considered the main group of phytoplankton using Si and influencing ecosystem Si fluxes. As mostly obligate silicifiers, diatoms take up dissolved silicate (dSi) in the form of silicic acid (H_4SiO_4) from the water and turn it into an opaline cell wall called a frustule (Lewin 1966; Darley and Volcani 1969). Historically, diatoms have been important components of the Lake Michigan food web and Si cycle, especially in the spring (Brooks and Torke 1977; Fahnenstiel and Scavia 1987). The dSi concentrations in Lake Michigan have been steadily rising since the 1980's (Pothoven and Fahnenstiel 2013; Cuhel and Aguilar 2013; Engevoold et al. 2015; Barbiero et al. 2018), notably in spring where concurrent declines in spring diatom blooms have been recorded (Fahnenstiel et al. 2010; Vanderploeg et al. 2010; Madenjian et al. 2015). Invasive dreissenid mussels likely play a key role in this increase but the exact mechanisms are unclear. The effects of dreissenid invasion could be due to nutrient limitation of the pelagic water column and "benthification" (Hecky et al. 2004), selective filtering of phytoplankton species by mussels (Vanderploeg et al. 2001, 2010), or coincident changes in benthic zooplankton (Cuhel and Aguilar 2013; Engevoold et al. 2015), along with reduced anthropogenic phosphorus loading, and increasing water clarity (Pothoven and Fahnenstiel 2013). Diatoms are still a major component of Lake

Michigan phytoplankton (Reavie et al. 2014; Simmons et al. 2016; Berges et al. 2021), so there may be another explanation for the recent dSi rises than simply reduced diatom biomass. Clearly there needs to be more investigation into the changes in the lower food web to be able to investigate the cause of the increase in dSi in Lake Michigan.

With the historic importance of diatoms to the Lake Michigan food web, diatoms were included in historic Si budgets for Lake Michigan in the 1980s (i.e. Schelske and Stoermer 1972), but there has been little consideration of how other phytoplankton species could be influencing Si cycling. With changes to the phytoplankton species composition of Lake Michigan (Fahnenstiel et al. 2010; Vanderploeg et al. 2010; Pothoven and Fahnenstiel 2013; Engevoild et al. 2015), we need more data on the potential influence of more diverse phytoplankton groups on Lake Michigan dSi concentrations. Some species within the groups Chrysophytes, Choanoflagellates, and Silicoflagellates can produce bSi structures (Preisig 1994; Sandgren et al. 1996; Finkel 2016; Marron et al. 2016b). Furthermore, marine *Synechococcus sp.* cells have been shown to have appreciable Si content (Baines et al. 2012; Brzezinski et al. 2017). In freshwater, many species of Charophytes have cellular Si concentrations higher than ambient water levels, suggesting bioaccumulation (Raven et al. 1986), and several other species of algae can form siliceous cysts or internal skeletons (Finkel 2016). A summary of published values of silicate content for a range of marine and freshwater diatoms and Chrysophytes are included in Table 1. To develop a more complete picture of freshwater

Si cycling, and to understand the marked changes in Lake Michigan Si cycling, any possibility of Si uptake by phytoplankton species other than diatoms needs to be investigated, including those not typically considered siliceous. This includes the Chrysophytes, which are a dominant group of phytoplankton in Lake Michigan (Reavie et al. 2014; Simmons et al. 2016) and cyanobacteria which are common and potentially increasing in abundance in Lake Michigan (Fahnenstiel et al. 2010; Reavie et al. 2014) and may accumulate Si (Baines et al. 2012).

To address this need, this study approached screening of freshwater phytoplankton taxa for use of Si by combining examination of growth requirements and employing germanium dioxide (GeO_2) which is known to inhibit diatom silicification and suppress growth in diatoms (Lewin 1966), but has rarely been used to examine Si use in non-diatom taxa. GeO_2 likely interferes with silicification by taking the place an Si atom would in a bSi structure, causing incorrectly or incompletely formed siliceous structures due to incorrect bonding and preventing cell division in diatoms (Azam et al. 1973; Safonova et al. 2007; Basharina et al. 2012). Choanoflagellates, which synthesize bSi loricae have been shown to be inhibited by $\text{Ge}(\text{OH})_4$ (Marron et al. 2016a). Since GeO_2 appears to directly affect Si use, growth experiments using GeO_2 may provide valuable information about Si requirements in diverse phytoplankton taxa.

To examine the potential players in Si cycling in Lake Michigan and other freshwater ecosystems, this thesis chapter is focused on two research questions:

1. Other than known silicifiers such as diatoms, can other taxa take up dissolved Si and accumulate biogenic Si?
2. Could changes in other phytoplankton taxa in Lake Michigan contribute to changes in dSi concentrations?

To address these questions, the research in this chapter focused on specific aims:

1. Determine Si growth requirements and bSi accumulation in diverse freshwater taxa.
2. Examine effect of GeO_2 on growth and Si uptake and accumulation in these taxa.
3. Use scanning electron microscopy with elemental analysis to examine Si content in selected taxa.
4. Relate Si content of diatoms and other taxa to Si cycling in Lake Michigan.

Materials and Methods

Cultures

Fifteen phytoplankton species within the Bacillariophyceae, Chrysophyceae, Cyanophyceae, and Chlorophyceae groups were grown in freshwater algal culture

medium DY-V (Anderson et al. 2005, see Appendix C). A list of cultures with their source locations can be found in Table 2. The cultures were monitored for growth and incorporation of Si into biogenic Si using cultures under three treatment conditions: nutrient replete DY-V medium (containing $57 \mu\text{M Na}_2\text{SiO}_3 \cdot 9\text{H}_2\text{O}$), a Si-free DY-V medium ($<1 \mu\text{M Si}$, hereafter Si-free), and nutrient replete DY-V with $30 \mu\text{M GeO}_2$ added (hereafter GeO_2). All cultures were conditioned to the DY-V medium for 2-3 generations in the same light conditions ($19\text{-}27 \mu\text{mol photons m}^{-2} \text{s}^{-1}$) that were used for the cultures prior to the experiment. Some cultures, namely cyanobacteria *Lyngbya purpureum* and *Oscillatoria lutea* and diatom *Navicula* sp. were grown in DY-V with nitrate increased to $549 \mu\text{M}$ and P increased to $25 \mu\text{M}$ to more closely match the levels found in the stock culturing medium (Bold's 3N; Starr and Zeikus 1993) and to increase biomass for inoculation of experimental cultures. Cyanobacteria took a long time to adjust to DY-V, likely due to adjustment from the high nutrient Bold's 3N medium, which contained no added Si source but did have the addition of soil water extract which was found to have Si concentrations higher than in DY-V ($\sim 80 \mu\text{M}$).

During the initial pre-conditioning of culture to DY-V, the tolerance of taxa to stirring was determined. If the species tolerated stirring, magnetic stir bars were used during the experiment to mitigate cell clumping. If the cultures did not grow well under stirring, the cultures were gently swirled by hand daily prior to measurement and were not magnetically stirred. Cultures were grown in round 0.5-1 L culture flasks that had

been soaked in distilled water (changed daily) for 3 days. This was shown to remove any significant Si leaching into the media. To test whether the presence of glass was affecting the results, most species were also grown in 0.5-1 L polycarbonate flasks (Nalgene) with Teflon tubing for aeration and sampling. All cultures were gently bubbled with ambient air supplied through a sterilized GF/F filter.

An initial growth experiment was carried out in 40 mL polycarbonate tubes with the diatom *Cyclotella meneghinana*, the Chrysophyte *Chrysocapsa sp.*, and the Chlorophyte *Chlamydomonas reinhardtii*. Only measurements of chl *a* fluorescence were collected daily for growth rates and bSi was analyzed at the end.

Growth Rates

Biomass was estimated from daily measurements of chlorophyll (chl) *a* fluorescence using a fluorometer (Turner Designs, TD-700) and flow cytometry (BD Accuri C6) if the cell morphology allowed. Approximately 5 mL samples were collected through a tube with a plastic syringe connected. About 1 mL was aliquoted into polypropylene microcentrifuge tubes for dSi measurements and the remainder put into borosilicate tubes for chl *a* fluorescence measurements and flow cytometry (FC). FC gates were established for FL3-H vs. FL2-H and FL3-H vs. FSC-H using cells from stock cultures used for inoculating experimental cultures. Most FC measurements were carried out with fast fluidics ($66 \mu\text{L min}^{-1}$) for less than 2 minutes, adjusting time and core size

as necessary for appropriate cell dimensions and culture density changes over time (Barker et al. 2012).

Growth rates were calculated from the slope of natural logged chl *a* fluorescence over time during the exponential growth period (Guillard and Ryther 1962). Growth rates were determined from chl *a* fluorescence data as all taxa were able to be measured using fluorometer, while some were not amenable to FC measurements (filamentous or colonial cells).

Dissolved and Biogenic Si determination

Cell-free media for dSi analysis was acquired by centrifuging the daily culture samples collected until cells were pelleted (16.1 RCF for 10-20 min). Supernatant solutions were transferred to new tubes and analyzed for soluble reactive silicate using ammonium molybdate method (Parsons et al. 1984).

Cultures were determined to have reached stationary phase when the plotted natural logged growth curve of Chl *a* fluorescence over time started to plateau rather than continue with linear growth. At this point of growth, biomass was filtered onto polycarbonate filters (0.8 μm , 25 mm, ATTP) for bSi analysis and 13 mm A/E filters (previously combusted at 460 °C for 5 hours in a furnace) for determination of C and N elemental analysis (FlashEA 1112 nitrogen and carbon analyzer, ThermoFinnigan). Filters were frozen at -20 °C until analysis. Culture bSi was determined by digesting polycarbonate filters in a 0.5% Na_2CO_3 w/v solution in a 85 °C water bath for 2 hours

(DeMaster 1981) followed by neutralization with 6N HCl, centrifugation, and analysis for soluble reactive Si as above. If a significant accumulation of bSi was found, cells were counted in a microscope (Olympus BX41, 40x objective) with a hemocytometer to calculate cellular bSi content. If cells grew as single cells, flow cytometry counts of cells per μL were also used.

For the diatoms *Navicula sp.* and *Synedra sp.*, biovolume estimates were made using photos taken of cells at 100x magnification (Olympus BX41, Olympus DP70 microscope camera) preserved in Lugol's iodine that were used for cell counts. The microscope scale was used to calibrate pixels using the program ImageJ (version 1.53k) to get measurements of length, width in valve view and length and depth in girdle view for 13 individuals (Schneider et al., 2012). Measurements were averaged and used to calculate a biovolume estimate using a three dimensional ellipsoid shape (Sun and Liu 2003).

Cell imaging and microscopy

The three species initially grown in 40 mL plastic tubes (*Cyclotella meneghiniana*, *Chrysocapsa sp.*, *Chlamydomonas reinhardtii*) were also grown with 0.4 mL of stock culture, 2.5 μL of 2-(4-pyridyl)-5-((4-(2-dimethylaminoethylaminocarbonyl)methoxy)phenyl)oxazole (PDMPO, also called LysoSensor, ThermoFisher L7545), and 20 mL DY-V medium (Shimizu et al. 2001). Cultures were allowed to grow for one day and then viewed with epifluorescence microscopy to visualize PDMPO fluorescence

localization within cells. Given the established growth rates of the species tested, one day was found to be enough time for a species which used Si to take up ambient concentrations and incorporate PDMPO into the bSi structure.

At the end of the growth experiment when cultures reached stationary phase, 800 μL subsamples were collected and preserved with 200 μL of 1:1 v/v mix of 25% glutaraldehyde solution and 0.1 M HEPES buffer (pH 6.8) to a final volume of 1 mL with final concentration 2.5% glutaraldehyde and 10 mM HEPES. These preserved samples were stored at 4°C before preparation for scanning electron microscopy (SEM). Preserved cells were sedimented onto 13 mm round plastic coverslips (Nunc™ Thermanox™, 13 mm, FisherScientific) which had been soaked in a solution of poly-L-Lysine (0.1% w/v in water, Sigma-Aldrich) and left to dry in a covered petri dish. Samples sedimented to coverslips were dehydrated with an increasing ethanol concentration series until samples were equilibrated in 100% ethanol. Samples were then critical point dried (Balzers Union CPD 020), mounted onto a 13 mm aluminum specimen mount, and carbon was evaporated (Coating system E306a, Edwards) on to the sample for viewing under SEM, edges were grounded with colloidal graphite (Ted Pella). The samples were viewed with a Hitachi S-4800 Field Emission-SEM, with an accelerating voltage (keV) of 3 keV or less for best secondary electron imaging. For energy dispersive X-ray elemental analysis (EDS), all samples were viewed at a working distance of 15 mm using an accelerating voltage of 15 keV to analyze elemental C and Si distribution in cells.

Statistical Analyses

Analyses for differences between growth rates and bSi content between treatments used a one-way ANOVA with treatment and growth rate as residuals in R (R Core Team, 2020). If statistically significant, a Tukey's post-hoc analysis was performed, also in R. Changes in dSi in the medium was examined using a linear regression in MS Excel.

Results

Growth rates

Across all the growth trials of three diatoms, two Chrysophytes, six cyanobacteria and five Chlorophytes, the only species that showed growth reductions in Si-free or +GeO₂ media relative to DY-V were known silicifiers, namely the diatoms and the silicifying Chrysophyte *Synura petersenii* (Table 3). Example growth curves of a Chlorophyte, diatom, and Cyanophyte are shown in Figure 1. There was no difference in growth when species were grown in glass vs. plastic ($p < 0.01$, one-way ANOVA, R). Species that showed diminished growth in Si-free or GeO₂ media showed the same results in both plastic and glass growth vessels (Table 3).

bSi content

The diatoms *Synedra sp.*, *Navicula sp.*, and *Cyclotella meneghiniana*, and the Chrysophyte *Synura petersenii* were the only taxa with extractable appreciable bSi

content ($p < 0.01$, one-way ANOVA, Figures 2, 3). The Chrysophyte *S. petersenii* showed bSi concentrations of 2.5 ± 1.1 pmol Si cell⁻¹ (error = SD) and the pennate *Synedra* showed 0.22 ± 0.083 pmol Si cell⁻¹. The pennate diatom *Navicula* was the most highly silicified of species tested with an average of 20.2 ± 6.3 pmol Si cell⁻¹ which was significantly higher than either *S. petersenii* or *Synedra* ($p < 0.05$, one way ANOVA, R). Cell counts were not carried out for *C. meneghinana* due to lack of preserved samples and later culture contamination preventing re-analysis. bSi per cell was calculated using the DY-V and Si-free cultures only, as GeO₂ was found to interfere with the bSi method as it was detected by the ammonium molybdate method, preventing distinguishing between bSi and background GeO₂. For non-silicifying species that had similar growth rates in Si-free and DY-V media, the cellular Si content was slightly higher in cells that were grown in Si-free than those grown in DY-V (Fig. 4). These differences were not statistically significant ($p > 0.05$, one-way ANOVA, R). *Synechocystis* and *Synechococcus* cultures measured absorbance values less than the carbonate digestion blank, despite having filtered 10⁸-10⁹ cells. For these cultures, a MilliQ water blank used to create the dSi standard curve was used to subtract background absorbance.

The cultures that showed bSi content extracted with chemical digestion also showed cellular localization of Si with the SEM-EDS method (Fig. 5). Taxa examined which did not have bSi content also showed no clear evidence for elemental Si content with SEM-EDS (Fig. 5). The growth of cultures with PDMPO also only showed bSi

incorporation and localization in the diatom *C. meneghiniana*, but no convincing labelling in *Chrysocapsa* (Fig. 6). *C. reinhardtii* also showed no fluorescence associated with PDMPO labelling, consistent with very low bSi content (Fig. 3).

Biovolume estimates for *Navicula* and *Synedra* showed an average biovolume of $71.9 \mu\text{m}^3$ and $105 \mu\text{m}^3$ respectively. This led to a calculated biovolume-scaled Si of $0.27 \pm 0.11 \text{ pmol Si}/\mu\text{m}^3$ for *Navicula* and $0.0021 \pm 0.00079 \text{ pmol Si}/\mu\text{m}^3$ for *Synedra*.

Depletion of dSi from medium

Only the diatoms *Navicula* and *Synedra* and Chrysophyte *Synura petersenii* showed any depletion of dissolved Si in the medium, as determined by regression analyses of dSi over time ($p < 0.01$, Fig. 7). Diatom *C. meneghiniana* was not measured for dSi removal from medium. Measurement of the medium of *S. petersenii* cultures showed depletion from $53 \mu\text{M}$ to $10 \pm 8.3 \mu\text{M}$ between 2 replicates at the end of the 18 day experiment. For *Synedra*, the dSi in DY-V was depleted from $57 \mu\text{M}$ to $0 \mu\text{M}$ within 7 days. *Navicula* was able to reduce the $120 \mu\text{M}$ in the doubled DY-V medium to $0 \mu\text{M}$ within 8 days. The rate of dSi depletion from the DY-V medium as determined by linear regression in *Synedra* and *Navicula* cultures were calculated for the exponential growth period. In *Synedra* this was $7.3 \pm 2.3 \mu\text{M d}^{-1}$ (days 4-7) and in *Navicula*, it was $6.4 \pm 1.9 \mu\text{M d}^{-1}$ (days 2-6) (mean \pm standard deviation, $n = 3$). Two distinct periods of depletion were noted during the growth period (Initial and exponential uptake on Fig. 7). For

Navicula, during days 0 -3, dSi was depleted at a rate of $2.6 \pm 0.81 \mu\text{M d}^{-1}$ and during days 3-6, dSi depletion was $32 \pm 0.36 \mu\text{M d}^{-1}$. The diatom *Synedra* showed dSi depletion of $13 \pm 1.8 \mu\text{M d}^{-1}$ for days 0 – 2, and $7.5 \pm 0.63 \mu\text{M d}^{-1}$ for days 3-6.

To relate the Si removal rates to cells present, cell counts from flow cytometry data were used to scale the decrease in dSi per day ($\mu\text{mol L}^{-1} \text{d}^{-1}$), to the cells L^{-1} on that day. This was calculated for the period of exponential growth for each diatom: *Navicula*, days 2-6 and *Synedra*, days 4-7. The average daily cellular Si depletion for cultures of *Synedra* was $72 \pm 250 \text{ pmol Si cell}^{-1} \text{d}^{-1}$ and *Navicula* was $56 \pm 6.9 \text{ pmol Si cell}^{-1} \text{d}^{-1}$ (averages are of 3 replicate cultures, error is standard deviation).

Discussion

Si Growth Requirements and Accumulation

The overarching goal of this study was to determine if phytoplankton taxa other than diatoms had the potential to make significant contributions to the Lake Michigan Si cycle. Across 15 different species in 4 different taxa, the species predicted to be affected by Si concentrations were the only ones that showed any significant Si incorporation or growth changes with Si depletion. The diatoms and *S. petersenii* were the only species shown to be actively taking up Si from the medium and producing any significant amount of bSi in their cells. The bSi content of any of these silicifiers was much greater than the other non-silicifying species, comparing both bulk culture biomass and cellular

content (Fig. 2-4). *C. meneghiniana*, *Synedra* sp., *Navicula* sp., and *Synura petersenii* had at least 1000x higher bSi per cell, than green algae and cyanobacteria tested.

In cultures grown in initially Si-replete conditions, the diatom *Navicula* had Si content scaled to cell biovolumes of 0.27 ± 0.11 pmol Si/ μm^3 and diatom *Synedra* had 0.0021 ± 0.00079 pmol Si/ μm^3 . The *Synedra* values were low for freshwater diatoms, and more similar to those found in marine species such as *Chaetoceros* sp. which had Si content of 0.0028 pmol Si/ μm^3 and *Thalassiosira* sp. with 0.0034 pmol Si/ μm^3 (Baines et al. 2010, Table 1). The bSi content of *Navicula* fell on the high end of freshwater diatoms, close to diatoms such as the centric diatom *Stephanodiscus astraea* which had 0.263 pmol Si/ μm^3 in culture, reported by Gibson et al. (1971) which estimated Si from cell dimensions and a Si content standard from Einsele & Grim (1938). In my experiments, *Navicula* was provided with higher Si content in the DY-V medium than the other diatoms, *Synedra* and *Cyclotella meneghiniana*. Dissolved P and N were not measured throughout the experiment, so it is not known if they had also depleted these macronutrients by the end of the experiment. If N and/or P were depleted, luxury Si uptake is possible (Lynn et al. 2000). However, given the elevated N (and P) content of the medium used for my *Navicula* experiment, the molar ratio of available Si:N was 1:5 whereas the luxury consumption of Si was reported with cultures given molar ratios of Si:N of 3:1 (Lynn et al. 2000), so N depletion probably would not have occurred before Si depletion. Further experimentation with the *Navicula* strain used in my experiments is

needed to determine if the silicification level is due to excess nutrients or if these diatoms are naturally more heavily silicified.

Cells of silicifying species were expected to have the highest Si content, and non-silicifying showed very low bSi content. Within these non-silicifying taxa, the Si-free grown cells showed relatively higher bSi content compared to Si-replete cells. This was not significant, but it was still a large relative difference in terms of a typically non-silicifying cell. We would expect the cells grown in Si-free to have less Si since there is less available in the ambient environment. $\text{Si}(\text{OH})_4$ may enter cells via simple diffusion (Thamatrakoln and Hildebrand 2008) and in the DY-V cultures, ambient Si concentrations were $57 \mu\text{M}$ which is likely higher than the intracellular concentrations, so the concentration gradient should have been favorable for Si to enter the cell via simple diffusion. This might result in some internal Si in the DY-V grown cultures of non-silicifying cultures. However internal dSi in the Si-free grown cells is difficult to explain. In diatoms, intracellular Si is likely bound to organic material, or stored in a vesicle, so high intracellular concentrations can be maintained relative to ambient extracellular levels (Martin-Jézéquel et al. 2000). It is also likely that the original purpose of silicon transport proteins (SITs) identified in diatoms were used to combat very high dSi in the PreCambrian ocean, thus supporting dSi *efflux*, so it didn't interfere with cellular processes; these transporters are believed later to 'turned around' by diatoms for uptake and influx of dSi (Marron et al. 2016b). One possibility for the non-silicifying cultures

showing higher bSi in Si-free treatments could be that in the DY-V medium, dSi was diffusing into the cell and cells were actively transporting it out. When grown in Si-free, there was minimal diffusion of dSi into cells and intracellular levels were below a threshold for stimulating any dSi efflux. The chemical digestion for bSi lyses cells and thus the bSi assay measures both bSi and any intracellular dSi. If cells grown in Si-free medium retained slightly higher intracellular dSi than DY-V cells, this may explain the bSi differences. However, the differences between Si-free cells and DY-V cells were not significant.

Depletion of Si(OH)₄ in medium

Diatoms clearly depleted the growth medium of dSi by the end of the experiment while non-diatoms did not have any effect on the medium dSi concentration. This was also reflected in the accumulated bSi in diatoms (+ *S. petersenii*) but very little bSi accumulation in non-diatoms. Rates of dSi depletion by diatoms were fastest during the exponential growth period and slower during lag and early stationary phase, although reduced dSi depletion during early stationary phase was also related to low remaining ambient dSi.

Cell specific uptake rates were higher for *Synedra* than *Navicula*. This could be due to differences in surface area, as the measured surface area of *Synedra* was 150 μm^2 and *Navicula* was 99 μm^2 (calculated from ImageJ measurements using geometric

models from Sun and Liu 2003). Flow cytometer cell counts worked well for *Navicula*, which was much less likely than *Synedra* to form aggregates. This aggregation could possibly lead to an underestimation of cell density and therefore an overestimation of cellular based dSi depletion in *Synedra* cultures.

Most published uptake rates of dSi uses variable concentrations for kinetic analysis (K_s and V_{max} parameters) and are inferred through isotope fractionation studies (e.g. Nelson et al. 1976; De La Rocha et al. 2000; Martin-Jézéquel et al. 2000; Brzezinski et al. 2003a). The focus of this study was not on specific uptake rates, but the daily depletion of Si on a cellular basis could be compared to some studies of diatom Si uptake rates. Literature values for Si uptake are typically on the scale of 10^{-6} to 10^{-7} $\mu\text{mol Si cell}^{-1} \text{d}^{-1}$ while our values were on the scale of 10^{-5} $\mu\text{mol Si cell}^{-1} \text{d}^{-1}$. Studies on freshwater diatom Si uptake reported rates of 1.9×10^{-6} $\mu\text{mol Si cell}^{-1} \text{d}^{-1}$ in *Diatoma elongatum* (Kilham et al. 1977), 8.59×10^{-7} $\mu\text{mol Si cell}^{-1} \text{d}^{-1}$ in *Asterionella formosa* and 3.6×10^{-7} $\mu\text{mol Si cell}^{-1} \text{d}^{-1}$ in *Cyclotella meneghiniana* (Tilman and Kilham 1976). Likely, differences in these uptake rates are due to methodology, with even the maximum dSi concentrations being less than the original starting concentrations of DY-V in this experiment. This experiment was not set up with variable starting dSi concentrations to measure uptake rates so comparisons with studies designed to examine this are limited.

Effects of GeO₂

This study confirmed the inhibitory effect of GeO₂ on diatom growth, but there were no indirect inhibitory effects on non-silicifying algae or cyanobacteria. These effects were not unexpected, as in diatoms GeO₂ is believed to inhibit SiO₂ uptake and interfere with Si polymerization in the frustule (Safonova et al. 2007). It is hard to distinguish between GeO₂ incorporation or depletion from the medium and Si (dSi and bSi) using the ammonium molybdate method because it also detects GeO₂. Because the dSi (plus dissolved GeO₂) in the medium was unchanged throughout the growth experiment, it suggests that GeO₂ prevented the depletion of dSi in the medium. This could either be due to stopping cell growth (no cells, no Si depletion) or by physically inhibiting the uptake of Si in silicifying organisms.

Si imaging

The SEM EDS analysis clearly showed that Si had been incorporated into the frustule of the diatom *Synedra*. EDS can detect elements if they make at least 0.1% of the total sample weight (Whallon et al. 1989). Both EDS and Synchrotron X-ray analysis (sXRF), employed by Baines et al. (2010), (see Table 1) detect elements present from the emission of characteristic x-rays from a sample. However, the source energy used to emit the characteristic x-rays is different, with XRF using X-rays or gamma rays and EDS using an electron beam from a SEM. To emit an X-ray, the energy needs to be high

enough to dislodge an inner valence electron from its orbital to force a higher valence electron to fill its spot and emit energy that can be detected. So EDS and sXRF should produce comparable results. In this study, the use of EDS methodology confirms the results of bSi quantification using chemical digestion.

The diatom *C. meneghinana* showed clear localization of incorporated bSi through PDMPO fluorescence (Fig. 6) although previous experiments have shown PDMPO labelling of frustules in *Navicula* (Pansch, Young, Jack, unpublished). A cell may need a silica deposition vesicle (SDV), to allow PDMPO to bind with any Si that is localized in the cell. Both diatoms and siliceous Chrysophytes (Synurophytes) are believed to utilize a SDV during bSi formation (Preisig 1994; Vrieling et al. 1999). The SDV of siliceous organisms controls silica polymerization by maintaining a low pH in the SDV (Vrieling et al. 1999; Hildebrand et al. 2018). PDMPO was originally developed for examining acidic vesicles in cells (Diwu et al. 1999). Since the SDV is acidic, PDMPO is able to bind to the polymerizing Si and show the localization of bSi after it is deposited (Shimizu et al. 2001). The Chrysophytes *Chrysocapsa* did not show convincing PDMPO localization (Fig. 6). However, *Chrysocapsa* also did not show any bSi with chemical analysis (Na_2CO_3) and did not show any difference in growth rates between the three media types, from which I conclude that it is not a silicifying Chrysophyte.

Lake Michigan Si cycling

In these growth experiments, initial dSi concentrations were not limiting for silicifying algae, but all diatoms tested depleted the dSi in the batch culture medium within a week. This would not happen in Lake Michigan, where pelagic concentrations are generally around 30-40 μM (Driskill, unpublished data from 2019) and cells are growing in much lower densities than in the cultures. Lake Michigan diatoms are more likely limited by phosphorus availability, especially in the pelagic open lake where invasive dreissenid mussels have disrupted P fluxes in the lake (Mosley and Bootsma 2015; Bockwoldt 2018). Diatoms in the nearshore are likely to experience higher fluctuations in dSi due to higher demand, and riverine inputs (Berges et al. 2021), but also have potentially greater access to P from mussel recycling than in the pelagic zone (Hecky et al. 2004). The available ratio of Si:P in the nearshore may support higher diatom growth nearshore than offshore (Berges et al. 2021).

To link the Si culture work to the Si cycle in Lake Michigan, the current phytoplankton composition of Lake Michigan needs to be considered. There are published data of phytoplankton composition, but they generally provide biovolumes at higher taxonomic levels (e.g. Cryptophytes) (Reavie et al. 2014; Simmons et al. 2016; Bramburger and Reavie 2016; Barbiero et al. 2018). However, if we use the data from Simmons et al. (2016), which provides cell abundances for specific sampling dates, we can compare the abundance of species that I tested with how much bSi they could

contribute to the lake. For example, the abundance of *Scenedesmus* on June 25, 2008 was 4150 cells in 150 mL integrated from 3 different depths of combined nearshore and offshore (Simmons et al. 2016). In my experiments, *Scenedesmus* cells contained 0.00063 pmol Si cell⁻¹. So if we assume that is the amount that each cell removed from the ambient water, the total number of *Scenedesmus* cells counted on June 25, 2008 could potentially have removed 0.028 μmols of Si L⁻¹ from the water. Based on the minimal bSi incorporation by phytoplankton taxa not traditionally associated with Si incorporation, it appears that non-siliceous algae will likely not have a significant effect on the Si cycle of Lake Michigan. Especially when current dSi concentrations in Lake Michigan are not limiting for algae, any passive dSi accumulation by these cells will make little difference to the overall Si cycle of Lake Michigan. Given the low cellular Si concentrations in the non-diatom phytoplankton studied in this experiment, it is not likely that these phytoplankton are actively removing anything substantial from the dSi pool. So diatoms are still the main players in the lake Si cycle. As diatom communities shift towards smaller diatoms, and spring phytoplankton composition shifts from diatom dominated to a more Cryptophyte and cyanobacterial dominated assemblages (Cuhel and Aguilar 2013; Reavie et al. 2014; Barbiero et al. 2018) spring dSi levels in open Lake Michigan may continue to increase. However it should be noted that Cryptophytes were not examined in this experiment.

Increased oligotrophication of Lake Michigan from a combination of decreased P loading (Pothoven et al. 2016) and increased nearshore P trapping by mussel filtration means there are potentially less diatoms to seed pelagic blooms and influence the spring dSi levels. *Aulacoseira*, which typically formed spring blooms, is a heavily silicified diatom that would be more likely to sink and could be more easily removed by mussel filtration (Vanderploeg et al. 2010). But reduced Si demand by these taxa may not be the only reason for the recent increases in dSi, especially in spring. With the ecosystem changes related to mussel establishment, there could be an increased rate of Si dissolution from diatom frustules. We have some data on diatom dissolution, but very little of it has been determined for freshwater environments, especially with realistic conditions for dissolution. Knowledge of the regeneration of dSi from freshwater diatoms is a crucial aspect in the lake-wide budget, and this was the focus of my research in Chapter 3.

Table 1. Review of published values of biogenic silicate (bSi) content for marine and freshwater diatoms and chrysophytes. The site of sampling for each isolate is listed, if known (EEP = Eastern Equatorial Pacific, SO = Southern Ocean). Where given, a culture clone is listed in parentheses if the data was from cultures. Values are \pm standard error.

Species	marine/ fresh	location/culture (clone)	[Si]cell (pmol/ μm^3)	N	Methodology	References
Diatoms						
<i>Chaetoceros concavicornis</i>	marine	EEP	0.00038 \pm 0.0001	2	Natural assemblages were analyzed using Synchrotron-based X-ray fluorescence microscopy (SXRF). Means \pm standard error or difference between observations when N=2. EEP = Eastern Equatorial Pacific, SO = Southern Ocean	(Baines et al. 2010)
<i>Thalassiosira sp.</i>	marine	EEP	0.0034 \pm 0.0012	3		
<i>Nitzschia bicapitata</i>	marine	EEP	0.0017 \pm 0.00010	8		
<i>Nitzschia sp.</i>	marine	EEP	0.00061 \pm 0.00040	2		
<i>Pseudo-nitzschia sp.</i>	marine	EEP	0.00066 \pm 0.0001	44		
<i>Chaetoceros sp.</i>	marine	SO	0.0028	1		
<i>Fragilariopsis cylindrus</i>	marine	SO	0.0041 \pm 0.0003	21		
<i>Navicula sp.</i>	marine	SO	0.0028	1		
<i>Stephanodiscus minutulus</i>	Fresh	Culture (Yellowstone L.)	0.00061 \pm 0.000025	7	100 μM Si, semi-continuous, 1.5% Na_2CO_3 digestion for bSi content	(Lynn et al. 2000)
<i>Achnanthes brevipes</i>	marine	culture (WAT7)	0.0011	1	Grown at 20°C, 100 $\mu\text{mol m}^{-2} \text{s}^{-1}$ (16:8 L/D) to exponential, 30-50 mL filtered on PC membranes, bSi digested with 0.1 M NaOH @ 100 °C	Conley, Zimba & Theriot 1990
<i>Ampiprora paludosa v. duplex</i>	marine	culture (73M)	0.079 \pm 0.050	4		
<i>Amphora sp.</i>	marine	culture (WTAM)	0.024	1		
<i>Nitzschia frustulum</i>	marine	culture (13M)	0.0047 \pm 0.0014	3		
<i>Stauroneis amphorooides</i>	marine	culture (11M)	0.010 \pm 0.0085	4		

<i>Achnathes c.f. minutissima</i>	fresh	culture (OKEE)	0.0011 ± 0.40	2		
<i>Achnathes c.f. minutissima</i>	fresh	culture (LOCH)	0.079 ± 0.14	2		
<i>Cocconeis placentula v. lineata</i>	fresh	culture (A-83)	0.024			
<i>Cymbella minuta</i>	fresh	culture (023)	0.0047			
<i>Gomphonema acuminatum v. pusilla</i>	fresh	culture (A-67)	0.010 ± 55	2	Grown 20°C, 100 µmol m ⁻² s ⁻¹ (16:8 L/D) to exponential, 30-50 mL filtered on PC membranes, bSi digested with 0.1 M NaOH @ 100 °C	Conley, Zimba & Theriot 1990
<i>Navicula cryptocephala</i>	fresh	culture (38/03/A)	0.0053			
<i>Navicula c.f. menisculus</i>	fresh	culture (OKEE)	0.0014 ± 0.22	2		
<i>Nitzschia palea</i>	fresh	Culture (OKEE)	0.069 ± 0.84	2		
<i>Nitzschia stigma</i>	fresh	culture (L-7)	0.076			
<i>Nitzschia subacicularis</i>	fresh	culture (OKEE)	0.013 ± 1.6	2		
<i>Pinnularia viridis</i>	fresh	culture A-53)	0.0059 ± 31	2		
<i>Surirella ovata</i>	fresh	culture (A-55)	0.0090 ± 13	2		
<i>Asterionella formosa</i>	fresh	Blelham Tarn	0.21		Lund tubes, SiO ₂ content estimated from uptake calculated from observed uptake	(Reynolds 1984)
<i>Fragilaria crotonensis</i>	fresh	Blelham Tarn	0.32			
<i>Stephanodiscus Astraea</i>	fresh	Lough Neagh,	0.26 ± 0.0048	4		
<i>Stephanodiscus hantzschii</i>	fresh	unknown	0.060			
Chrysophytes						
<i>Synura petersenii</i>	fresh	culture (CDS-SYNRPET-2)	0.00029		Grown 15°C, Si-limited cultures, post-spike uptake measured	(Sandgren et al. 1996)
<i>Synura petersenii</i>	fresh	culture	0.00078		Batch cultures, growth and Si uptake measured	Leadbeater & Barker in Sandgren et al. 1995
<i>Paraphysomonas vestita</i>	fresh	culture	0.00041			
<i>Paraphysomonas imperforata</i>	fresh	culture	0.00034			

Table 2. List of cultures used for the experiments and their source locations. If available, strain identification is also provided.

Species	Strain	Group	Origin
<i>Cyclotella meneghiniana</i>		Diatom	Linda Graham lab, UW Madison
<i>Navicula sp.</i>		Diatom	Carolina Biologicals
<i>Synedra sp.</i>	A13-866	Diatom	Jones Island waste water isolate (courtesy of Bob Anderson)
<i>Chrysocapsa sp.</i>		Chrysophyte	Craig Sandgren lab isolate from Firefly Lake (Vilas county Wisconsin)
<i>Synura petersenii</i>		Chrysophyte	Sportsman Lake, San Juan Island, WA, USA (isolated by Craig Sandgren, 1/24/1977)
<i>Lyngbya purpureum</i>	UTEX LB 2716	Cyanophyte	Culture collection of algae at the University of Texas at Austin
<i>Microcystis aeruginosa</i>	CPCC 299	Cyanophyte	Canadian Phycological Culture Collection
<i>Nostoc sp.</i>	PCC 7120	Cyanophyte	Bob Haselkorn lab, University of Chicago
<i>Oscillatoria lutea var. contorta</i>	UTEX LB 390	Cyanophyte	Culture collection of algae at the University of Texas at Austin
<i>Synechococcus sp.</i>	UTEX LB 2390	Cyanophyte	Culture collection of algae at the University of Texas at Austin
<i>Synechocystis sp.</i>	UTEX 2470	Cyanophyte	Culture collection of algae at the University of Texas at Austin
<i>Chlamydomonas reinhardtii</i>	C-9 wt	Chlorophyte	Chlamydomonas culture collection
<i>Pediastrum boryanum</i>	UTEX LB 471	Chlorophyte	Culture collection of algae at the University of Texas at Austin
<i>Raphidocelis subcapitata</i>	CPCC37	Chlorophyte	Canadian Phycological Culture Collection
<i>Scenedesmus sp.</i>	CPCC 10	Chlorophyte	Canadian Phycological Culture Collection

Table 3: Growth rates of fifteen phytoplankton species based on changes in chl *a* fluorescence over time during the exponential growth period. Growth in plastic or glass flasks is noted. Bold values indicate these cultures grow significantly better in Si-replete DY-V media ($p < 0.05$, $n = 9$).

Species	Algal type	Plastic			Glass		
		DYV	Si-Free	GeO ₂	DYV	Si-Free	GeO ₂
<i>Cyclotella meneghiniana</i>	Bacillariophyte				0.93 ± 0.11	0.036 ± 0.033	-0.11 ± 0.016
<i>Navicula sp.</i>	Bacillariophyte	0.91 ± 0.074	-0.029 ± 0.038	-0.071 ± 0.066			
<i>Synedra sp.</i>	Bacillariophyte	1.5 ± 0.17	-0.18 ± 0.19	-0.2 ± 0.051	0.42 ± 0.12	-0.10 ± 0.019	-0.083 ± 0.051
<i>Chrysocapsa sp.</i>	Chrysophyte	0.35 ± 0.066	0.35 ± 0.49	0.35 ± 0.034			
<i>Synura petersenii</i>	Chrysophyte				0.47 ± 0.056	0.15 ± 0.11	-0.44 ± 0.28
<i>Lyngbya purpureum</i>	Cyanophyte	0.37 ± 0.20	0.28 ± 0.10	0.34 ± 0.091			
<i>Microcystis aeruginosa</i>	Cyanophyte				0.27 ± 0.010	0.28 ± 0.010	0.26 ± 0.013
<i>Nostoc sp.</i>	Cyanophyte				0.55 ± 0.12	0.4 ± 0.13	0.55 ± 0.040
<i>Oscillatoria lutea var. contorta</i>	Cyanophyte	0.58 ± 0.038	0.54 ± 0.081	0.47 ± 0.091			
<i>Synechococcus sp.</i>	Cyanophyte	0.77 ± 0.016	0.6 ± 0.20	0.62 ± 0.18	0.48 ± 0.22	0.6 ± 0.0080	0.52 ± 0.15
<i>Synechocystis sp.</i>	Cyanophyte	0.56 ± 0.048	0.49 ± 0.027	0.51 ± 0.026			
<i>Scenedesmus sp.</i>	Chlorophyte	0.71 ± 0.13	0.81 ± 0.052	0.79 ± 0.032	0.88 ± 0.0030	0.89 ± 0.056	0.88 ± 0.040
<i>Chlamydomonas reinhardtii</i>	Chlorophyte				0.94 ± 0.12	0.98 ± 0.024	0.90 ± 0.14
<i>Pediastrum boryanum</i>	Chlorophyte				0.23 ± 0.014	0.39 ± 0.01	0.28 ± 0.026
<i>Raphidocelis subcapitata</i>	Chlorophyte	0.53 ± 0.050	0.57 ± 0.15	0.62 ± 0.24	0.83 ± 0.088	0.87 ± 0.048	0.89 ± 0.030

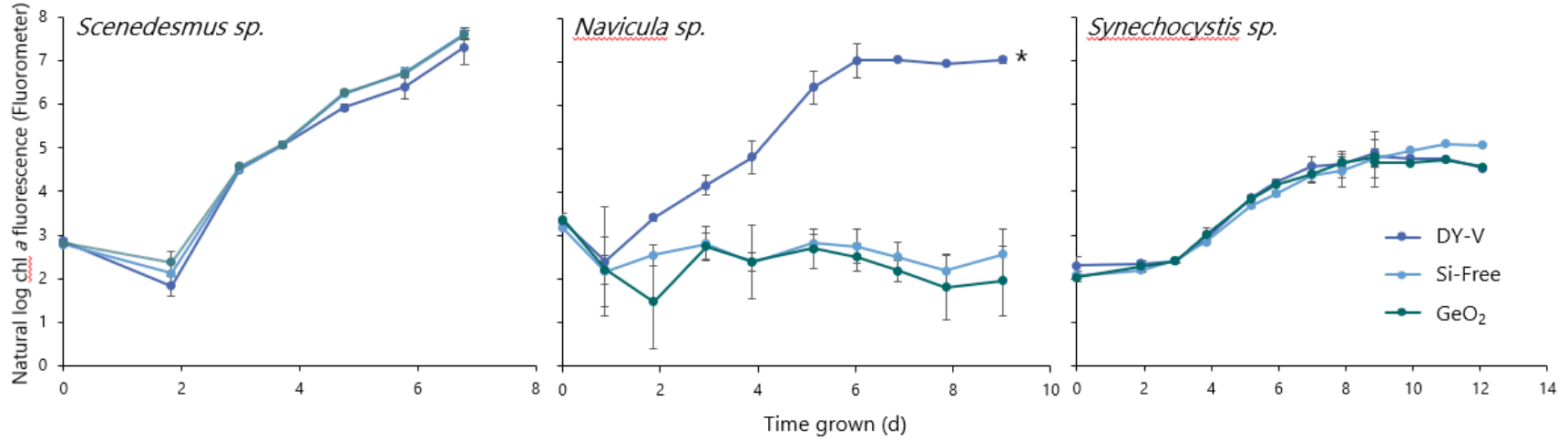


Figure 1. Representative growth curves of algae and cyanobacteria grown under three Si conditions, Si-replete (DYV), Si-free and Si replete with GeO₂. Curves are shown for the Chlorophyte *Scenedesmus sp.*, diatom *Navicula sp.*, and Cyanophyte *Synechocystis sp.* Each point represents an average of values from 3 replicate cultures. Error bars represent standard deviation (n=3). Growth rates were calculated from the slope of cultures during exponential phase, excluding lag and stationary phases. Only the diatom shows any significant difference in growth between the 3 Si treatment conditions.

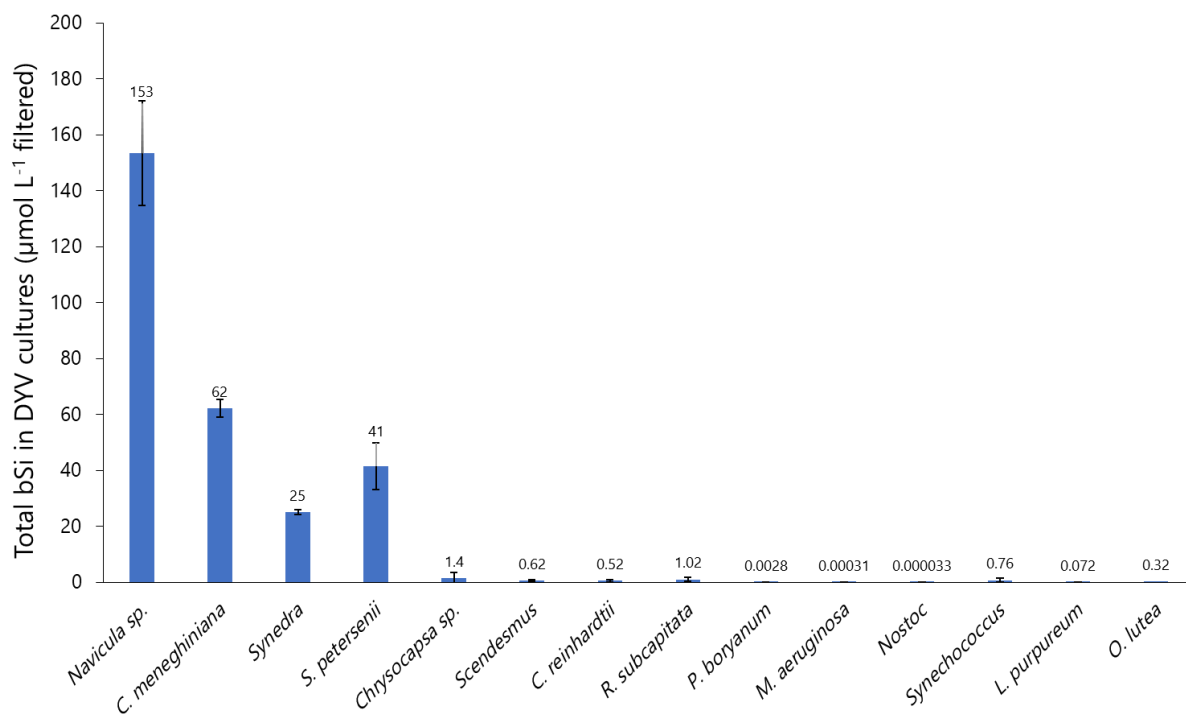


Figure 2. bSi content for 15 phytoplankton species grown in culture with 57 µM silicic acid available (DY-V cultures). bSi was analyzed with hot Na₂CO₃ digestion of biomass collected on filters. bSi content was analyzed for whole culture, then in taxa with significant accumulation, cells were counted to calculate a cellular Si content (see Figure 3). Bars are means of values from three replicate cultures (only two for *S. petersenii*) and error bars are standard deviation.

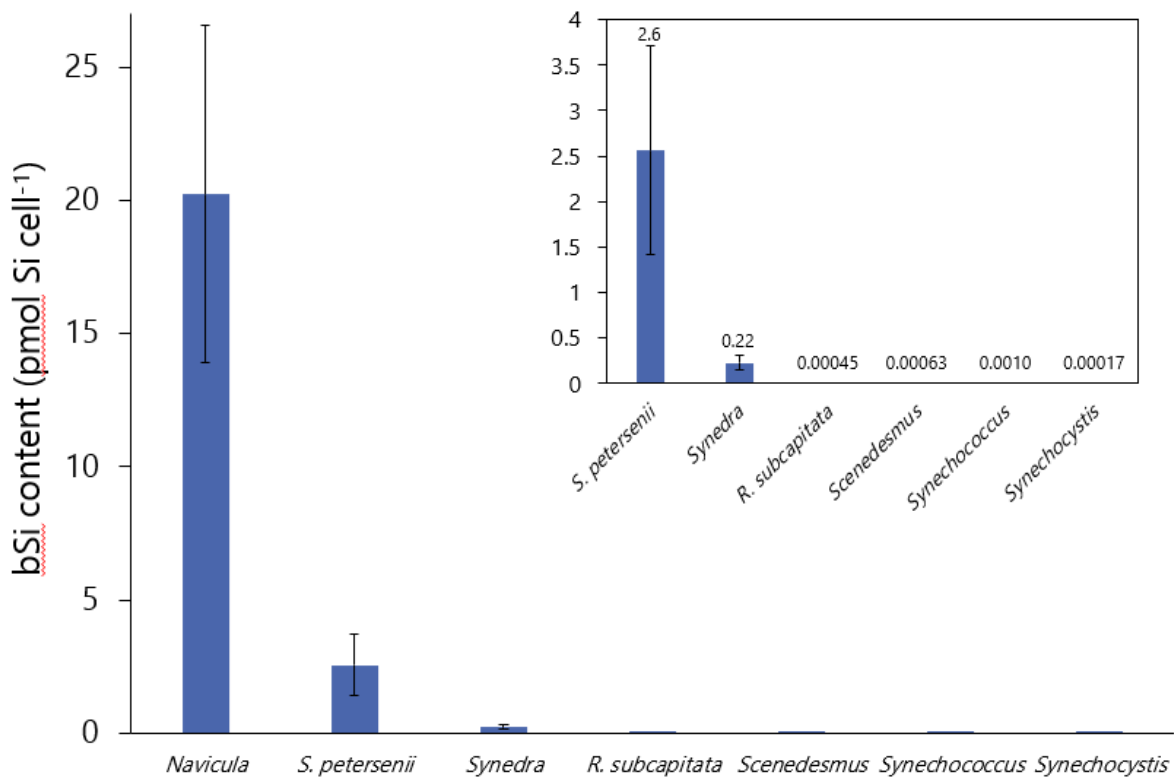


Figure 3. Cellular Si content of selected taxa grown in DY-V medium with 57 μM Si. *Navicula* was the most silicified of species tested. Cell counts for siliceous species were carried out with a hemocytometer. All non-siliceous phytoplankton were counted with a flow cytometer and confirmed to not have formed any aggregates by microscopy. Bars are mean values and error bars represent standard deviation of values from 3 replicates cultures. Insert shows the same graph with *Navicula* removed for better resolution.

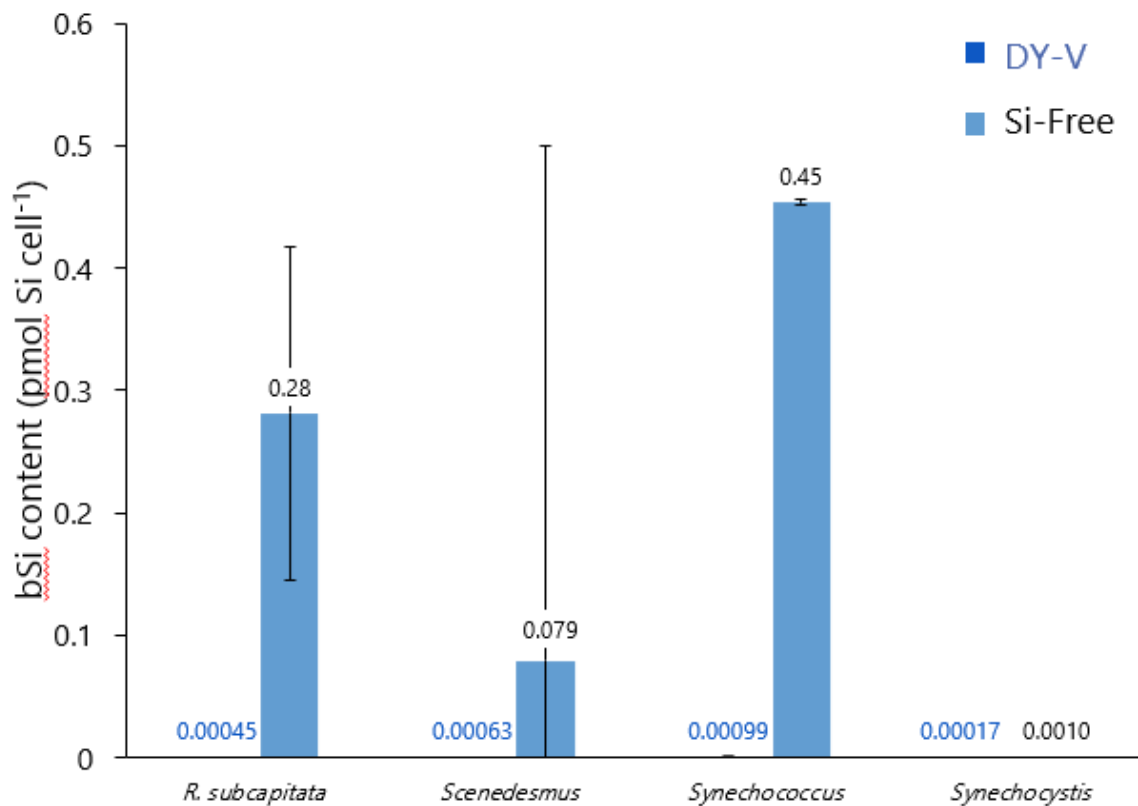


Figure 4. Comparison of Si content of non-siliceous taxa. There was no statistically significant difference between bSi content in the cells grown in Si-free and those grown in DY-V. However for three species, there was an apparent slight increase in cellular Si content in cells grown in Si-free compared to those grown in the Si-replete DY-V. Error bars represent standard deviation of 3 replicate cultures.

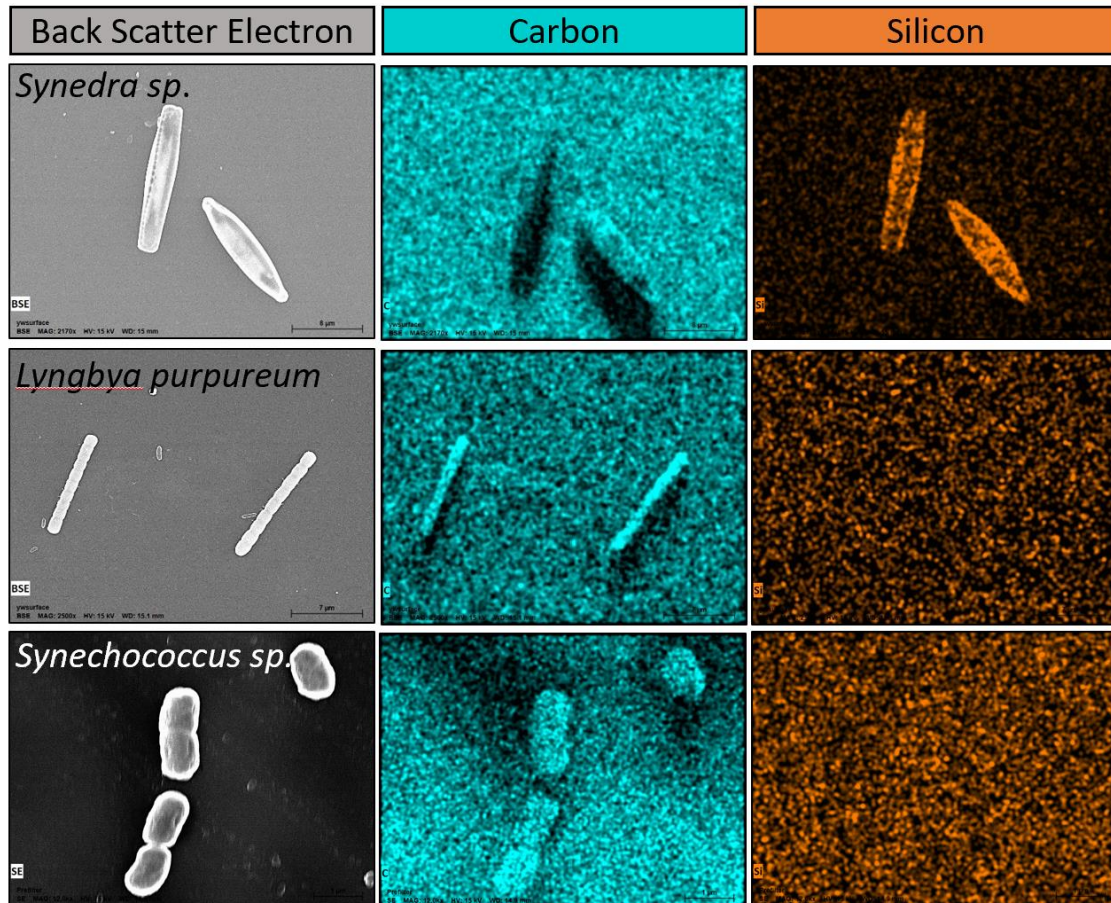


Figure 5. SEM images of cells grown in DY-V medium with 57 μM Si. Three species are shown – the diatom *Synedra* (top row), cyanobacterium *Lyngbya purpureum* (middle row), and cyanobacterium *Synechococcus* (bottom row). The first column shows a backscatter electron image which provides a surface image of the cells, the second column and third columns show the localization using EDS of elemental C and Si (respectively) on those same cells.



Figure 6. Light microscope image and PDMPO localization (green) of bSi in the diatom *C. meneghiniana* (**A & B**) and *Chrysocapsa* (**C & D**) exposed to PDMPO for 1 day during growth in Si-replete DY-V medium. Clear silicification is seen on the frustule of the diatom, whereas mostly chlorophyll autofluorescence (red) is seen in the chrysophytes. Some dots of PDMPO fluorescence can be seen, but they are not likely actual localization of bSi.

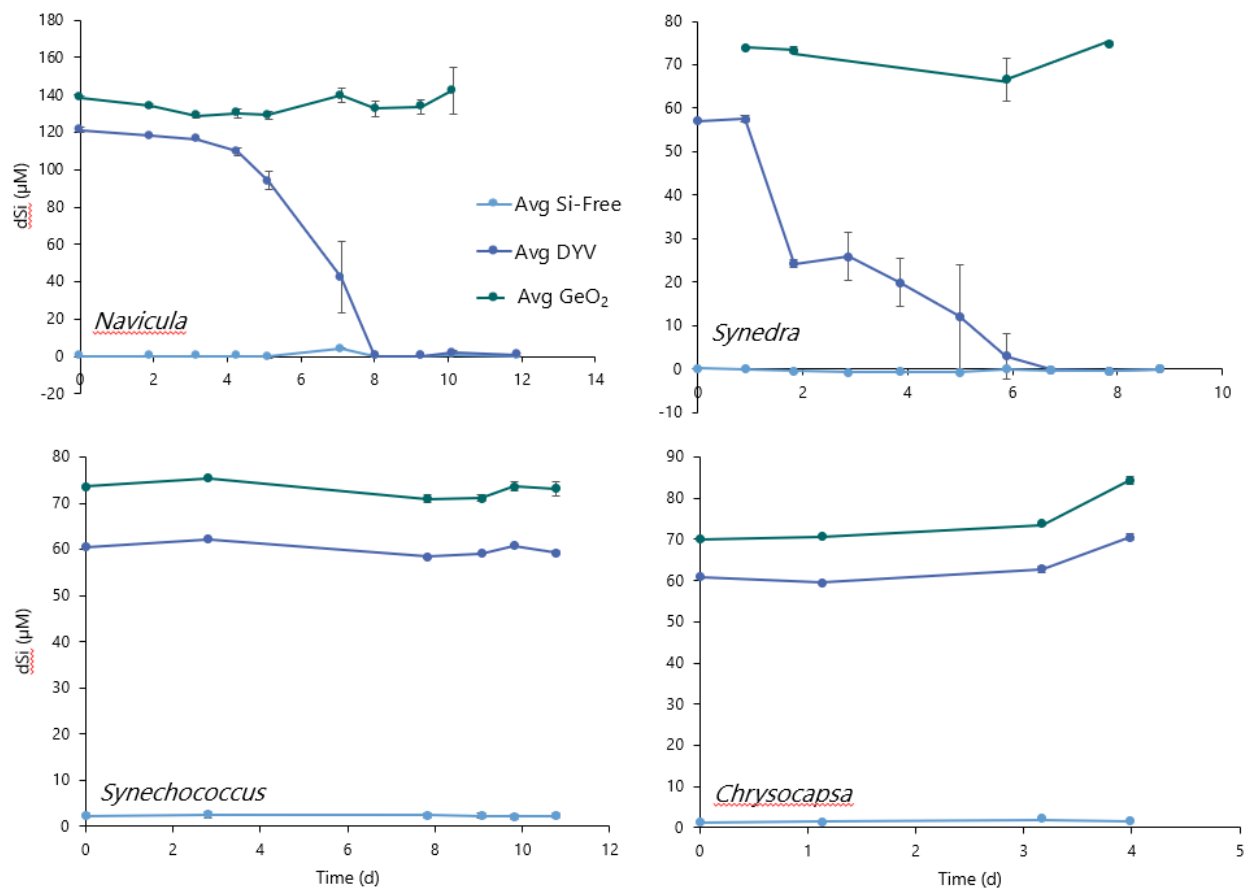


Figure 7. Changes in dSi over time during culture growth of 4 phytoplankton cultures. *Navicula* and *Synedra* are diatoms and show clear uptake of Si from the DY-V medium. The Cyanobacterium *Synechococcus* and the Chrysophyte *Chrysocapsa* do not show any significant changes in dSi in any of the medium conditions tested. Error bars are standard deviations of 3 replicate cultures.

CHAPTER 3: DISSOLUTION OF FRESHWATER DIATOM FRUSTULES WITH NATURAL BACTERIAL ASSEMBLAGES

Introduction

Si dissolution: the transfer of bSi to the dSi pool

Dissolved Si in the water column can be regenerated from biogenic Si (bSi) in siliceous phytoplankton cells through bSi dissolution. The rates of dissolution of bSi to the dissolved Si fraction (dSi) are important in biogeochemical cycling of Si in aquatic ecosystems. The physical process and rates of dissolution have been most thoroughly studied in diatom frustules (Lewin 1961; Martin-Jézéquel et al. 2000; Tréguer and De La Rocha 2013; Krause et al. 2015). To prevent the dissolution of a diatom frustule while it is alive, the frustule is coated with glycoproteins that prevent the silica in the frustule from readily dissolving in the water (Lewin 1961). After a cell dies, dissolution is accelerated by bacterial degradation and removal of this protective glycoprotein coat, allowing for chemical dissolution of the polymerized bSi (Bidle and Azam 1999, 2001). As phytoplankton cells senesce, they can exude larger molecular weight organic molecules which can attract bacteria (Bell and Mitchell 1972; Amin et al. 2012; Seymour et al. 2017). Colonization by bacteria during senescence could accelerate bacteria-mediated dissolution of the bSi in the frustule after cell demise.

Dissolution vs. Sedimentation

Dissolution can happen in the water column, recycling Si where phytoplankton grow, and represents a major component of marine Si cycles (Brzezinski et al. 2003b; Struyf and Conley 2012; Tréguer and De La Rocha 2013; Krause et al. 2015; Tréguer et al. 2021). While a diatom is growing, Si frustule weight can be offset by less dense osmolytes, lipids, and other organics, but sedimentation rates increase during senescence or after death of cells (Reynolds 1984; Boyd and Gradmann 2002; Brzezinski et al. 2003b; Assmy et al. 2013). If a dead diatom does sink to the sediment, it could get buried and permanently removed from the pelagic Si cycle. Since the ocean is so deep, diatoms that sediment take their silica (and carbon) with them and sequester it in the deep ocean sediments (Smetacek and Naqvi 2008; Baines et al. 2010; Assmy et al. 2013; Krause et al. 2015; Collins et al. 2015; Smetacek 2018; Tréguer et al. 2018; McNair et al. 2018). Lake dynamics are different from the ocean due to differences in size and depth of the lakes compared to the ocean. A holomictic lake diatom can sink to the sediments and have a good chance of resuspension into the water column. If it does undergo dissolution on the sediments, the dSi released can be transferred to the photic zone where new diatoms can use it during upwelling events which bring nutrient waters to the surface, or during water column mixing when lake stratification breaks down (Schelske 1985; Wetzel 2001; Pothoven and Fahnenstiel 2013). Silicate that has dissolved in the sediment can be flushed out of the porewater by burrowing amphipods and

bioturbation by other sediment organisms (Quigley and Robbins 1984). Likely dissolution occurs most at surface of the sediment, with aerobic bacteria playing an important role (Holstein and Hensen 2010). Zooplankton grazing can also influence the rate of dissolution of diatom frustules (e.g. Krause et al. 2010), but that is not going to be covered in this thesis.

Dissolution differences between marine and freshwater environments

Dissolution typically occurs at a slower rate in freshwater than in saltwater (Loucaides et al. 2008). Chemical dissolution of bSi is affected by pH (higher pH increases dissolution rates), temperature (higher temperatures increase dissolution and dSi solubility), salinity (higher salinity increases dissolution), and pressure (generally higher dissolution with higher pressure) (Lewin 1961; Kamatani and Riley 1979; Loucaides et al. 2012). Cleaned frustules of marine diatom *Thalassiosira punctigera* dissolved at only a fifth of the rate when placed in freshwater compared to placement in saltwater (Loucaides et al. 2008), but there has been some evidence suggesting that freshwater diatoms are more heavily silicified than their marine counterparts (Conley et al. 1989; Martin-Jézéquel et al. 2000) also see Table 2.1 of this thesis. Biological factors can also influence dissolution. The extent of frustule silicification can also affect dissolution, as lightly silicified diatoms are likely to undergo dissolution more readily and rapidly. Species-specific factors including frustule surface area may also affect dissolution, with larger surface area providing more targets for bacteria, increasing

likelihood of encounter and bacterial cells adhering to cells and mediating degradation of the organic layer (Seymour et al. 2017). Higher surface areas also lend themselves to faster dissolution as well (Hurd and Birdwhistell 1983; Van Cappellen et al. 2002).

Though there have been several studies looking at freshwater diatom bSi dissolution, most of these focus on sediment cores. Cores are more likely to include mineral silicate which is also partially dissolved by chemical extraction methods for bSi, which could in bSi estimates which are higher than the real bSi concentration if no correction is made (Barão et al. 2015). Cores also contain heavier silicified diatoms as these cells are more likely to stay intact than lighter silicified diatoms which can completely dissolve during sedimentation (Ryves et al. 2003). Many dissolution rate estimates are from studies using frustules which have had the organic coating removed, so they don't necessarily represent functional ecosystem rates. The resistance of some freshwater diatom frustules to dissolution is important in paleolimnological studies and even have been used to provide forensic dating of human bodies immersed in natural waters (Kaye and Meltzer 2020). With lakes having structural and chemical differences from marine environments, the freshwater Si cycle will be different, and so dissolution rates need to be better quantified in freshwaters, with more realistic environmental conditions.

To address this need, this thesis chapter focused on the following research questions:

1. How quickly can bSi in freshwater diatom frustules undergo dissolution and re-enter the dissolved Si pool (dSi)?
 - a. How do dissolution rates differ between warm (summer epilimnion) and cold (hypolimnion year-round) temperature conditions?
 - b. How do dissolution rates differ between a pennate and centric freshwater diatom of different sizes?
2. What is the role of Lake Michigan sediment bacteria in the bSi dissolution process?
 - a. How does the rate of frustule dissolution in dead diatoms including the natural organic layer compare to the chemical dissolution of a cleaned diatom frustule stripped of the organic layer?

Materials and Methods

Two similar experiments were conducted with freshwater diatoms. The first one compared the rate of dissolution in freshwater of the same species at two different temperatures, 4 °C and 18 °C, while the second compared the rate of dissolution from two different diatom species, a pennate and a centric, at 4°C. The experimental design used for these experiments is outlined in Table 1.

Experiment I: Temperature comparison

Diatom inoculum prep

The diatom *Synedra sp.* (source details in Chapter 1) was used as the bSi inoculum in both temperature treatments. To prepare the diatom detritus, three 1 L glass, round growth flasks were filled halfway with DY-V (Appendix C), inoculated with *Synedra* and grown up to stationary phase. Cultures were bubbled gently with filtered air (GF/F, 25 mm). These cultures were gently stirred to minimize sticking to the sides of the flask, but there was still some growth on the sides of the flask, which was scraped off with a flame sterilized metal loop at the time of harvest. All 3 cultures were combined into a 2 L autoclaved polycarbonate flask (Nalgene) and allowed to settle. Most of the supernatant fluid was poured off and the concentrated culture was collected in 11 sterile 50 mL conical tubes. Tubes were centrifuged at 4500 RPM for 10 min, the supernatant discarded, and the pellet resuspended in 10 mL of Si-free DY-V (pH 8). This centrifugation and washing resuspension with Si-free medium was repeated two more times to remove unincorporated dSi. All media exchanges were carried out in a laminar flow cabinet (Purifier Vertical Clean bench, Labconco). After the washes, the cell pellets were resuspended with 2 mL of Si-free medium and conical tubes of concentrated cells were placed in a hot water bath at 85 °C for 15 min to kill cells. After heat killing, 2 tubes were set aside for frustule cleaning. Tubes with heat killed cells were filled to 10 mL with Si-free DY-V medium. The tubes set aside for frustule cleaning were centrifuged,

supernatant removed, and 2 mL of 30% H₂O₂ added. Tubes were heated in water bath at 85 °C for 3.5 hours to strip the organic coating from the frustules (Ryves et al. 2001).

Lake water sampling and preparation

Lake water was collected aboard the *RV Neeskay* from a 20 m depth station (43°6.000 N, 87°51.0000 W) off the Milwaukee coast on Lake Michigan, WI, USA in on 28 October 2020. This station is monitored daily in the summer and data is available to the public (GLOS database). Two ponar grabs were used to collect sediment and water was collected with a 2 L Niskin sampler at 1, 5, 10, 15, and 18 m. Water samples were pooled together immediately into an autoclaved polycarbonate carboy. A total of 1,971 mL was filtered through 0.8 µm PC filters (ATTP, Millipore) to remove diatoms and zooplankton. Filters were analyzed for bSi using methods to determine bSi concentrations in the lake at the time using methods described in Chapter 2. Filtered water was autoclaved in a 10 L PC carboy (Nalgene) to sterilize. After autoclaving, ambient air was bubbled into the carboy through a 0.45 µm filter (PHWP, Millipore, 25mm) overnight to re-adjust the pH and carbonate equilibrium.

Three 0.2 µm (25 mm, Isopore) filters were used to collect seston from water samples for DNA extraction, with water volumes measured in autoclaved glass graduated cylinders and filtering done in a sterile hood or with an open flame on an ethanol sanitized work bench. The carboy was swirled in between pouring water for filtration to homogenize.

Sediment was picked through using sterilized metal tools to remove large pieces of rock and mussel shells. Two ~2 g samples of sediment were frozen at -70 °C for DNA analysis. To create a bacterial inoculum, 240 g sediment was combined with 1660 mL the filtered lake water and shaken vigorously to combine. This sediment 'cocktail' was strained through a series of ethanol sanitized Nitex screens (Dynamic Aqua-Supply Ltd.) – 153 µm → 53 µm → 20 µm → 5µm → 1 µm to remove zooplankton, algae, cyanobacterial filaments but preserve bacteria in the filtrate. This bacterial 'cocktail' was collected in autoclaved containers and Nitex screens were rinsed with ethanol to sanitize followed by MilliQ rinse. After the series of Nitex screens, GF/F filters with a nominal pore size of 0.7 µm were used with gentle vacuum to allow only bacteria through (Bidle and Azam 2001).

Experimental set up

The experiment was carried out in 60 mL polypropylene jars (53 mm diameter opening, Fisherbrand). A total of 30 jars were used at each of the two temperatures, 4 °C and 18 °C. The jars were equally divided between 3 different inoculation treatments (10 jars per treatment). The first treatment contained the bacterial cocktail and killed diatoms (EXP treatment hereafter). The second treatment used autoclaved lake water and killed diatoms, which was designed as a negative control for bacterial-mediated dissolution (C1, dead diatoms + sterile water hereafter). The third treatment used autoclaved lake

water with cleaned diatom frustules, to provide a baseline comparison of the rate of chemical dissolution after the outer organic coating had been removed (C2, frustules + sterile water hereafter). Each jar received 50 mL of lake water (autoclaved or filtered bacterial cocktail) and 1 mL of concentrated diatom inoculum (killed diatoms or cleaned frustules). Jars were grouped in trays of 6, with 2 replicates of each treatment per tray (2x EXP, 2x C1, 2x C2). Trays were placed into black felt sacks to block out light from all sides. A subsample of the filtered bacterial cocktail used to inoculate dissolution jars was filtered (0.2 μm) and filters were frozen at $-70\text{ }^{\circ}\text{C}$ for future DNA analysis of initial bacteria in experimental treatments. Jars were inoculated with the lake water and diatoms, inverted to mix, and allowed to settle for 20 minutes. 1 mL samples were collected from near the surface of the water in the jars for initial dSi measurements. Jars were incubated at $4\text{ }^{\circ}\text{C}$ in a refrigerator, or at $18\text{ }^{\circ}\text{C}$ in the algal growth chamber. The refrigerator used for the experiment was exclusively used for this experiment, so temperature fluctuations due to opening were minimal and ranged between -1 and $6\text{ }^{\circ}\text{C}$. There was never any evidence of freezing or frosting of the jars during the experiment duration. Samples collected for dSi were centrifuged for 20 min at 13.2 RPM, then 500 μL of supernatant was analyzed for dSi using the ammonium molybdate blue method (Parsons et al. 1984) outlined in Chapter 2.

Sampling method

Each tray of jars was destined to be terminally harvested for bSi determination at particular times (6, 12, 62, 104 and 176 days) so these 5 trays allowed coverage of dSi and bSi sampling over a longer period of time (Table 1). Prior to the terminal harvesting for bSi, each jar was sampled 6 times for dSi, including the zero time point. Each day a dSi sample was scheduled, the entire tray of jars was inverted to mix and was allowed to settle for at least 20 min before sampling water for dSi from near the top of the jars described above for time zero sample. One mL samples were centrifuged and supernatant analyzed for dSi.

At each designated jar terminal harvest date, jars were inverted and small volumes were collected for epifluorescence counts of bacterial abundance and for SEM imaging of frustule dissolution progress and bacterial loads. Epifluorescence replicates were 900 μ L of sample preserved with 100 μ L 25% glutaraldehyde (2.5% final conc.). SEM sample preservation was also in 2.5% glutaraldehyde with HEPES buffer (see Chapter 2). After sample collection and preservation in a sterile hood, 30 mL of sample was filtered on to 0.8 μ m polycarbonate (PC) filters for bSi analysis. After filtration, filters were dried for at least 2 hours or overnight, then weighed and frozen at -20 °C until analysis. On the last day of the experiment, 10 mL from the experimental (+ bacteria) jars were collected and frozen at -70 °C for later DNA analysis.

Experiment II: Diatom Species Comparison

Experiment II was run with similar methods to Experiment I but tested two different diatom species (one centric and one pennate) at the same temperature (4°C).

Diatom inoculum preparation

Two different diatoms were used, the same pennate of the genus *Synedra* that was used in Experiment I as well as a centric diatom isolated from water off the McKinley Marina in Lake Michigan. This *Cyclotella*-like diatom will be called *Cyclotella* for simplicity. This provides a contrast both for cell shape (pennate vs centric) and also for cell size.

Because of the amount of dissolution observed in C2 controls in Experiment I, I used antibiotic treatment to exclude bacteria not explicitly introduced during Experiment II.

Three culture flasks were grown up of the diatoms in DY-V medium as for Experiment II.

After growth to stationary phase, cultures were allowed to settle and some of the medium decanted. The concentrated cell culture at the bottom was centrifuged and

medium supernatant removed. The pellets were re-suspended in 4.9 mL of Si-free medium and 0.1 mL of an antibiotic cocktail of ampicillin and streptomycin (Fisher

Scientific), to a final concentration of 0.2 mg mL⁻¹ streptomycin and 2 mg mL⁻¹

ampicillin. These antibiotics were chosen because they were shown not to have an

adverse effect on diatoms in previous studies (D'Costa and Anil 2012). The cells were

centrifuged and medium replaced with fresh antibiotics and medium three times to hinder the growth of any bacteria already associated with the diatom cultures.

Prior to use as the inoculum for dissolution experiments, the cultures were washed through several rounds of centrifugation and resuspension with medium to remove any remaining antibiotics, before the heat-killing step at 85 °C for 30 min. After the hot water bath, tubes were plunged into a tray of ice and put into the freezer until contents were frozen.

To be able to compare the surface area of the diatoms, length and width of girdle and the diameter of the valve of *Cyclotella* was measured using the free software ImageJ (version 1.53k, Schneider et al. 2012). Most cells were found in girdle view, so 18 cells were measured in girdle view and 7 measured in valve view. The pixels in the scale bar were put into ImageJ and used to calculate the distance of lines drawn across cells in imageJ. The measurements were used to calculate surface area using equations from (Sun and Liu 2003). The measurements for *Synedra* from Chapter 1 were used to calculate a surface area to compare to *Cyclotella*.

Lake water sampling

Lake water was sampled from the *RV Neesky* in July 2021 from a 55 m pelagic Lake Michigan site (43°05.679 N, 87°46.2321 W). This station has been extensively monitored (e.g. Mosley and Bootsma 2015). Samples were collected with a Niskin sampler at

depths of 2, 8, 15, 20, 24, 38, and 50 m. These samples were pooled into an autoclaved carboy for transport to the laboratory. 1.5 L of water was filtered through a 0.8 μm filter (25 mm, ATTP) and autoclaved similar to Experiment I. For the sediment bacterial cocktail, ~300 g sediment was shaken with 1 L lake water and filtered through successive Nitex mesh sizes (243 μm \rightarrow 153 μm \rightarrow 53 μm \rightarrow 37 μm \rightarrow 20 μm \rightarrow 15 μm \rightarrow 10 μm \rightarrow 6 μm) which had been sterilized with ethanol. After filtering through the mesh, the filtrate was passed through 2 μm and then 0.8 μm polycarbonate (PC) filters with vacuum filtration. All filtering was done by an open flame or in the sterile hood to maintain a sterile environment. This produced a lake water and sediment bacterial 'cocktail' for use in the experiment.

For DNA analysis of water and sediment collected, 20 mL of sediment water was filtered for bacterial DNA analysis, along with 2 sediment samples (<1 g) and frozen at -70 °C for DNA extraction and gene sequencing (to be carried out later).

Experimental set up

The same set-up as in Experiment I was used for this experiment, with 30 autoclaved polypropylene jars inoculated with 1 mL of killed *Synedra* cells or cleaned frustules, the other 30 jars inoculated with *Cyclotella* cells or frustules. Into each jar, 49 mL of either autoclaved lake water or filtered bacteria cocktail was added. The three experimental types (EXP, C1 – dead diatoms + sterile water C2 – frustules + sterile water) were the

same as above, except that in the C1 treatment, 0.5 mL of 50 mL autoclaved water was replaced with 0.5 mL of the same antibiotic cocktail used in experimental preparation, for a final concentration of 0.2 mg mL⁻¹ streptomycin and 2 mg mL⁻¹ ampicillin.

One tray of jars was filled with 50 mL of the bacteria cocktail or the autoclaved water to monitor natural fluctuations in dSi without any bSi added. Two jars had 50 mL of autoclaved water; 4 jars had 50 mL of the filtered Lake Michigan bacteria cocktail. The jars with the filtered Lake Michigan bacteria were also used as “blank controls” so that the change in bacteria without the influence of diatom detritus could be monitored and compared to experimental treatments sampled at the same time.

Sampling was carried out as for Experiment I, but 0.5 mL instead of 1 mL was collected, allowing jars to rest and settle for at least a day before to avoid the need for centrifuging before dSi analyses. This experiment was shorter (77 days) and concentrated more sampling for dSi release in the beginning of the experiment (Table 1). Subsamples from jars were collected more frequently for analysis of changes in dSi in the water and changes in bSi were measured by filtration. Samples were filtered for DNA analysis on day 8 and day 77 (last day) for the experimental treatments and the jars inoculated with only the bacterial cocktail with no added diatoms (blank controls).

Statistical analyses and rate calculations

The dSi and bSi values from each sampling point for a jar were plotted in groups for each treatment (C1, C2, EXP). This provided a picture of dissolution over time, compared

for each treatment, as calculated rates of increase in dSi and decrease in bSi over time. To examine rates of change over the 6 dSi sampling points in individual jars from inoculation to the terminal sampling date, the initial dSi concentration at T_0 was subtracted from the dSi concentrations at each sampling time. The changes over time were analyzed by linear regression in R for both dSi and bSi, grouped together by treatment type.

To compare the change in individual jars across the different treatments, temperatures, and species, the overall rate of change in dSi from the inoculation of the jar to its filtration end date was calculated as the slope of a linear regression line. The rate of change from the start of the experiment to the end of the experiment was calculated as the slope of a linear regression line for each treatment at each temperature (Expt I) or for each species used (Expt II). The individual jars contributing to the linear regression inputs were considered independent and not subjected to repeated measures analysis. Temperature or species, treatment and final harvest day were all considered independent factors and the change in dSi over time (calculated jar slope) was the dependent response variable for a nested two-way ANOVA analysis using R (R Core Team 2020). This ANOVA compared treatments and determined interactions of temperature or species with treatment (EXP, C1, or C2) and final harvest day sampled on the slopes of the dSi and bSi changes over time.

Previous studies (e.g. Bidle and Azam 2001; Passow et al. 2011) calculated rates of Si dissolution (V_{diss}) using an equation from Hurd and Birdwhistell (1983), which normalized the dSi measured at time (t) to the bSi inoculated (bSi_0), using the following equation:

$$V_{diss} = -\left(\frac{1}{t}\right) \ln\left(\frac{bSi_0 - dSi_t}{bSi_0}\right)$$

This gives the rate of bSi dissolution to dSi for a specific time point. The equation assumes that starting dSi is zero, whereas the experiment started with $\sim 30 \mu\text{M}$ as the dSi concentration in the Lake Michigan water. To address this, the values used for dSi in the equation were adjusted to starting dSi concentrations ($dSi_t - dSi_0$). To get rates of change the entire experiment, the second half of the equation ($-\ln((bSi_0 - dSi)/bSi_0)$) was plotted over time and the slope of that line was used as the overall rate of dissolution (d^{-1}), normalized to starting bSi values, i.e. the diatom bSi inoculum added (Hurd and Birdwhistell 1983). To compare rates to published values, this rate of change was calculated over not just the entire experimental run, but also between time periods where dissolution rates seemed to be highest. Passow et al. (2011) used the period from the onset of dissolution (excluding any initial lag period) to the point where the dissolution rate started to decrease to represent “initial dissolution”. To compare with these experiments, an initial dissolution rate was determined for these experiments by graphing raw dSi values over time. For Experiment I, initial dissolution rates appeared to

be over days 0-12 for *Synedra* at 18 °C and days 0-62 for *Synedra* at 4 °C. dSi concentrations in Experiment II were more variable, so it was difficult to select a time period to represent initial linear dissolution. Given that Experiment I with *Synedra* showed linear dissolution from 0-62 days and the duration of Experiment II was a similar period of 77 days, the entire period was chosen to represent the initial dissolution rate for *Synedra*. For *Cyclotella*, days 0-34 were used.

Scanning Electron Microscopy

Four samples were chosen from Experiment II to analyze how the diatom frustule degraded over time and how bacteria colonized the diatom cells. One experimental treatment replicate was chosen to represent days 8 and 75 for *Cyclotella* and *Synedra* each. Nunc™ Thermanox™ polyester coverslips (13mm, ThermoFisher) were soaked in a solution of 2mL filtered (0.2 μm pore size) and 200 μL of poly-L-Lysine solution (0.1% w/v in water, Sigma-Aldrich). The solution covered the coverslips completely and were left submerged for 5 minutes each. Coverslips were dried in a petri dish with qualitative filter paper on the bottom to absorb excess. They were stored at room temperature in the petri dish until use.

Each SEM sample (preserved in 2.5% glutaraldehyde and 0.01 M HEPES) was brought to room temperature and 200 μL was pipetted using sterile techniques onto the coverslips. Cells were allowed to sediment for 1 hour and then placed (still wet) into a critical point drying basket (brass/nickel plated coverslip holder, Electron Microscopy

Sciences) which was submerged in a 10% ethanol solution, so cells were never allowed to dry out. The critical point drying basket was transferred to solutions with increasing percentages of ethanol (10% → 20% → 40% → 60% → 80% → 100%), soaking in each solution for 20-30 minutes before transfer. The samples were transferred to 100% ethanol twice before placing into 100% dry ethanol for 20 min. The critical point drying basket was transferred to the chamber of the critical point dryer, which was previously filled with dry ethanol enough to submerge basket (SAMDRI-790A, Tousimis). In the critical point dryer, ethanol was exchanged for liquid CO₂. Once all liquid had been exchanged, it was brought to the critical point of CO₂ to convert all liquid to gas but maintain the cell shape as if it was still completely hydrated. Critical point dried coverslips were placed into a desiccator jar with until they were mounted (< 1 hour). Coverslips were mounted onto 13 mm aluminum stubs with double sided conductive carbon tabs (PELCO Tabs™, Ted Pella Inc). The stubs with coverslips were placed on mounts and coated with carbon using a semi-planetary rotary work holder so that all sides of the sample would be coated evenly (Coating System E306A, Edwards). Carbon fiber was evaporated onto the rotating samples in approximately 10 second bursts until the string broke (2-3 pulses of coating). Edges of the coverslips and areas where charging might occur and areas where charging might occur were painted with colloidal graphite (Ted Pella Inc). Samples were viewed a Hitachi S-4800 field emission scanning electron microscope (FE-SEM).

Results

Experiment I – Effects of Temperature

Changes in dSi

Regressions of each treatment showed a significant increase in dSi over time for all treatments ($p < 0.01$) except for diatom frustules at 4 °C (C2, $p > 0.5$). For the 18 °C treatments, regressions of plots of dSi in treatments with heat-killed diatom cells inoculum (EXP and C1) had R^2 values > 0.91 , while the R^2 values for jars kept at 4 °C were lower (0.25 for EXP and 0.73 for C1, Fig. 1).

Across both temperatures and all treatments, the fastest rate of dSi increase in the jars was from day 0 to 12 (Fig. 2, $p < 0.00001$, nested two-way ANOVA, $n=60$). The treatment (type of diatom inoculum and lake water used) did not have a significant effect on the rate of overall dSi release into the water at either temperature ($p > 0.5$, $n=30$). However, temperature did significantly affect dSi release, with dissolution happening faster at 18 °C than 4 °C (Fig. 2; $p < 0.01$, $n = 60$). Changes in dSi over time were best described with linear regression (Fig. 1), except for C1 (dead diatoms + sterile water) at 18 °C which was best fit with a logarithmic curve (Fig. 4, $R^2=0.91$). Negative slope values were mainly due to the subtraction of the dSi values at the time of sampling being lower than the initial time points (dSi_t from dSi_0). Since the change in dSi was minimal for the first few

sampling time points, this resulted in negative values for the first date range of jars at the 4 °C temperature (Fig. 2).

Given the possibility of different initial bSi among treatments, the change in dSi at a specific time point was subtracted from the initial bSi, following the second half of the formula from Hurd and Birdwhistell (1983), $\ln(bSi_0 - dSi_t) / bSi_0$. When plotted against time, the slopes give the dissolution rate over that time period (Fig. 3). First, the overall rates of dissolution (0-176 days) were 0.0025 d⁻¹(EXP), 0.0074 d⁻¹ (C1), and 0.0037 d⁻¹ (C2) at 4 °C. At 18 °C, the values were 0.00469 d⁻¹ (EXP), 0.0056 d⁻¹ (C1), and 0.0042 d⁻¹ (C2).

These changes in dSi over the whole experiment were significant for C1 and C2 at 4 °C, and EXP and C1 at 18 °C ($p < 0.001$). Because there seemed to be faster increases in dSi in the jars during the first days, a period of initial dissolution from 0 to 62 days for 4 °C, 0-12 days for 18 °C was also analyzed by linear regression (Fig. 3). All treatments at both temperatures had a significant increase in dSi over time for this period of initial dissolution, except for C2 at 18 °C ($p < 0.01$).

Changes in bSi

There was a significant decrease in bSi across all treatments over time. At both temperatures, the slopes for bSi decline in jars with heat-killed diatoms with bacteria (EXP) and with autoclaved water (C1) were not significantly different (one-way ANOVA, $p > 0.01$), but both were higher than bSi changes in jars that contained frustules and

autoclaved water (C2) (Fig. 4) (one-way ANOVA, $p < 0.01$). By the end of the experiment (day 176), less than 0.05% of bSi inoculum was left for both temperatures and all treatments. Normalizing bSi measured at different time points to the experimental inoculum ($(bSi_0 - dSi_t)/bSi_0$) and doing a regression over time showed an average of $\sim 0.5\% d^{-1}$ decrease in the bSi in the original inoculum for all dead diatom treatments at both temperatures. Frustules showed an average of $0.2\% d^{-1}$ dissolution.

In this experiment, it was assumed that the bSi of the diatom cell inoculum ($8.7 \pm 0.56 \mu M$) for EXP and C1, average of 4 replicates of leftover inoculum *Synedra* cells and $3.4 \mu M$ for frustule, C2 treatments) would be converted to the dSi fraction. So with 100% dissolution, there would be $\sim 8.7 \mu M$ increase in the dSi over the experiment. In this experiment, starting dSi concentrations were $\sim 42.2 \mu M$ (EXP), $35.6 \mu M$ (C1) and $35.8 \mu M$ (C2). The change in bSi at the end of the experiment was near 100% for all treatments at all temperatures, so there would be an expected increase to $51.2 \mu M$ (EXP), $44.3 \mu M$ (C1), and $39.4 \mu M$ (C2). Actual end (day 176) dSi concentrations at $4^\circ C$ were $45.9 \mu M$ (EXP), $42.2 \mu M$ (C1), and $37.5 \mu M$ (C2). At $18^\circ C$ end dSi concentrations were $58.0 \mu M$ (EXP), $47.0 \mu M$ (C1), and $38.7 \mu M$ (C2). In the C1 and EXP treatments provided with dead diatom frustules, the end date dSi concentrations are higher than the calculated dSi concentrations at $18^\circ C$. The opposite is true for the jars kept at colder temperatures, where all of the treatments (EXP, C1, C2) end at a dSi concentration lower than what is calculated from the change in bSi over that time period.

Experiment II – Effect of Diatom Species

Differences in sizes and shapes of diatom inoculum species

Synedra is a pennate diatom (Fig. 5) with an average height of $3.23 \pm 0.48 \mu\text{m}$ (error = SD, $n = 13$), valve width of $3.37 \pm 0.50 \mu\text{m}$ ($n=13$), and valve length of $12.8 \pm 1.6 \mu\text{m}$ ($n=26$). Cells were measured for length in both valve and girdle view but width only in valve view and height in girdle view. Surface area was calculated as $150 \mu\text{m}^2$.

Cyclotella was a centric diatom, with an average valve diameter of $3.6 \pm 0.4 \mu\text{m}$ ($n= 25$) and height of $5.0 \pm 1.3 \mu\text{m}$ ($n= 18$). Cells were measured for diameter in both valve and girdle view and height in girdle view. Surface area was calculated as $78.0 \mu\text{m}^2$.

Changes in dSi

The release of dSi for this experiment was more variable than Experiment I, but there was still a significant increase in dSi concentrations in the EXP and C1 treatments for *Synedra* and the EXP and C2 treatments for *Cyclotella* (Fig. 6, linear regression, $p < 0.01$).

Cyclotella had a significantly higher rate of dissolution than *Synedra* (nested two-way ANOVA, $p < 0.01$, $n=60$). For *Synedra*, the date sampled did not have a significant effect on slope, but for *Cyclotella* the two earliest jars (0-2.5, 0-9 days, Fig. 7) had a significantly lower slope (negative) than the jars sampled at later times ($p < 0.01$, one-

way ANOVA, n=30). There was no significant difference found between the slopes of different treatments for either species ($p > 0.1$, one-way ANOVA). Rates of dSi increase for *Cyclotella* were faster over the length of the whole experiment (0-77 days) compared to *Synedra*, across all treatments.

Rates of change in dSi normalized to initial bSi starting values (Fig. 8) showed significant increases in dSi for *Synedra* EXP (dead diatoms + bacteria) and *Cyclotella* EXP and C1 (dead diatoms + sterile water) (linear regression, $p < 0.01$). The overall rates of dissolution for the *Synedra* jars (days 0-77) 0.0028 d^{-1} (EXP), 0.0021 d^{-1} (C1), and -0.0037 d^{-1} (C2) (Fig. 8). For comparison, the rates of *Synedra* at $4 \text{ }^{\circ}\text{C}$ from days 0-77 in Experiment I showed faster rates for all treatments except for EXP: 0.010 d^{-1} (EXP), 0.0040 d^{-1} (C1), and 0.0036 d^{-1} (C2). For *Cyclotella*, the EXP and C1 treatments showed significant increases in dSi over the full 76 days of the experiment (Fig. 7, linear regression, $p < 0.01$). When the rates were calculated for the "initial" dissolution value, from days 0-34, only the EXP treatment showed significant increases in dSi (linear regression, $p < 0.0001$).

Changes in bSi

The rates of dissolution of bSi in *Cyclotella* were generally faster than in *Synedra*. The bSi in the jars significantly decreased over time for *Synedra* in the EXP (dead diatoms + bacteria) and C2 (frustules + sterile water) treatments (Fig. 9, regression, $p < 0.001$). For

Cyclotella, only the C1 (dead diatoms + sterile water) showed a significant decrease in bSi over time (Fig. 9, regression, $p < 0.05$). Comparisons of the slopes of bSi over time with a one-way ANOVA showed that only the *Synedra* EXP (dead diatoms + bacteria) was significantly different from the other treatments ($p < 0.01$, one-way ANOVA, R). There was no significant difference between treatments for *Cyclotella*. bSi concentrations at the end of the experiment had decreased to about 50% of the original concentration for the *Synedra* experimental treatment and about 30% had dissolved in the *Synedra* C2 frustule treatment (Fig. 8). The C1 *Synedra* was more variable, but there was between 20 and 40% dissolution between replicate jars. Comparing to the time period 0-62 days in Experiment I, *Synedra* had more dissolution in the dead diatoms + bacteria (EXP) treatments (average of $70.7\% \pm 14\%$ in Experiment I and $54.3\% \pm 1.5\%$ in Experiment II). The dissolution for the frustule + sterile water (C2) was very similar between the two different experiments, with $69.9\% \pm 1.4\%$ in Experiment II and $72.1\% \pm 3.2\%$ in Experiment I. The dead diatoms + sterile water (C1) were very different not only between the different replicate jars within that treatment, but also compared from Experiment I to Experiment II. In Experiment I, it seemed that very little dissolution had happened by day 62 in the C1 jars, with an average of $2.3\% \pm 4.5\%$ dissolution. In Experiment II, C1 jars showed an average of $32.2 \pm 11.8\%$ dissolution. It should be noted that the dissolution of C1 over time by looking at the percent of bSi dissolved jumped after day 62 to ~80% dissolution by day 104. In *Cyclotella*, there was considerable

variability between all jars because of the clumpy nature of the cells, but by the end of the experiment, there has been ~20% dissolution in the experimental treatments (EXP), ~50% dissolution in the C1 treatments, and 7-50% dissolution in C2.

Si mass balance was calculated in the same way as Experiment I. The starting dSi values (dSi_0) ranged between 23 μM and 43 μM across different treatments, with an average bSi inoculum of 16.5 μM for *Synedra* and 17.5 μM for *Cyclotella* (though this species was much more variable due to clumping). Using the calculated difference in bSi from inoculum to end date sampling, the last day dSi theoretical dSi values were calculated. The ending dSi values for *Synedra* were calculated to be ~46 μM (EXP), 36 μM (C1), and 40 μM (C2). The actual *Synedra* end date dSi values were 38.3 μM (EXP), 31.4 μM (C1), and 37.8 μM (C2). For *Cyclotella*, theoretical end date dSi was calculated to be 41.7 μM , 29.4 μM (C1), 40.2 μM (C2). The actual end date dSi values were much consistently 4-10 μM lower with 31.6 μM (EXP), 24.8 μM (C1), and 34.8 μM (C2).

Scanning electron microscopy

The scanning electron microscopy images showed much more bacterial colonization of *Cyclotella* cells than of *Synedra* cells (Fig. 10). *Cyclotella* were also much more likely to appear in clumps than *Synedra* cells were. It appeared that there were broken shards of frustules by day 75 for *Cyclotella* which were still in clumps surrounded by bacteria. *Synedra* showed some frustules that looked mostly intact, but there is

separation between the valve and the girdle band where the early images from day 8 show a much more tightly held together cell.

Si concentrations in water from Lake Michigan at start of experiments

In Experiment I, the bSi in the water at the time of sampling was of $11.5 \pm 6.3 \mu\text{mols Si L}^{-1}$ ($n = 3$) in a depth-integrated sampling of the water column. The dSi concentrations of this depth integrated water column was $34.8 \mu\text{M}$. This was during late October, when the water column temperature stratification was breaking down. Temperatures near the surface and throughout the water column were about $8 \text{ }^\circ\text{C}$ (uwm.edu/glos/data). In Experiment II, water was collected in late July when there was a stable stratification. The depth integrated bSi concentration was $1.19 \pm 0.30 \mu\text{mols Si L}^{-1}$ ($n=3$), and the dSi concentration was $36.9 \mu\text{M}$. CTD casts from that day showed a surface temperature of $19.6 \text{ }^\circ\text{C}$ and a hypolimnion temperature of $5.4 \text{ }^\circ\text{C}$.

Discussion

Dissolution Rates and Effects of Temperature

Temperature had a significant effect on dissolution rate, which was clear from Experiment I and comparisons to previous studies. The greatest change in dSi at either temperature happened within the first 0-12 days. This could be due to the breaking open of the diatoms to release internal dSi pools. Based on the changes in bSi over that time period, this is the most likely explanation for the $4 \text{ }^\circ\text{C}$ treatment. The $18 \text{ }^\circ\text{C}$

treatment showed similar changes in dSi to the changes in bSi over that time period so there could be frustule dissolution starting to happen within the first 12 days for the warmer temperature. Experiment I had samples collected for SEM during each jar harvest date, removing some bSi for microscopic analysis, which was helpful to confirm frustule degradation. Experiment II only had samples removed for SEM on day 8 and the last day (76).

Other studies have shown that higher temperatures increase dissolution. Passow et al. (2011) summarized several marine studies examining the dissolution of dead diatoms (both natural and cultured assemblages and single species) and live (untreated) cells. The dissolution rates were normalized to the starting bSi concentration, so comparisons with the current study need to use the V_{diss} values calculated from dSi values normalized to initial bSi (see slopes in Figs 3, 7). In some cases, the rates of dissolution of these diatoms in freshwater seem faster than published values for marine diatoms. The marine diatom *Thalassiosira weissflogii* incubated with local bacteria had a V_{diss} of 0.023-0.036 after 7 days, dissolving ~50% of available bSi in the diatom (Bidle et al. 2002). In my experiment at 18 °C with *Synedra* and Lake Michigan bacteria (Experiment I EXP), V_{diss} over 8 days was $0.060 \pm 0.0071 \text{ d}^{-1}$. C1 treatment for the same time period, which likely still contained some bacteria originating from the non-axenic *Synedra* cultures, had higher V_{diss} rates (days 0-8) of $0.092 \pm 0.022 \text{ d}^{-1}$, however only 25-37% (range between replicate jars) of available bSi had dissolved by day 12 in this

treatment. Another experiment with *T. weissflogii* and *Chaetoceros simplex* at 18 °C with natural marine bacteria showed V_{diss} rates of 0.015-0.035 d⁻¹ (*T. weissflogii*) and 0.026-0.051 d⁻¹ (*C. simplex*) over 14 days (Bidle and Azam 2001). With *Synedra* at 18 °C (Experiment I) V_{diss} rates were within a similar range with 0.035 ± 0.0011 d⁻¹ for EXP and 0.080 ± 0.015 d⁻¹ for C1 in this experiment. Dissolution of diatom frustules in freshwater may not have been as different from marine species as previously thought, but it is important to note that Lake Michigan is rather alkaline, at a pH of about 8, which is more favorable to dissolution than acidic conditions (Loucaides et al. 2008).

To compare the 4 °C experiments with similar marine conditions, reported initial dissolution rates of *Chaetoceros debilis* and *Fragilaria kerguelensis* at 5 °C were 0.0074 d⁻¹ (0-102 days) and 0.0017 d⁻¹ (14-123 days), respectively (Passow et al. 2011), whereas with *Synedra* in Experiment I, from 0 to 117 days V_{diss} was 0.0046 ± 0.0031 d⁻¹ for EXP and 0.0064 ± 0.0011 d⁻¹ for C1. These are slightly slower than marine, but the more similar rates for *F. kerguelensis* to our C1 *Synedra* treatment may indicate the influence of bacteria communities.

Dissolution of the cleaned frustule treatments was faster at 18 °C than 4 °C. Naked frustule treatments (C2) showed higher rates of dissolution during days 0-12 than other treatments at both temperatures (Fig. 2) indicating the effect of temperature on chemical dissolution (since the organic coating had been removed). From days 0-12 for both experiments, the rate of dissolution (V_{diss}) at 18 °C is 0.05 d⁻¹ compared to 0.012 d⁻¹

¹, an almost 5x increase with increased temperature. Unlike in the other two treatments with intact diatoms, the H₂O₂ treatment to remove the organic coating of the frustule would also have opened the cells. The subsequent washing with Si-free media should have removed any intracellular dSi pools that were released during the chemical processing of the frustule. The removal of the organic coating, either by slow bacterial activity or in C2 treatment with peroxide-heat treatments, exposes the Si for chemical dissolution, so a higher rate of bSi to dSi dissolution is observed (Lewin 1961). In several marine species, dissolution rates of naked frustules increase with temperature (Kamatani and Riley 1979; Hurd and Birdwhistell 1983) as this is a chemical process, which may increase with temperature.

Dissolution rates from different diatom species

Dissolution rates were also significantly affected by the species, *Synedra* or *Cyclotella*, inoculated into the dissolution jar, possibly due to surface area differences between the diatoms. Higher surface area increases the rates of dissolution of cleaned diatom frustules (Hurd and Birdwhistell 1983; Van Cappellen et al. 2002), so one might expect differences between a pennate and centric diatoms. Measured surface area for *Cyclotella* was 78 μm^2 while *Synedra* was 150 μm^2 so we would expect *Synedra* to dissolve at a faster rate, but this was not the case. V_{diss} rates for the entire experimental

time period were slightly higher for *Cyclotella* than for *Synedra* for all treatments, but *Cyclotella* also had considerably more variability (see R² values in Fig. 8).

The clumping of *Cyclotella* may have caused much more variability in the total bSi inoculated into each jar. This partially explains the variability in the mass balance calculations, since the differences between the starting bSi inoculum and the actual measured at the end would be affected if there wasn't a consistent starting bSi value for each jar. In future studies, there should be a bSi taken from each jar itself, which may help alleviate this potential disparity between the actual bSi inoculated and that calculated from the remaining detritus like this experiment used.

Cell counts on the *Cyclotella* inoculum for this experiment were difficult with the clumping of cells, so the non-ionic surfactant Pluronic F-68 (MP Biomedicals) was added to a final concentration of 0.1%, but lysed all the cells destroying the aliquot for cell counts. bSi and cell counts from other *Cyclotella* cultures grown at the same time derived a bSi content of 0.063 ± 0.020 pmol cell⁻¹, suggesting this centric species was more lightly silicified than *Synedra*, at 0.26 pmol cell⁻¹. Lightly silicified diatoms are more likely to undergo dissolution than heavier silicified diatoms (Bidle and Azam 1999; Ryves et al. 2003). *Cyclotella* also had a higher bacterial load even after antibiotic treatment (Fig. 9, 10), and may have fostered bacterial communities that enhanced dissolution more efficiently than those attached to *Synedra*. Because *Cyclotella* was more likely to

aggregate, this could mean that around cell clumps, there were niches for bacteria that were protected from the antibiotics used to control bacteria in the inoculum.

Bacterial mediation of dissolution in freshwater

Diatom frustules when alive have an organic coating which needs to be degraded, probably by bacteria or passage through the gut of a zooplankter, before chemical dissolution of the Si can occur. The experimental treatments with Lake Michigan bacteria examined the role of bacteria in dissolution. Bacteria have been shown to accelerate dissolution rates by stripping the organic coating of diatoms and exposing the frustule beneath (Bidle and Azam 1999, 2001; Holstein and Hensen 2010). Living diatoms are colonized with increasing numbers of bacteria as they senesce, likely sending out exopolymeric substances that attract bacteria (Bell and Mitchell 1972; Abell and Bowman 2005; Znachor et al. 2012; Seymour et al. 2017). In Experiment I, I expected that heat-killing the diatoms would kill the bacteria too, but that was apparently not the case. Light microscopy showed that bacteria was still present around the diatom cells after inoculation. If bacteria survived the C1 heat treatment, they were transferred to lake water in jars. With the nutrients present in the lake water, little competition after autoclaving, and with the bacterial cells already being associated with diatom cells, they were likely well equipped to enhance the breakdown of the organic layer and increase dissolution of that diatom cell. In the experimental treatment, bacteria were explicitly

added and were likely competing with any surviving phycosphere bacteria, possibly reducing direct action on the diatom organic layer. This may explain the higher rates of dissolution of the C1 (dead diatoms + sterile water) for Experiment I (Fig. 3). This is especially evident in the warmer, 18 °C treatment. Since the diatoms used for this experiment were grown at that same temperature, the bacteria that were growing with these cultures would already have been growing competitively at this temperature. In Experiment II, I actively tried to reduce the bacteria inoculated into cultures by pre-treating with antibiotics. However, there were unforeseen chemical reactions of jars treated with antibiotics (C1 jars). During the ammonium molybdate dSi reaction, the addition of ammonium molybdate to the samples which contained antibiotics resulted in a cloudy precipitate. This disappeared when the acidic reducing reagent was added, suggesting a pH mediated reaction. The reaction appeared to develop color normally, so the results were used. Addition of glutaraldehyde to samples containing antibiotics (during preservation for SEM and epifluorescence) resulted in bright yellow color change. No documented explanation for this could be found in the literature and the reasons are unclear. This effect likely does not change the results of the experiment, but it is notable. The dissolution rates and bacterial community composition that are most ecologically relevant are those in the EXP treatments. Comparing *Synedra* dissolution in Experiments I and II, these were inoculated with bacteria collected from Lake Michigan at different time points. The V_{diss} from Experiment I, using bacteria collected in October, were 0.011

$\pm 0.012 \text{ d}^{-1}$ and faster than the rate in Experiment II, using bacteria collected in July, $0.0028 \pm 0.00020 \text{ d}^{-1}$. The incubation temperature and species inoculated were the same, and V_{diss} is normalized to starting bSi concentrations. Therefore, bacterial communities may be the key differences in the experiments resulting in different dissolution rates. The bSi in the water column at the time of sampling in October (Experiment I) was higher than the bSi in the water column in July (Experiment II), aligning with previous reports of highest seasonal bSi in northern Lake Michigan occurring in November (Schelske 1988). Furthermore, during the slowest period of phytoplankton growth during the colder season, there may be more dead diatoms falling to the sediment. These two factors may mean that the water column and sediment bacteria collected in October may have been enriched in microbial taxa which can degrade organic material related to silica frustules. These communities may also have been better acclimated to use these food sources than the communities collected in July which had a different supply of organic substrates. This hypothesis could be examined when the filters preserved for DNA are analyzed for bacterial community composition using 16S rRNA gene sequencing at a later date.

Ecological context

The implications of this research for understanding diatom Si dissolution and Si cycling in Lake Michigan suggest that dSi can be regenerated from freshwater diatoms

cells within a year, providing they are not buried in the sediments. The longer time frame covered by Experiment I showed almost complete bSi breakdown and dissolution by the end of 176 days (>99%, Fig. 4). Based on this rate, the bSi incorporated within a diatom bloom forming in April could be completely returned to the dSi pool by September. There could also be diatom blooms in fall (Brooks and Torke 1977), with highest concentrations of bSi in northern Lake Michigan being found in November in 1975 (Schelske 1988). Since the managed reduction of anthropogenic phosphorus loading resulting from the 1972 Great Lakes Water Quality Agreement, the lake has become more oligotrophic (Burlakova et al. 2018). Invasive dreissenid mussel density has increased (Vanderploeg et al. 2002; Nalepa et al. 2010), which has almost certainly affected recent Si cycling (Berges et al. 2021). In marine ecosystems, the release of dSi from mussel was higher than pseudofeces, but both showed dSi regeneration over 235 days in seawater (Van Broekhoven et al. 2015). Diatoms that have been grazed on by mussels through filter feeding may have their Si content ejected as feces or pseudofeces, and aggregates encapsulate other nutrients and bacteria. This may increase the chance of bacteria colonization of frustules and dead diatom cells, including via stronger signaling for chemotactic bacteria or by increasing encounter rate with bacteria (Seymour et al. 2017). The sediment bacteria collected for the experiments were likely influenced by mussel colonization, as mussels have colonized much of

western Lake Michigan nearshore, and mussel shells were found in the Ponar grabs of both experiments.

Mussels could potentially increase the rate of dissolution for diatoms in Lake Michigan. If a diatom falls to the sediments during normal senescence, the benthic space occupied by mussels may also change the fate of this diatom cell. Before extensive mussel colonization, the diatom could land on the sediment where it could be consumed by benthic amphipods. For example, *Diporeia sp.* typically relied on sedimenting cells from the spring diatom bloom (Madenjian et al. 2015). Cells could also become buried, or undergo dissolution on the sediment surface. If the benthos is covered by mussels, this may mean that sedimenting diatoms instead become food for mussels, or a diatom that reaches a crevice between mussels may be trapped and more likely to get buried under the mussel ejecta. More research on the role of dreissenid mussels on dSi regeneration is needed to determine exactly how they could be affecting the Si cycle in Lake Michigan. This study showed that under natural conditions, diatom frustule bSi can dissolve and this process can be mediated by Lake Michigan bacteria at temperatures common in the lake throughout the year.

Table 1. Description of different treatments, sampling days, temperatures, and species used in both Si dissolution experiments. Bold values show the last day the jar was sampled for dSi and was filtered for bSi, (+DNA) indicates that part of the jar was filtered for DNA analysis.

Experiment I Temperature comparison with <i>Synedra</i> diatoms						
Temperature	4 °C			18 °C		
	Experimental (EXP)	Control 1 (C1)	Control 2 (C2)	Experimental (EXP)	Control 1 (C1)	Control 2 (C2)
Treatments	Dead diatoms + lake bacteria	Dead diatoms + sterile water	Cleaned frustules + sterile water	Dead diatoms + lake bacteria	Dead diatoms + sterile water	Cleaned frustules + sterile water
Sampling (days from start of experiment)						
Jars 1-6	0, 1, 2, 3, 4, 6			0, 1, 2, 3, 4, 6		
Jars 7-12	0, 2, 4, 6, 8, 12			0, 2, 4, 6, 8, 12		
Jars 13-18	0, 6, 12, 25, 40, 62			0, 6, 12, 25, 40, 62		
Jars 19-24	0, 12, 25, 40, 85, 104			0, 12, 25, 40, 85, 104		
Jars 25-30	0, 25, 76, 117, 153, 176 (+ DNA)			0, 25, 76, 117, 153, 176 (+ DNA)		
Experiment II: Species comparison at 4 °C						
Species	<i>Synedra sp.</i>			<i>Cyclotella sp.</i>		
	Experimental (EXP)	Control 1 (C1)	Control 2 (C2)	Experimental (EXP)	Control 1 (C1)	Control 2 (C2)
Treatments	Dead diatoms + lake bacteria	Dead diatoms + sterile water	Cleaned frustules + sterile water	Dead diatoms + lake bacteria	Dead diatoms + sterile water	Cleaned frustules + sterile water
Sampling (days from start of experiment)						
Jars 1-6	0, 0.5, 1, 1.5, 2, 2.5			0, 0.5, 1, 1.5, 2, 2.5		
Jars 7-12	0, 5, 7, 8, 9 (+ DNA)			0, 5, 7, 8, 9 (+ DNA)		
Jars 13-18	0, 2.5, 9, 17, 27, 35			0, 2.5, 9, 17, 27, 35		
Jars 19-24	0, 13, 27, 35, 45, 50			0, 13, 27, 35, 45, 50		
Jars 25-30	0, 17, 45, 56, 68, 76 (+ DNA)			0, 17, 45, 56, 68, 76 (+ DNA)		

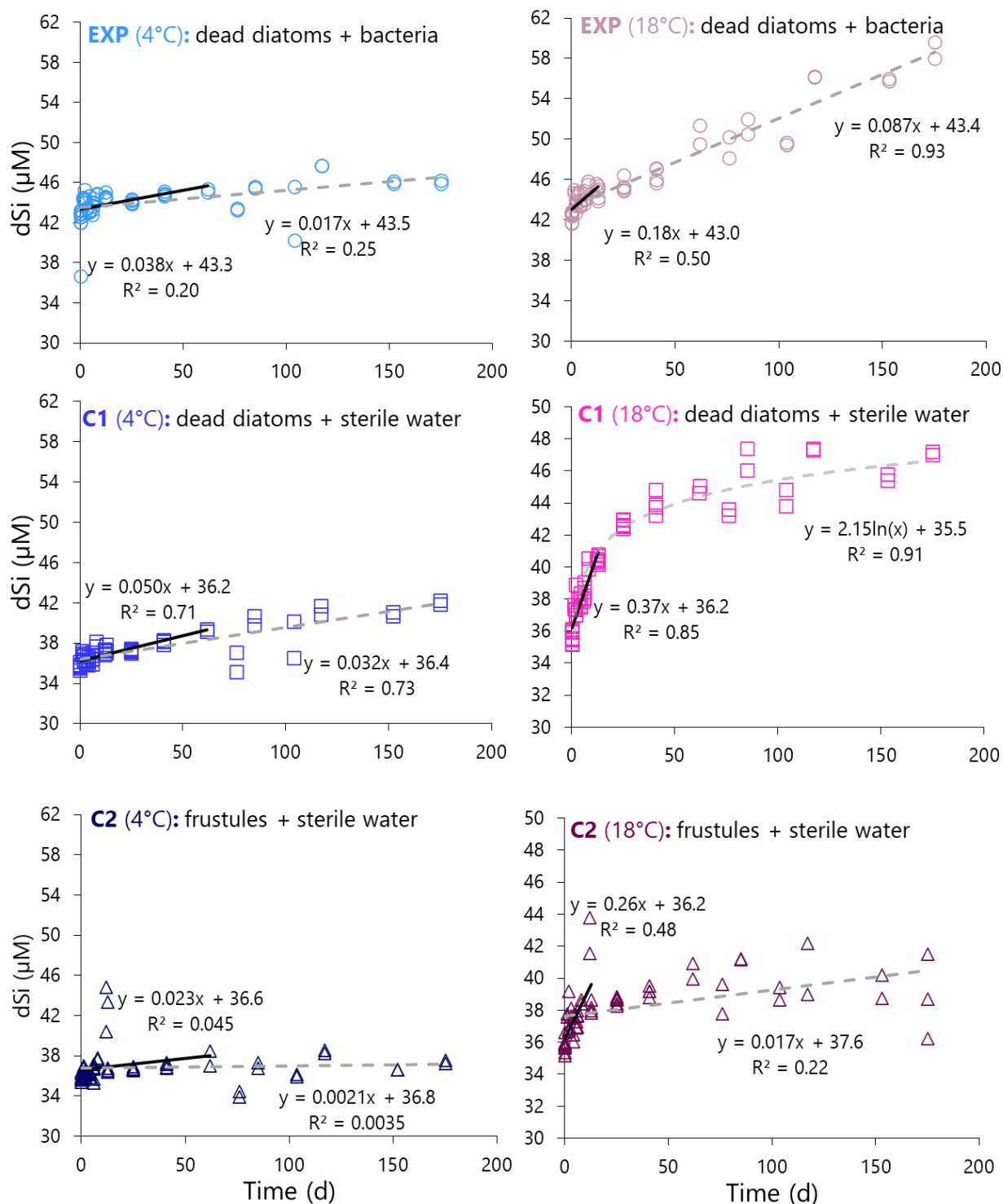


Figure 1. Raw dSi concentrations for all jars (not normalized to starting dSi) in Experiment I for each of the three treatments – EXP (dead diatoms + lake bacteria), C1 (dead diatoms + sterile water), and C2 (frustules + sterile water), using *Synedra* cells as the bSi inoculum. Black linear regressions show the time period used for “initial” dissolution for V_{diss} calculations. Dashed lines represent overall change in dSi over the full experimental period.

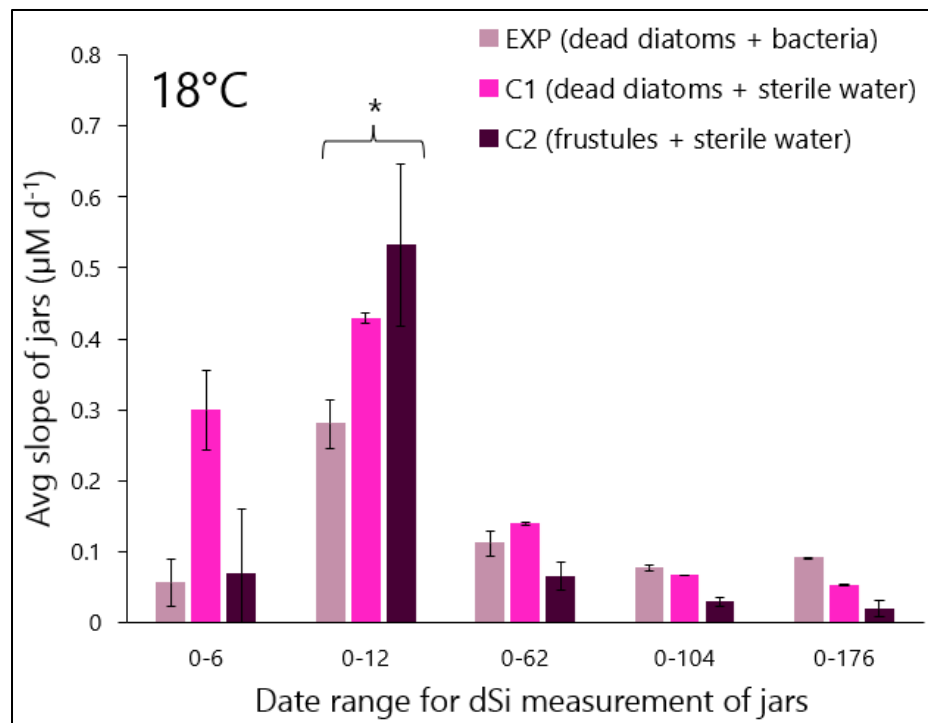
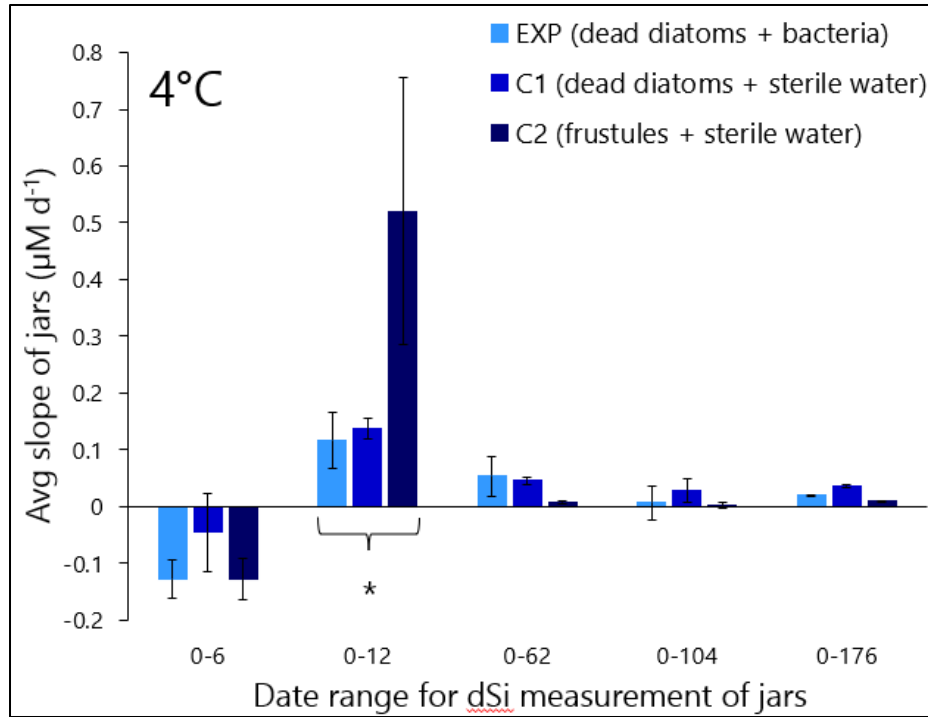


Figure 2. Average change in dSi from inoculation to bSi sample date for replicate jars. Each bar is the average of 2 jars inoculated and ended at the same time, with slopes measured from dSi changes in these individual jars. Error bars represent standard deviation. Asterisks signify a change that was significantly different than other jar replicates (one-way ANOVA, $p < 0.01$).

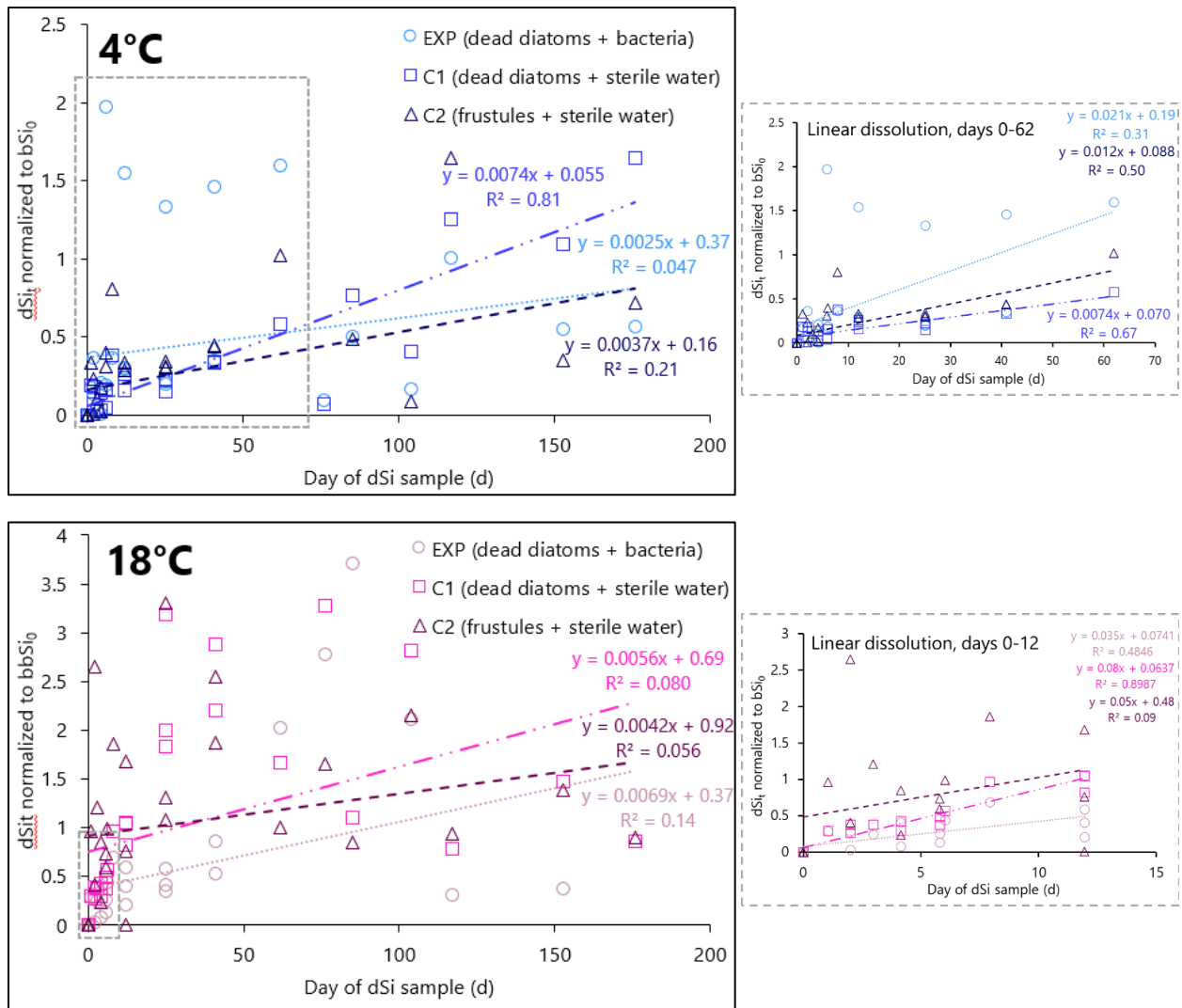


Figure 3. Change in dSi relative to the initial bSi added in the starting inoculum. The y axis shows the dSi normalized to initial bSi calculated using the formula $\ln(bSi_0 - dSi_t / bSi_0)$, plotted over time (t, d) to give the V_{diss} rates per day (Hurd & Birdwhistell 1983). Subsections outlined in the larger graphs are plotted next to their respective original graph and represent the period of initial dissolution that was determined from Fig. 1.

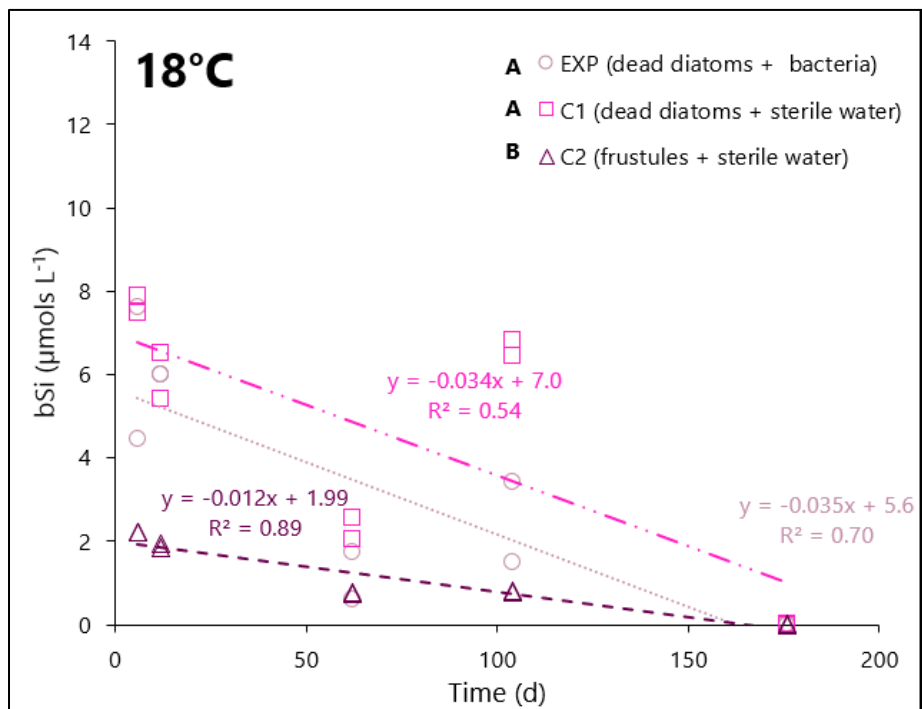
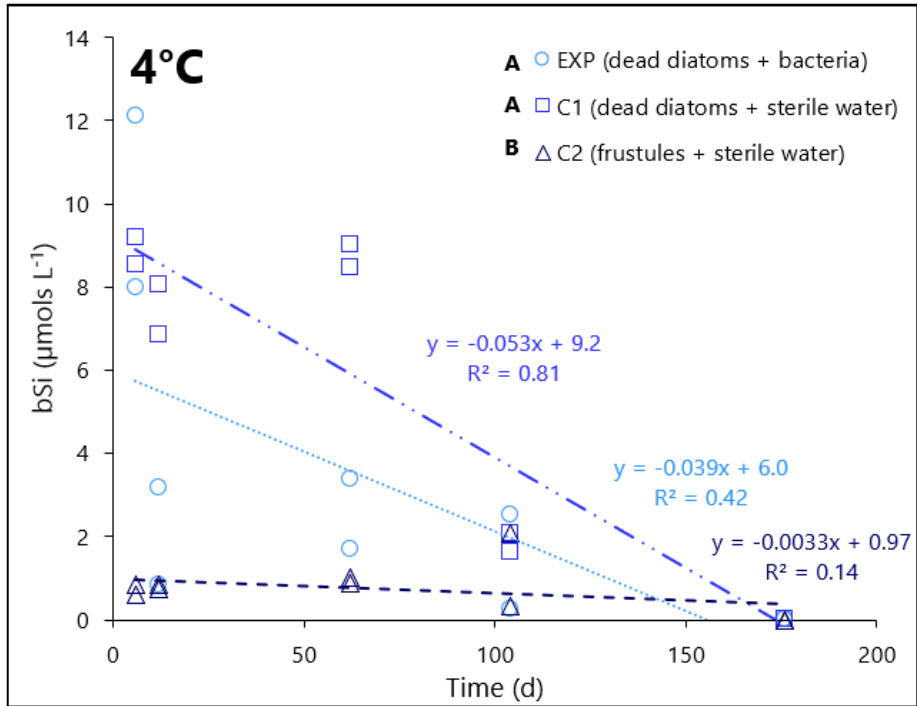


Figure 4. Change in bSi over time. Each point represents the bSi at the terminal harvest sampling date for each jar. Different letters against the legend indicate treatment slopes that were significantly different from the others ($p < 0.01$, one-way ANOVA).

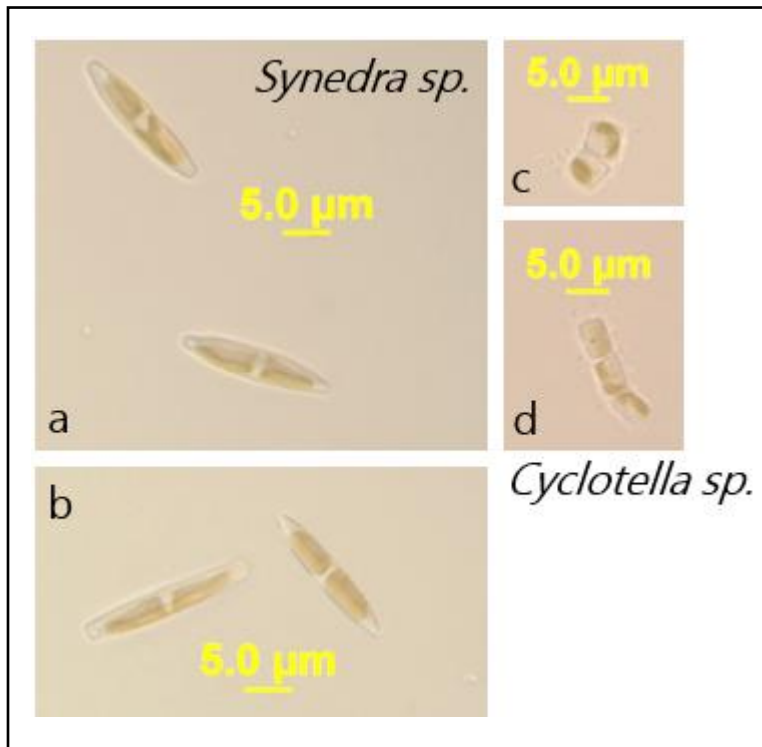


Figure 5. Light micrographs of the diatom species used as inoculum in Si dissolution experiments. Pictures are scaled to represent actual differences in size between the two diatoms.

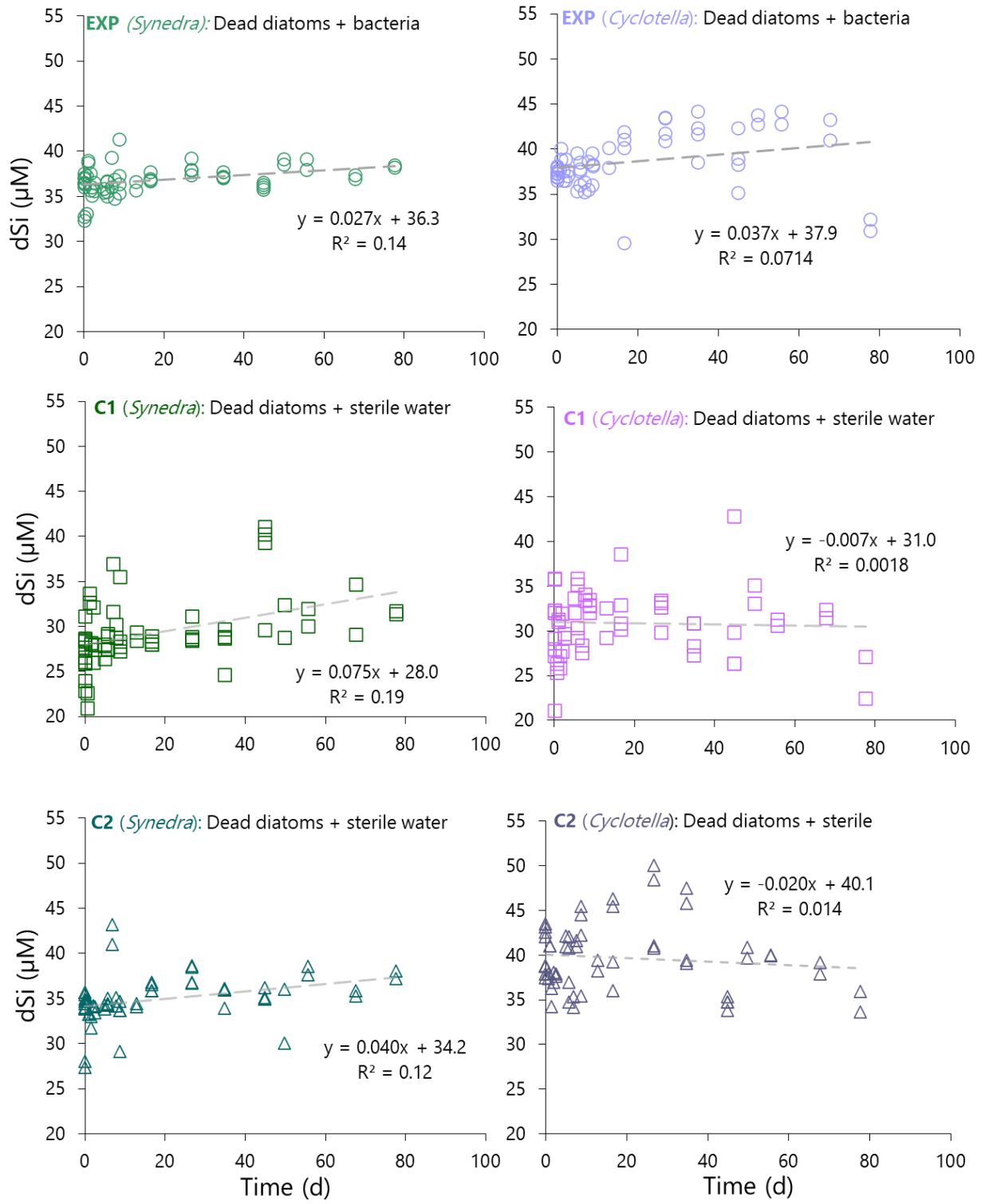


Figure 6. Raw dSi concentrations over time for all jars in Experiment II with two different diatom species, each with three treatments – EXP (dead diatoms + lake bacteria), C1 (dead diatoms + sterile water control) and C2 (diatom frustules + sterile water control) at 4 °C. Dashed lines represent overall change in dSi over the full experimental period.

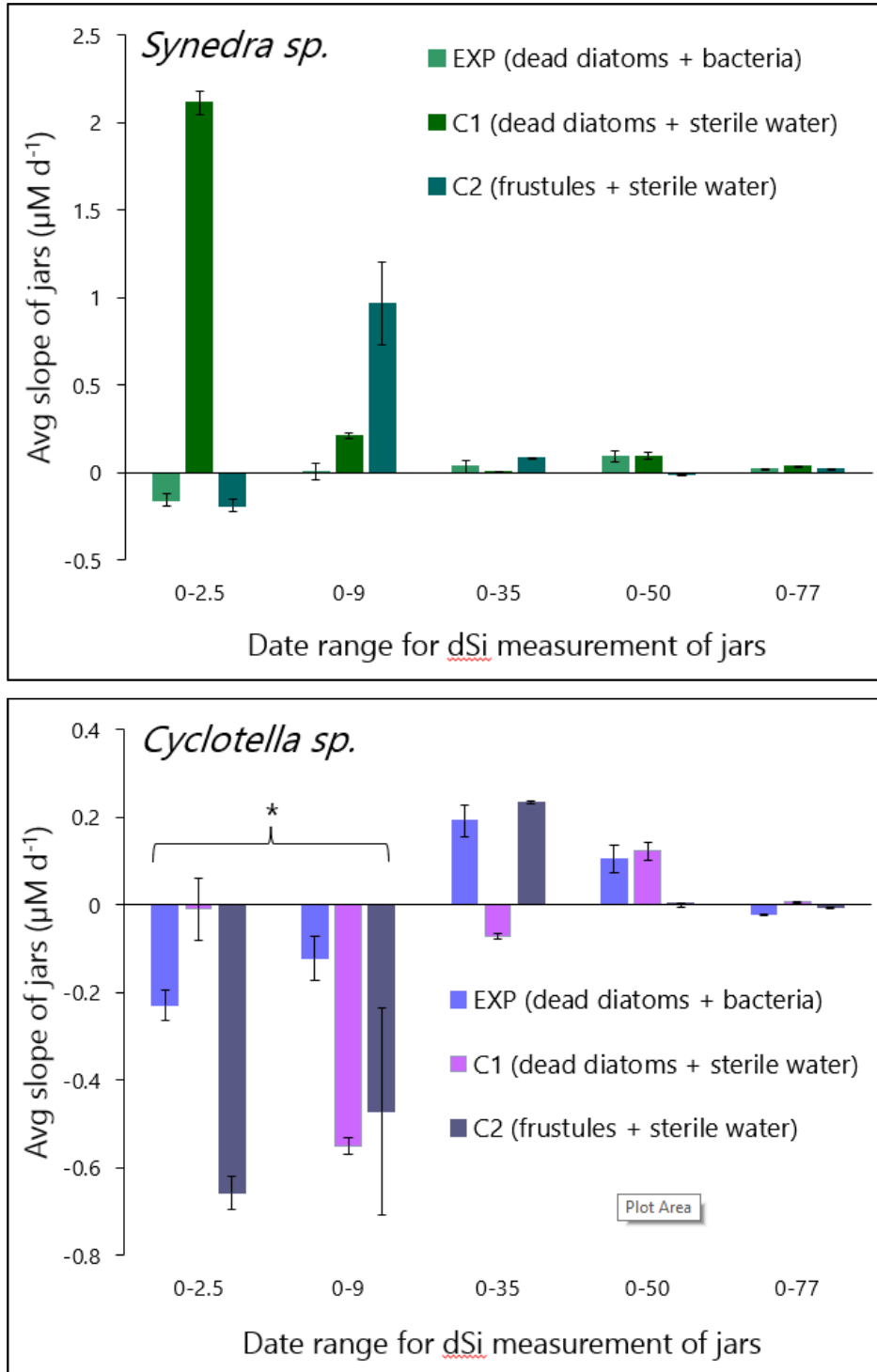


Figure 7. Average change in dSi from inoculation to bSi sample date (see table 1) for replicate jars. Error bars represent standard deviation of 2 jars. Asterisks signify a change in dSi for a certain time period that was significantly different than other time periods.

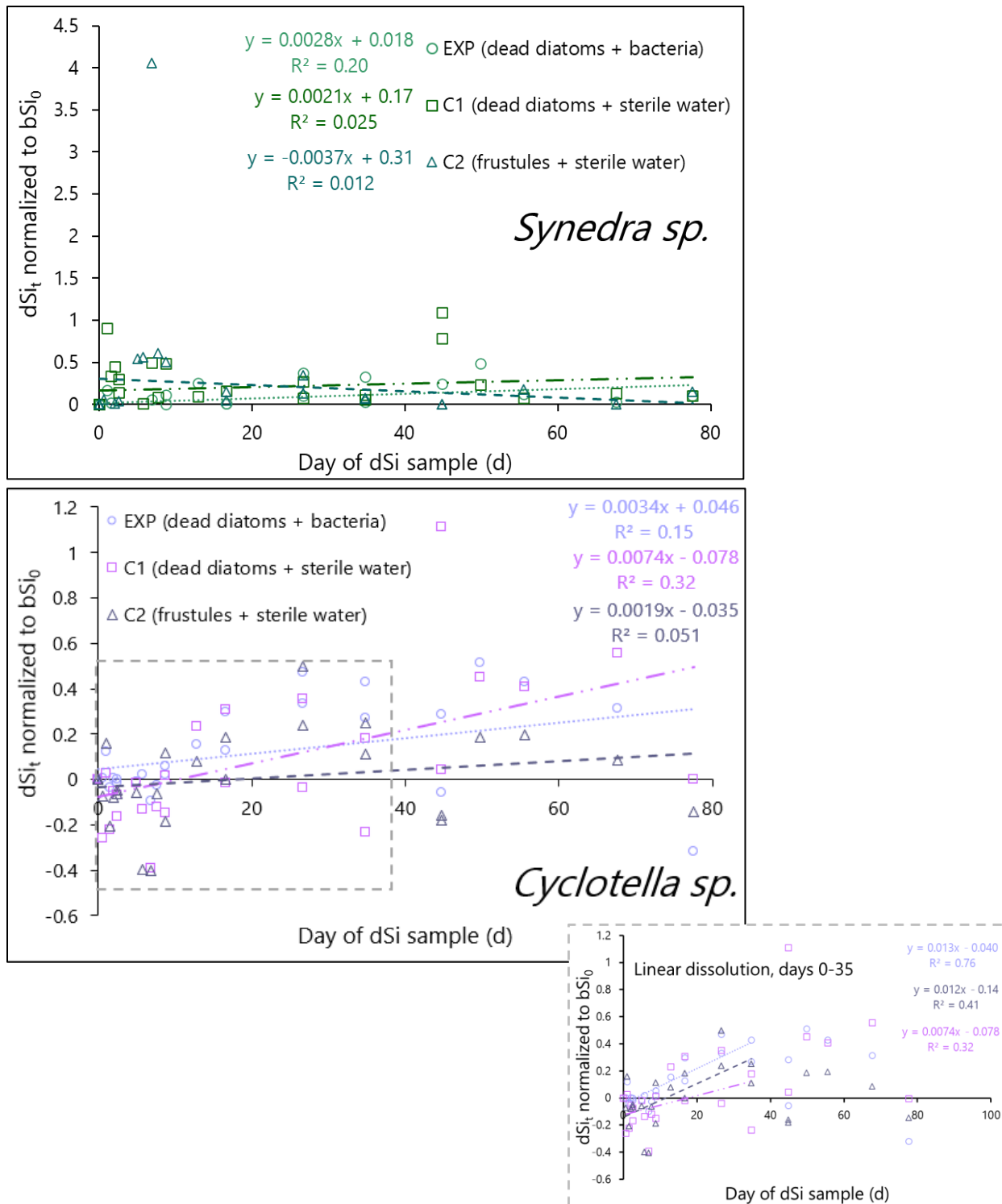


Figure 8. Change in dSi relative to the initial bSi added in the starting inoculum in dissolution experiment with two diatom species. The y axis shows the change in dSi normalized to initial bSi concentrations using the formula $\ln(bSi_0 - dSi_t / bSi_0)$, plotted over time (t, d) to give the V_{diss} rates per day (Hurd & Birdwhistell 1983). Subsections outlined in the *Cyclotella* graph are plotted next to the original graph and represent the period of initial dissolution that was determined from Fig. 6.

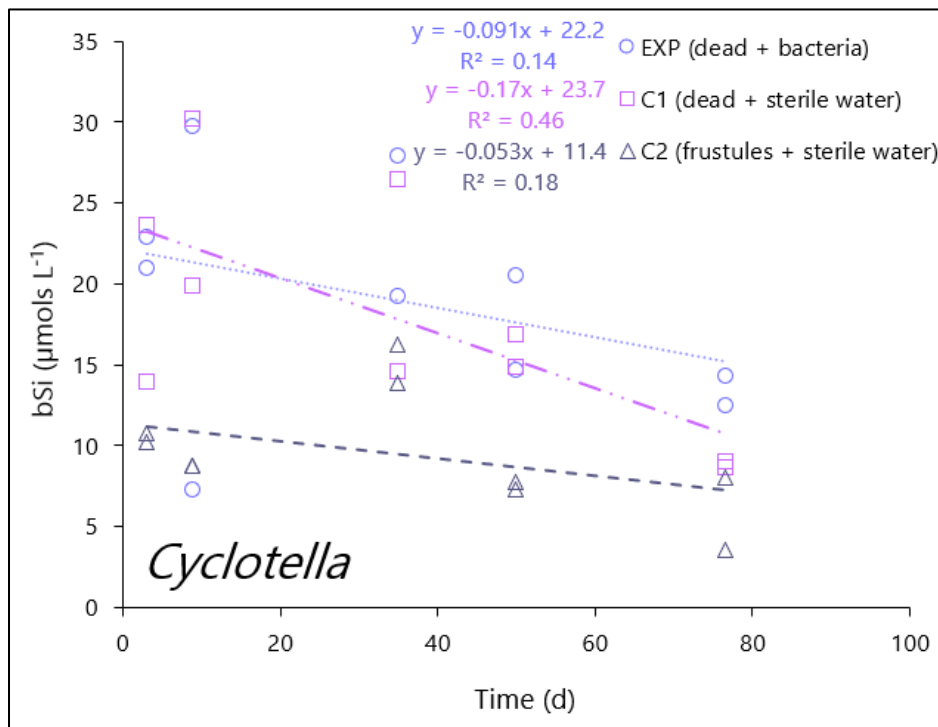
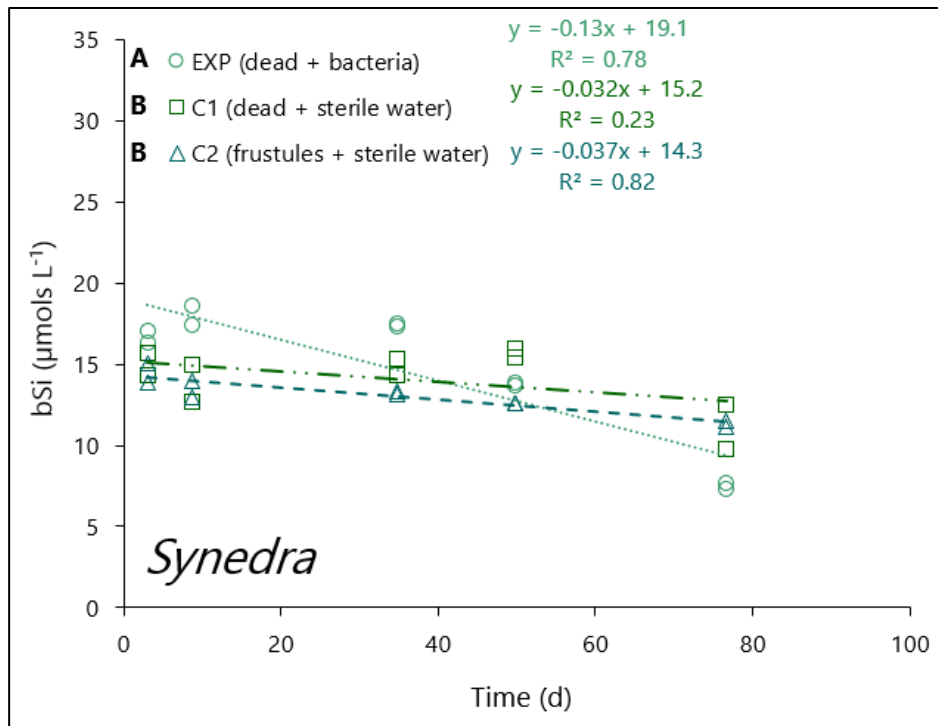


Figure 9. Change in bSi over time in dissolution experiment with two diatom species. Each point represents the bSi at the terminal harvest sampling date for each jar. Different letters against the legend indicate treatment slopes that were significantly different from the others ($p < 0.01$, one-way ANOVA).

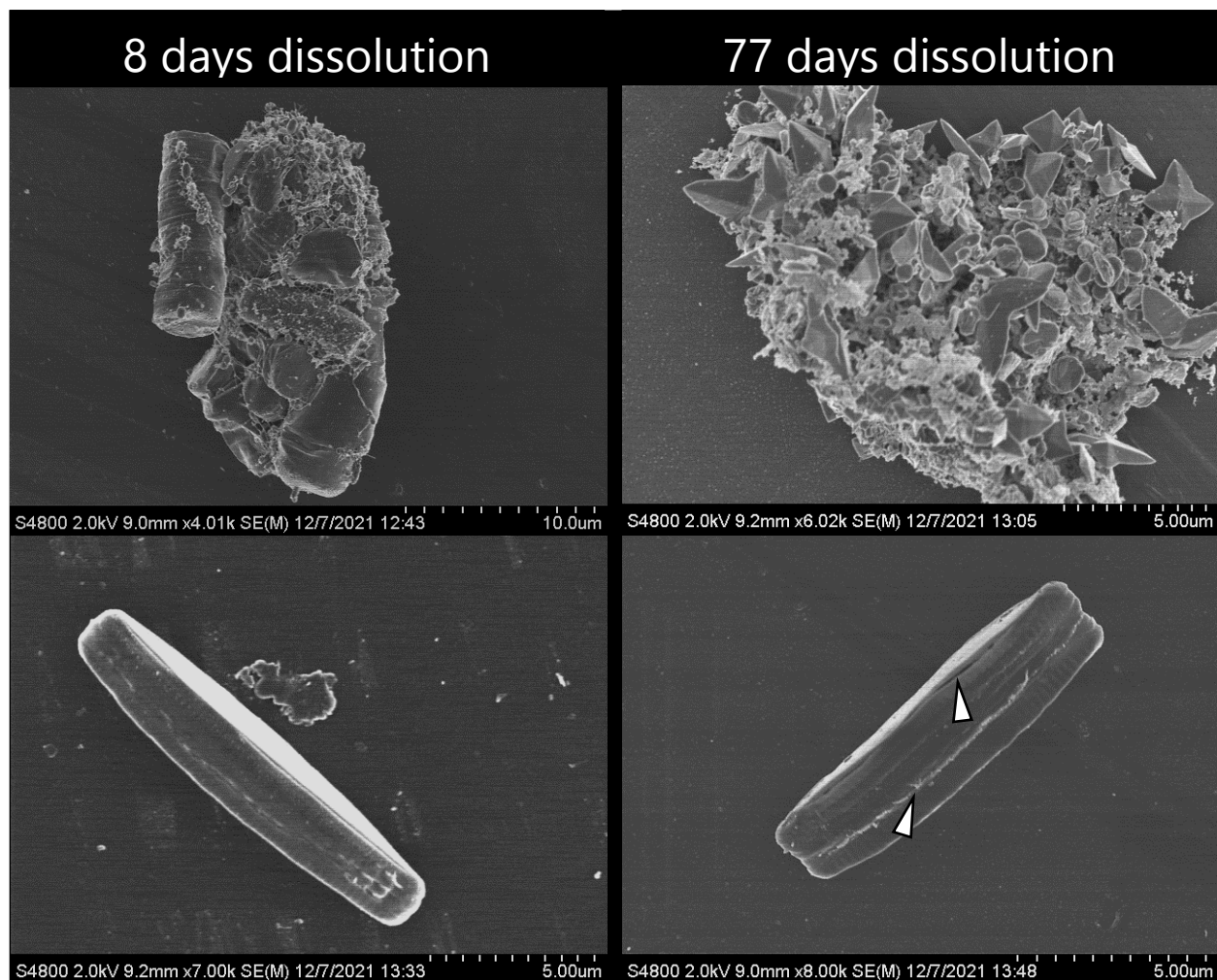


Figure 10. SEM images of *Cyclotella* (top) and *Synedra* (bottom) sampled during dissolution experiment, on day 8 (left) and the last day of Experiment II (day 77, right). *Cyclotella* showed heavy bacterial colonization from early in the experiment and showed more detritus and potential broken frustules by day 77. *Synedra* showed much less bacteria colonization at any stage, but showed some degradation of frustule integrity by day 77 (arrows).

REFERENCES

- Abell, G. C. J., and J. P. Bowman. 2005. Colonization and community dynamics of class Flavobacteria on diatom detritus in experimental mesocosms based on Southern Ocean seawater. *FEMS Microbiol. Ecol.* **53**: 379–391. doi:10.1016/j.femsec.2005.01.008
- Amin, S. A., M. S. Parker, and E. V. Armbrust. 2012. Interactions between Diatoms and Bacteria. *Microbiol. Mol. Biol. Rev.* **76**: 667–684. doi:10.1128/membr.00007-12
- Anderson, R. A., J. A. Berges, P. J. Harrison, and M. M. Watanabe. 2005. Recipes for freshwater and seawater media, p. 429–538. *In* R.A. Anderson [ed.], *Algal Culturing Techniques*. Elsevier.
- Assmy, P., V. Smetacek, M. Montresor, and others. 2013. Thick-shelled, grazer-protected diatoms decouple ocean carbon and silicon cycles in the iron-limited Antarctic Circumpolar Current. *Proc. Natl. Acad. Sci. U. S. A.* **110**: 20633–20638. doi:10.1073/pnas.1309345110
- Azam, F., B. B. Hemmingsen, and B. E. Volcani. 1973. Germanium incorporation into the silica of diatom cell walls. *Arch. für Mikrobiol.* **92**: 11–20. doi:10.1007/BF00409507
- Baines, S. B., B. S. Twining, M. A. Brzezinski, J. W. Krause, S. Vogt, D. Assael, and H. McDaniel. 2012. Significant silicon accumulation by marine picocyanobacteria. *Nat. Geosci.* **5**: 886–891. doi:10.1038/ngeo1641
- Baines, S. B., B. S. Twining, M. A. Brzezinski, D. M. Nelson, and N. S. Fisher. 2010. Causes and biogeochemical implications of regional differences in silicification of marine diatoms. *Global Biogeochem. Cycles* **24**. doi:10.1029/2010GB003856
- Barão, L., F. Vandevenne, W. Clymans, P. Frings, O. Ragueneau, P. Meire, D. J. Conley, and E. Struyf. 2015. Alkaline-extractable silicon from land to ocean: A challenge for biogenic silicon determination. *Limnol. Oceanogr. Methods* **13**: 329–344. doi:10.1002/lom3.10028
- Barbiero, R. P., B. M. Lesht, G. J. Warren, L. G. Rudstam, J. M. Watkins, E. D. Reavie, K. E. Kovalenko, and A. Y. Karatayev. 2018. A comparative examination of recent changes in nutrients and lower food web structure in Lake Michigan and Lake Huron. *J. Great Lakes Res.* **44**: 573–589. doi:10.1016/J.JGLR.2018.05.012

- Barbiero, R. P., M. L. Tuchman, G. J. Warren, and D. C. Rockwell. 2002. Evidence of recovery from phosphorus enrichment in Lake Michigan. *Can. J. Fish. Aquat. Sci.* **59**: 1639–1647. doi:10.1139/f02-132
- Barker, J. P., R. A. Cattolico, and E. Gatz. 2012. Multiparametric Analysis of Microalgae for Biofuels Using Flow Cytometry. *BD Biosci.* 1–12.
- Basharina, T. N., E. N. Danilovtseva, S. N. Zelinskiy, I. V. Klimenkov, Y. V. Likhoshway, and V. V. Annenkov. 2012. The Effect of Titanium, Zirconium and Tin on the Growth of Diatom *Synedra Acus* and Morphology of Its Silica Valves. *Silicon* **4**: 239–249. doi:10.1007/s12633-012-9119-x
- Bell, W., and R. Mitchell. 1972. Chemotactic and Growth Responses of Marine Bacteria to Algal Extracellular Products. *Biol. Bull.* **143**: 265–277.
- Bennett, P., J. Rogers, W. Choi, and F. Hiebert. 2001. Silicates, Silicate Weathering, and Microbial Ecology. *Geomicrobiol. J.* **18**: 3–19. doi:10.1080/01490450151079734
- Berges, J. A., A. M. Driskill, E. J. Guinn, K. Pokrzywinski, J. Quinlan, B. von Korff, and E. B. Young. 2021. Role of nearshore benthic algae in the Lake Michigan silica cycle. *PLoS One* **16**: 1–14. doi:10.1371/journal.pone.0256838
- Bidle, K., and F. Azam. 1999. Accelerated dissolution of diatom silica by marine bacterial assemblages. *Nature* **397**: 508–512. doi:10.1038/17351
- Bidle, K. D., and F. Azam. 2001. Bacterial control of silicon regeneration from diatom detritus: Significance of bacterial ectohydrolases and species identity. *Limnol. Ocean.* **46**: 1606–1623.
- Bidle, K. D., M. Manganelli, and F. Azam. 2002. Regulation of oceanic silicon and carbon preservation by temperature control on bacteria. *Science (80-.)*. **298**: 1980–1984. doi:10.1126/science.1076076
- Bockwoldt, K. 2018. Spatial and Temporal Variation of Phytoplankton Production in Lake Michigan. University of Wisconsin - Milwaukee.
- Bootsma, H. A., R. E. Hecky, T. C. Johnson, H. J. Kling, and J. Mwita. 2003. Inputs, Outputs, and Internal Cycling of Silica in a Large, Tropical Lake. *J. Gt. Lakes Res. Internat. Assoc. Gt. Lakes Res* **29**: 121–138.

- Bootsma, H. A., E. B. Young, and J. A. Berges. 2004. Temporal and spatial patterns of *Cladophora* biomass and nutrient stoichiometry in Lake Michigan, p. 81–88. In H.A. Bootsma, E.T. Jensen, E.B. Young, and J.A. Berges [eds.], *Cladophora* research and management in the great lakes: Special Report 2005-01.
- Boyd, C. M., and D. Gradmann. 2002. Impact of osmolytes on buoyancy of marine phytoplankton. *Mar. Biol.* **141**: 605–618. doi:10.1007/s00227-002-0872-z
- Bramburger, A. J., and E. D. Reavie. 2016. A comparison of phytoplankton communities of the deep chlorophyll layers and epilimnia of the Laurentian Great Lakes. *J. Great Lakes Res.* **42**: 1016–1025. doi:10.1016/j.jglr.2016.07.004
- Van Broekhoven, W., H. Jansen, M. Verdegem, E. Struyf, K. Troost, H. Lindeboom, and A. Smaal. 2015. Nutrient regeneration from feces and pseudofeces of mussel *Mytilus edulis* spat. *Mar. Ecol. Prog. Ser.* **534**: 107–120. doi:10.3354/meps11402
- Brooks, A. S., and B. G. Torke. 1977. Vertical and Seasonal Distribution of Chlorophyll *a* in Lake Michigan. *J. Fish. Res. Board Canada* **34**: 2280–2287. doi:10.1139/f77-306
- Brzezinski, M. A. 1985. The Si:C:N ratio of marine diatoms: Interspecific variability and the effect of some environmental variables. *J. Phycol.* **21**: 347–357. doi:10.1111/j.0022-3646.1985.00347.x
- Brzezinski, M. A., M. L. Dickson, D. M. Nelson, and R. Sambrotto. 2003a. Ratios of Si, C and N uptake by microplankton in the Southern Ocean. *Deep. Res. Part II Top. Stud. Oceanogr.* **50**: 619–633. doi:10.1016/S0967-0645(02)00587-8
- Brzezinski, M. A., J. L. Jones, K. D. Bidle, and F. Azam. 2003b. The balance between silica production and silica dissolution in the sea: Insights from Monterey Bay, California, applied to the global data set. *Limnol. Ocean.* **48**: 1846–1854.
- Brzezinski, M. A., J. W. Krause, S. B. Baines, J. L. Collier, D. C. Ohnemus, and B. S. Twining. 2017. Patterns and regulation of silicon accumulation in *Synechococcus* spp. M. Posewitz [ed.]. *J. Phycol.* **53**: 746–761. doi:10.1111/jpy.12545
- Burlakova, L. E., E. K. Hinchey, A. Y. Karatayev, and L. G. Rudstam. 2018. U.S. EPA Great Lakes National Program Office monitoring of the Laurentian Great Lakes: Insights from 40 years of data collection. *J. Great Lakes Res.* doi:10.1016/j.jglr.2018.05.017
- Van Cappellen, P., S. Dixit, and J. van Beusekom. 2002. Biogenic silica dissolution in the oceans: Reconciling experimental and field-based dissolution rates. *Global Biogeochem. Cycles* **16**. doi:10.1029/2001gb001431

- Carrick, H. J., and R. L. Lowe. 2007. Nutrient limitation of benthic algae in Lake Michigan: The role of silica. *J. Phycol.* **43**: 228–234. doi:10.1111/j.1529-8817.2007.00326.x
- Collins, J. R., B. R. Edwards, K. Thamatrakoln, J. E. Ossolinski, G. R. DiTullio, K. D. Bidle, S. C. Doney, and B. A. S. Van Mooy. 2015. The multiple fates of sinking particles in the North Atlantic Ocean. *Global Biogeochem. Cycles* **29**: 1471–1494. doi:10.1002/2014GB005037
- Conley, D. J., S. S. Kilham, and E. Theriot. 1989. Differences in silica content between marine and freshwater diatoms. *Limnol. Ocean.* **34**: 205–207.
- Conley, D. J., C. L. Schelske, and E. F. Stoermer. 1993. Modification of the biogeochemical cycle of silica with eutrophication. *Mar. Ecol. Prog. Ser.* **101**: 179–192. doi:10.3354/meps101179
- Conway, H. L., J. I. Parker, E. M. Yaguchi, and D. L. Mellinger. 1977. Biological utilization and regeneration of silicon in Lake Michigan. *J. Fish. Res. Board Canada* **34**: 537–544. doi:10.1139/f77-085
- Corsi, S. R., M. A. Borchardt, S. K. Spencer, P. E. Hughes, and A. K. Baldwin. 2014. Human and bovine viruses in the Milwaukee River watershed: Hydrologically relevant representation and relations with environmental variables. *Sci. Total Environ.* **490**: 849–860. doi:10.1016/J.SCITOTENV.2014.05.072
- Cuhel, R. L., and C. Aguilar. 2013. Ecosystem Transformations of the Laurentian Great Lake Michigan by Nonindigenous Biological Invaders. *Ann. Rev. Mar. Sci.* **5**: 289–320. doi:10.1146/annurev-marine-120710-100952
- D’Costa, P. M., and A. C. Anil. 2012. The effect of antibiotics on diatom communities. *Curr. Sci.* **102**: 1552–1559.
- Darley, W. M., and B. E. Volcani. 1969. Role of silicon in diatom metabolism. A silicon requirement for deoxyribonucleic acid synthesis in the diatom *Cylindrotheca fusiformis*. *Exp. Cell Res.* **58**: 334–342. doi:10.1016/0014-4827(69)90514-X
- DeMaster, D. J. 1981. The supply and accumulation of silica in the marine environment. *Geochim. Cosmochim. Acta* **45**: 1715–1732. doi:10.1016/0016-7037(81)90006-5
- Diwu, Z., C.-S. Chen, C. Zhang, D. H. Klaubert, and R. P. Haugland. 1999. A novel acidotropic pH indicator and its potential application in labeling acidic organelles of live cells. *Chem. Biol.* **6**: 411–418. doi:10.1016/S1074-5521(99)80059-3

- Ehrlich, H. L. 1996. How microbes influence mineral growth and dissolution. *Chem. Geol.* **132**: 5–9.
- Einsele W. & J. Grim. 1938. Über den kiesel säuregehalt planktischer diatomeen und dessen bedeutung für einige fragen ihrer ökologie. *Zeitschrift für Botanik.* **32**: 545-590
- Elser, J. J., M. E. S. Bracken, E. E. Cleland, and others. 2007. Global analysis of nitrogen and phosphorus limitation of primary producers in freshwater, marine and terrestrial ecosystems. *Ecol. Lett.* **10**: 1135–1142. doi:10.1111/j.1461-0248.2007.01113.x
- Engevold, P. M., E. B. Young, C. D. Sandgren, and J. A. Berges. 2015. Pressure from top and bottom: Lower food web responses to changes in nutrient cycling and invasive species in western Lake Michigan. *J. Great Lakes Res.* **41**: 86–94. doi:10.1016/j.jglr.2015.04.015
- Fahnenstiel, G. L., and D. Scavia. 1987. Dynamics of Lake Michigan phytoplankton: primary production and growth. *Can. J. Fish. Aquat. Sci.* **44**: 499–508. doi:10.1139/f87-062
- Fahnenstiel, G., S. Pothoven, H. Vanderploeg, D. Klarer, T. Nalepa, and D. Scavia. 2010. Recent changes in primary production and phytoplankton in the offshore region of southeastern Lake Michigan. *J. Great Lakes Res.* **36**: 20–29. doi:10.1016/j.jglr.2010.03.009
- Falkowski, P. G., R. T. Barber, and V. Smetacek. 1998. Biogeochemical controls and feedbacks on ocean primary production. *Science (80-.)*. **281**: 200–206. doi:10.1126/science.281.5374.200
- Finkel, Z. V. 2016. Silicification in the Microalgae, p. 289–300. *In* M.A. Borowitzka, J. Beardall, and J.A. Raven [eds.], *The Physiology of Microalgae*. Springer International Publishing.
- Galloway, J. N., A. M. Leach, A. Bleeker, and J. W. Erisman. 2013. A chronology of human understanding of the nitrogen cycle. *Philos. Trans. R. Soc. B Biol. Sci.* **368**: 20130120. doi:10.1098/RSTB.2013.0120
- Gibson, C. E., G. Wang, and R. H. Foy. 2000. Silica and diatom growth in Lough Neagh : the importance of internal recycling. *Freshw. Biol.* **45**: 285–293.

- Gibson, C. E., R. B. Wood, E. L. Dickson, and D. H. Jewson. 1971. The succession of phytoplankton in L. Neagh 1968—70. *SIL Commun. 1953-1996* **19**: 146–160. doi:10.1080/05384680.1971.11903927
- Guillard, R. R. L., and J. H. Ryther. 1962. Studies of marine planktonic diatoms. I. *Cyclotella nana Hustedt*, and *Detonula confervacea* (Cleve) Grun. *Can. J. Microbiol.* **8**: 229–239. doi:10.1139/m62-029
- Hecky, R. E., R. E. H. Smith, D. R. Barton, S. J. Guildford, W. D. Taylor, M. N. Charlton, and T. Howell. 2004. The nearshore phosphorus shunt: a consequence of ecosystem engineering by dreissenids in the Laurentian Great Lakes. *Can. J. Fish. Aquat. Sci.* **61**: 1285–1293. doi:10.1139/F04-065
- Hildebrand, M., S. J. L. Lerch, and R. P. Shrestha. 2018. Understanding diatom cell wall silicification—moving forward. *Front. Mar. Sci.* **5**. doi:10.3389/fmars.2018.00125
- Hildebrand, M., B. E. Volcani, W. Gassmann, and J. I. Schroeder. 1997. A gene family of silicon transporters. *Nature* **385**: 688–689.
- Hoffmann, L. J., I. Peeken, and K. Lochte. 2007. Co-limitation by iron, silicate, and light of three Southern Ocean diatom species. *Biogeosciences Discuss.* doi:10.5194/bgd-4-209-2007
- Holstein, J. M., and C. Hensen. 2010. Microbial mediation of benthic biogenic silica dissolution. *Geo-Marine Lett.* **30**: 477–492. doi:10.1007/s00367-009-0181-3
- Hurd, D. C., and S. Birdwhistell. 1983. On producing a more general model for biogenic silica dissolution. *Am. J. Sci.* **283**: 1–28. doi:10.2475/ajs.283.1.1
- Hutchins, D. A., and K. W. Bruland. 1998. Iron-limited diatom growth and Si:N uptake ratios in a coastal upwelling regime. *Nature* **393**: 561–564. doi:10.1038/31203
- Iler, R. K. 1979. *Chemistry of Silica - Solubility, Polymerization, Colloid and Surface Properties and Biochemistry*, John Wiley & Sons.
- Kamatani, A., and J. P. Riley. 1979. Rate of dissolution of diatom silica walls in seawater. *Mar. Biol.* **55**: 29–35. doi:10.1007/BF00391714
- Karatayev, A. Y., L. E. Burlakova, K. Mehler, R. P. Barbiero, E. K. Hinchey, P. D. Collingsworth, K. E. Kovalenko, and G. Warren. 2018. Life after *Dreissena*: The decline of exotic suspension feeder may have significant impacts on lake ecosystems. *J. Great Lakes Res.* **44**: 650–659. doi:10.1016/J.JGLR.2018.05.010

- Kaye, T. G., and M. Meltzer. 2020. Diatoms constrain forensic burial timelines: case study with DB Cooper money. *Sci. Rep.* **10**: 1–9. doi:10.1038/s41598-020-70015-z
- Kerfoot, W. C., F. Yousef, S. A. Green, J. W. Budd, D. J. Schwab, and H. A. Vanderploeg. 2010. Approaching storm: Disappearing winter bloom in Lake Michigan. *J. Great Lakes Res.* **36**: 30–41. doi:10.1016/j.jglr.2010.04.010
- von Keyserlingk, M. A. G., N. P. Martin, E. Kebreab, and others. 2013. Invited review: Sustainability of the US dairy industry. *J. Dairy Sci.* **96**: 5405–5425. doi:10.3168/jds.2012-6354
- Kilham, S. S., C. L. Kott, and D. Tilman. 1977. Phosphate and Silicate Kinetics for the Lake Michigan Diatom *Diatoma Elongatum*. *J. Great Lakes Res.* **3**: 93–99. doi:10.1016/S0380-1330(77)72233-6
- Krause, J. W., M. A. Brzezinski, M. R. Landry, S. B. Baines, D. M. Nelson, K. E. Selph, A. G. Taylor, and B. S. Twining. 2010. The effects of biogenic silica detritus, zooplankton grazing, and diatom size structure on silicon cycling in the euphotic zone of the eastern equatorial Pacific. *Limnol. Oceanogr.* **55**: 2608–2622. doi:10.4319/lo.2010.55.6.2608
- Krause, J. W., M. R. Stukel, A. G. Taylor, D. A. A. Taniguchi, A. De Verneil, and M. R. Landry. 2015. Net biogenic silica production and the contribution of diatoms to new production and organic matter export in the Costa Rica Dome ecosystem. *J. Plankton Res.* **38**: 216–229. doi:10.1093/plankt/fbv077
- De La Rocha, C. L., D. A. Hutchins, M. A. Brzezinski, and Y. Zhang. 2000. Effects of iron and zinc deficiency on elemental composition and silica production by diatoms. *Mar. Ecol. Prog. Ser.* **195**: 71–79. doi:10.3354/meps195071
- Leblanc, K., and D. A. Hutchins. 2005. New applications of a biogenic silica deposition fluorophore in the study of oceanic diatoms. *Limnol. Oceanogr. Methods* **3**: 462–476. doi:10.4319/lom.2005.3.462
- Lewin, J. 1966. Silicon metabolism in diatoms. V. Germanium dioxide, a specific inhibitor of diatom growth. *Phycologia* **6**: 1–12. doi:10.2216/i0031-8884-6-1-1.1
- Lewin, J. C. 1961. The dissolution of silica from diatom walls. *Geochim. Cosmochim. Acta* **21**: 182–198. doi:10.1016/s0016-7037(61)80054-9
- Loucaides, S., P. Van Cappellen, and T. Behrends. 2008. Dissolution of biogenic silica from land to ocean: Role of salinity and pH. *Limnol. Ocean.* **53**: 1614–1621.

- Loucaides, S., P. Van Cappellen, V. Roubex, B. Moriceau, and O. Ragueneau. 2012. Controls on the Recycling and Preservation of Biogenic Silica from Biomineralization to Burial. *Silicon* **4**: 7–22. doi:10.1007/s12633-011-9092-9
- Lynn, S. G., S. S. Kilham, D. A. Kreeger, and S. J. Interlandi. 2000. Effect of nutrient availability on the biochemical and elemental stoichiometry in the freshwater diatom *Stephanodiscus minutulus*. *J. Phycol.* **36**: 510–522. doi:10.1046/j.1529-8817.2000.98251.x
- Madenjian, C. P., D. B. Bunnell, D. M. Warner, and others. 2015. Changes in the Lake Michigan food web following dreissenid mussel invasions: A synthesis. *J. Great Lakes Res.* **41**: 217–231. doi:10.1016/J.JGLR.2015.08.009
- Malkin, S. Y., R. J. Sorichetti, J. A. Wiklund, and R. E. Hecky. 2009. Seasonal abundance, community composition, and silica content of diatoms epiphytic on *Cladophora glomerata*. *J. Great Lakes Res.* **35**: 199–205. doi:10.1016/j.jglr.2008.12.008
- Marron, A. O., H. Chappell, S. Ratcliffe, and R. E. Goldstein. 2016a. A model for the effects of germanium on silica biomineralization in choanoflagellates. *J. R. Soc. Interface* **13**. doi:10.1098/rsif.2016.0485
- Marron, A. O., S. Ratcliffe, G. L. Wheeler, R. E. Goldstein, N. King, F. Not, C. De Vargas, and D. J. Richter. 2016b. The evolution of silicon transport in eukaryotes. *Mol. Biol. Evol.* **33**: 3226–3248. doi:10.1093/molbev/msw209
- Martin-Jézéquel, V., M. Hildebrand, and M. A. Brzezinski. 2000. Silicon metabolism in diatoms: Implications for growth. *J. Phycol.* **36**: 821–840. doi:10.1046/j.1529-8817.2000.00019.x
- McCarthy, M. J., W. S. Gardner, M. F. Lehmann, A. Guindon, and D. F. Bird. 2016. Benthic nitrogen regeneration, fixation, and denitrification in a temperate, eutrophic lake: Effects on the nitrogen budget and cyanobacteria blooms. *Limnol. Oceanogr.* **61**: 1406–1423. doi:10.1002/lno.10306
- McNair, H. M., M. A. Brzezinski, C. P. Till, and J. W. Krause. 2018. Taxon-specific contributions to silica production in natural diatom assemblages. *Limnol. Oceanogr.* **63**: 1056–1075. doi:10.1002/lno.10754
- Mida, J. L., D. Scavia, G. L. Fahnenstiel, S. A. Pothoven, H. A. Vanderploeg, and D. M. Dolan. 2010. Long-term and recent changes in southern Lake Michigan water quality with implications for present trophic status. *J. Great Lakes Res.* **36**: 42–49. doi:10.1016/j.jglr.2010.03.010

- Moore, L. F., and J. A. Traquair. 1976. Silicon, a required nutrient for *Cladophora glomerata* (L) Kütz. (Chlorophyta). *Planta* **128**: 179–182. doi:10.1007/BF00390321
- Mortimer, C. H., and G. T. Csanady. 1975. Physical limnology of Lake Michigan., Argonne National Laboratory.
- Mosley, C., and H. Bootsma. 2015. Phosphorus recycling by profunda quagga mussels (*Dreissena rostriformis bugensis*) in Lake Michigan. *J. Great Lakes Res.* **41**: 38–48. doi:10.1016/j.jglr.2015.07.007
- Nalepa, T. F., D. L. Fanslow, and S. A. Pothoven. 2010. Recent changes in density, biomass, recruitment, size structure, and nutritional state of *Dreissena* populations in southern Lake Michigan. *J. Great Lakes Res.* **36**: 5–19. doi:10.1016/j.jglr.2010.03.013
- Nelson, D. M., J. J. Goering, S. S. Kilham, and R. R. L. Guillard. 1976. Kinetics of Silicic Acid Uptake and Rates of Silica Dissolution in the Marine Diatom *Thalassiosira Pseudonana*. *J. Phycol.* **12**: 246–252. doi:10.1111/j.1529-8817.1976.tb00510.x
- Nelson, D. M., P. Tréguer, M. A. Brzezinski, A. Leynaert, and B. Quéguiner. 1995. Production and dissolution of biogenic silica in the ocean: Revised global estimates, comparison with regional data and relationship to biogenic sedimentation. *Global Biogeochem. Cycles* **9**: 359–372. doi:10.1029/95GB01070
- Opfergelt, S., E. S. Eiriksdottir, K. W. Burton, A. Einarsson, C. Siebert, S. R. Gislason, and A. N. Halliday. 2011. Quantifying the impact of freshwater diatom productivity on silicon isotopes and silicon fluxes: Lake Myvatn, Iceland. *Earth Planet. Sci. Lett.* **305**: 73–82. doi:10.1016/J.EPSL.2011.02.043
- Panizzo, V. N., G. E. A. Swann, A. W. Mackay, L. Vologina, L. Alleman, L. André, V. H. Pashley, and M. S. . Horstwood. 2017. Constraining Modern Day Silicon Cycling in Lake Baikal. *Global Biogeochem. Cycles* **31**: 558–574. doi:10.1002/2016GB005518
- Parsons, T. R., Y. Maita, and C. M. Lalli. 1984. A manual of chemical and biological methods for seawater analysis, Pergamon Press.
- Passow, U., M. A. French, and M. Robert. 2011. Biological controls on dissolution of diatom frustules during their descent to the deep ocean: Lessons learned from controlled laboratory experiments. *Deep. Res. Part I Oceanogr. Res. Pap.* **58**: 1147–1157. doi:10.1016/j.dsr.2011.09.001

- Pauer, J. J., A. M. Anstead, W. Melendez, R. Rossmann, K. W. Taunt, and R. G. Kreis. 2008. The Lake Michigan Eutrophication Model, LM3-Eutro: Model Development and Calibration. *Water Environ. Res.* **80**: 853–861. doi:10.2175/106143008x304686
- Pondaven, P., M. Gallinari, S. Chollet, E. Bucciarelli, G. Sarthou, S. Schultes, and F. Jean. 2007. Grazing-induced Changes in Cell Wall Silicification in a Marine Diatom. *Protist* **158**: 21–28. doi:10.1016/J.PROTIS.2006.09.002
- Pothoven, S. A., and G. L. Fahnenstiel. 2013. Recent change in summer chlorophyll a dynamics of southeastern Lake Michigan. *J. Great Lakes Res.* **39**: 287–294. doi:10.1016/j.jglr.2013.02.005
- Pothoven, S. A., G. L. Fahnenstiel, H. A. Vanderploeg, and T. F. Nalepa. 2016. Changes in water quality variables at a mid-depth site after proliferation of dreissenid mussels in southeastern Lake Michigan. *Fundam. Appl. Limnol.* **188**: 233–244. doi:10.1127/fal/2016/0883
- Preisig, H. R. 1994a. Siliceous structures and silicification in flagellated protists, p. 29–42. *In* R. Wetherbee, R.A. Anderson, and J.D. Pickett-Heaps [eds.], *The Protistan Cell Surface*. Springer Vienna.
- Preisig, H. R. 1994b. Siliceous structures and silicification in flagellated protists. *Protoplasma* **181**: 29–42. doi:10.1007/BF01666387
- Quigley, M. A., and J. A. Robbins. 1984. Silica Regeneration Processes in Nearshore Southern Lake Michigan. *J. Great Lakes Res.* **10**: 383–392. doi:10.1016/S0380-1330(84)71854-5
- Ragueneau, O., E. De Blas Varela, P. Treguer, B. Queguiner, and Y. Del Amo. 1994. Phytoplankton dynamics in relation to the biogeochemical cycle of silicon in a coastal ecosystem of western Europe. *Mar. Ecol. Prog. Ser.* **106**: 157–172.
- Raven, J. A., F. A. Smith, and N. A. Walker. 1986. Biomineralization in the Charophyceae *sensu lato*, p. 125–139. *In* B.S.C. Leadbeater and R. Riding [eds.], *Biomineralization in lower plants and animals*.
- Raven, J. A., and A. M. Waite. 2004. The Evolution of Silicification in Diatoms: Inescapable Sinking and Sinking as Escape? *Source New Phytol.* **162**: 45–61. doi:10.1111/j.1469-8137.2004.01022.x
- Reavie, E. D., R. P. Barbiero, L. E. Allinger, and G. J. Warren. 2014. Phytoplankton trends in the Great Lakes, 2001–2011. *J. Great Lakes Res.* **40**: 618–639. doi:10.1016/j.jglr.2014.04.013

- Reavie, E. D., G. V. Sgro, L. R. Estep, and others. 2017. Climate warming and changes in *Cyclotella sensu lato* in the Laurentian Great Lakes. *Limnol. Oceanogr.* **62**: 768–783. doi:10.1002/lno.10459
- Reynolds, C. S. 1984. *The ecology of freshwater phytoplankton*, Cambridge University Press.
- Reynolds, C. S. 1986. Diatoms and the geochemical cycling of silicon, p. 269–289. *In* B.S.C. Leadbeater and R. Riding [eds.], *Biom mineralization in lower plants and animals*. Published for the Systematics Association by the Clarendon Press.
- Robertson, D. M., and D. A. Saad. 2011. Nutrient Inputs to the Laurentian Great Lakes by Source and Watershed Estimated Using SPARROW Watershed Models. *J. Am. Water Resour. Assoc.* **47**: 1011–1033. doi:10.1111/jawr.12060
- Rowe, M. D., E. J. Anderson, H. A. Vanderploeg, S. A. Pothoven, A. K. Elgin, J. Wang, and F. Yousef. 2017. Influence of invasive quagga mussels, phosphorus loads, and climate on spatial and temporal patterns of productivity in Lake Michigan: A biophysical modeling study. *Limnol. Oceanogr.* **62**: 2629–2649. doi:10.1002/lno.10595
- Ryves, D. B., D. H. Jewson, M. Sturm, R. W. Battarbee, R. J. Flower, A. W. Mackay, N. G. Granin, and V. Titov. 2003. Quantitative and qualitative relationships between planktonic diatom communities and diatom assemblages in sedimenting material and surface sediments in Lake Baikal, Siberia The transmission of biogenic environmental signals from the upper water column of deep water bodies to the sediment. *Limnol. Oceanogr.* **48**: 1643–1661.
- Ryves, D. B., S. Juggins, S. C. Fritz, and R. W. Battarbee. 2001. Experimental diatom dissolution and the quantification of microfossil preservation in sediments. *Palaeogeogr. Palaeoclimatol. Palaeoecol.* **172**: 99–113. doi:10.1016/S0031-0182(01)00273-5
- Safonova, T. A., V. V. Annenkov, E. P. Chebykin, E. N. Danilovtseva, Y. V. Likhoshway, and M. A. Grachev. 2007. Aberration of Morphogenesis of Siliceous Frustule Elements of the Diatom *Synedra acus* in the Presence of Germanic Acid. *Biochem.* **72**: 1261–1269. doi:10.1134/S0006297907110132
- Sandgren, C. D., S. A. Hall, and S. B. Barlow. 1996. Siliceous scale production in chrysophyte and synurophyte algae. I. Effects of silica-limited growth on cell silica content, scale morphology, and the construction of the scale layer of *Synura petersenii*. *J. Phycol.* **32**: 675–692. doi:10.1111/j.0022-3646.1996.00675.x

- Sandgren, C. D., and J. T. Lehman. 1990. Response of chlorophyll-*a*, phytoplankton, and microzooplankton to the invasion of Lake Michigan by *Bythotrephes*. *Verhandlungen des Int. Verin Limnol.* **24**: 386–392. doi:10.1080/03680770.1989.11898764
- Schelske, C. L. 1985. Biogeochemical silica mass balances in Lake Michigan and Lake Superior. *Biogeochemistry* **1**: 197–218. doi:10.1007/BF02187199
- Schelske, C. L. 1988. Historic Trends in Lake Michigan Silica Concentrations. *Int. Rev. der gesamten Hydrobiol. und Hydrogr.* **73**: 559–591. doi:10.1002/iroh.19880730506
- Schelske, C. L., and E. F. Stoermer. 1972. Phosphorus, silica, and eutrophication of Lake Michigan. *Am. Soc. Limnol. Oceanogr.* **1**: 157–171.
- Schneider, C. A., W. S. Rasband, and K. W. Eliceiri. 2012. NIH Image to ImageJ: 25 years of image analysis. *Nat. Methods* **9**: 671–675. doi:10.1038/nmeth.2089
- Schoelynck, J., A. L. Subalusky, E. Struyf, and others. 2019. Hippos (*Hippopotamus amphibius*): The animal silicon pump. *Sci. Adv.* **5**: eaav0395. doi:10.1126/sciadv.aav0395
- Seymour, J. R., S. A. Amin, J.-B. Raina, and R. Stocker. 2017. Zooming in on the phycosphere: the ecological interface for phytoplankton–bacteria relationships. *Nat. Microbiol.* **2**: 17065. doi:10.1038/nmicrobiol.2017.65
- Shimizu, K., Y. Del Amo, M. A. Brzezinski, G. D. Stucky, and D. E. Morse. 2001. A novel fluorescent silica tracer for biological silicification studies. *Chem. Biol.* **8**: 1051–1060. doi:10.1016/S1074-5521(01)00072-2
- Siegel, D. A., K. O. Buesseler, M. J. Behrenfeld, and others. 2016. Prediction of the Export and Fate of Global Ocean Net Primary Production: The EXPORTS Science Plan. *Front. Mar. Sci.* **3**: 22. doi:10.3389/fmars.2016.00022
- Simmons, L. J., C. D. Sandgren, and J. A. Berges. 2016. Problems and pitfalls in using HPLC pigment analysis to distinguish Lake Michigan phytoplankton taxa. *J. Great Lakes Res.* **42**: 397–404. doi:10.1016/j.jglr.2015.12.006
- Smetacek, V. 2018. FROM THE ARCHIVES Seeing is Believing: Diatoms and the Ocean Carbon Cycle Revisited. *Protist* **169**: 791–802. doi:10.1016/j.protis.2018.08.004
- Smetacek, V., and S. Naqvi. 2008. The next generation of iron fertilization experiments in the Southern Ocean. *Philos. Trans. A. Math. Phys. Eng. Sci.* **366**: 3947–67. doi:10.1098/rsta.2008.0144

- Smis, A., S. Van Damme, E. Struyf, and others. 2011. A trade-off between dissolved and amorphous silica transport during peak flow events (Scheldt river basin, Belgium): Impacts of precipitation intensity on terrestrial Si dynamics in strongly cultivated catchments. *Biogeochemistry* **106**: 475–487. doi:10.1007/s10533-010-9527-1
- Starr, R. C., and J. A. Zeikus. 1993. UTEX—The culture collection of algae at the university of Texas at Austin 1993 list of cultures. *J. Phycol.* **29**: 1–106. doi:10.1111/j.0022-3646.1993.00001.x
- Street-Perrott, F. A., and P. A. Barker. 2008. Biogenic silica: a neglected component of the coupled global continental biogeochemical cycles of carbon and silicon. *Earth Surf. Process. Landforms* **33**: 1436–1457. doi:10.1002/esp.1712
- Struyf, E., and D. J. Conley. 2012. Emerging understanding of the ecosystem silica filter. *Biogeochemistry* **107**: 9–18. doi:10.1007/s10533-011-9590-2
- Struyf, E., A. Smis, S. Van Damme, and others. 2010. Historical land use change has lowered terrestrial silica mobilization. *Nat. Commun.* **1**. doi:10.1038/ncomms1128
- Sun, J., and D. Liu. 2003. Geometric models for calculating cell biovolume and surface area for phytoplankton. *J. Plankton Res.* **25**: 1331–1346. doi:10.1093/plankt/fbg096
- Tesson, B., S. J. L. Lerch, and M. Hildebrand. 2017. Characterization of a New Protein Family Associated With the Silica Deposition Vesicle Membrane Enables Genetic Manipulation of Diatom Silica. *Sci. Rep.* **7**: 13457. doi:10.1038/s41598-017-13613-8
- Thamatrakoln, K., and M. Hildebrand. 2008. Silicon Uptake in Diatoms Revisited: A Model for Saturable and Nonsaturable Uptake Kinetics and the Role of Silicon Transporters. *PLANT Physiol.* **146**: 1397–1407. doi:10.1104/pp.107.107094
- Tilman, D. 1981. Tests of Resource Competition Theory Using Four Species of Lake Michigan Algae. *Ecology* **62**: 802–815.
- Tilman, D., and S. S. Kilham. 1976. Phosphate and Silicate Growth and Uptake Kinetics of the Diatoms *Asterionella Formosa* and *Cyclotella Meneghiniana* in Batch and Semicontinuous Culture. *J. Phycol.* **12**: 375–383. doi:10.1111/j.1529-8817.1976.tb02860.x
- Tréguer, P., C. Bowler, B. Moriceau, and others. 2018. Influence of diatom diversity on the ocean biological carbon pump. *Nat. Geosci.* **11**: 27–37. doi:10.1038/s41561-017-0028-x

- Tréguer, P. J., and C. L. De La Rocha. 2013. The World Ocean Silica Cycle. *Ann. Rev. Mar. Sci.* **5**: 477–501. doi:10.1146/annurev-marine-121211-172346
- Tréguer, P. J., J. N. Sutton, M. Brzezinski, and others. 2021. Reviews and syntheses: The biogeochemical cycle of silicon in the modern ocean. *Biogeosciences* **18**: 1269–1289. doi:10.5194/bg-18-1269-2021
- Tréguer, P., D. M. Nelson, A. J. Van Bennekom, D. J. DeMaster, A. Leynaert, and B. Quéguiner. 1995. The silica balance in the world ocean: A reestimate. *Sci. Earth, Atmos. Aquat. Sci. Database* pg **268**: 375–379.
- Vanderploeg, H. A., J. R. Liebig, W. W. Carmichael, M. A. Agy, T. H. Johengen, G. L. Fahnenstiel, and T. F. Nalepa. 2001. Zebra mussel (*Dreissena polymorpha*) selective filtration promoted toxic *Microcystis* blooms in Saginaw Bay (Lake Huron) and Lake Erie. *Can. J. Fish. Aquat. Sci.* **58**: 1208–1221. doi:10.1139/cjfas-58-6-1208
- Vanderploeg, H. A., J. R. Liebig, T. F. Nalepa, G. L. Fahnenstiel, and S. A. Pothoven. 2010. *Dreissena* and the disappearance of the spring phytoplankton bloom in Lake Michigan. *J. Great Lakes Res.* **36**: 50–59. doi:10.1016/j.jglr.2010.04.005
- Vanderploeg, H. A., T. F. Nalepa, D. J. Jude, E. L. Mills, K. T. Holeck, J. R. Liebig, I. A. Grigorovich, and H. Ojaveer. 2002. Dispersal and emerging ecological impacts of Ponto-Caspian species in the Laurentian Great Lakes. *Can. J. Fish. Aquat. Sci.* **59**: 1209–1228. doi:10.1139/f02-087
- Vandevenne, F. I., A. L. Barão, J. Schoelynck, A. Smis, N. Ryken, S. Van Damme, P. Meire, and E. Struyf. 2013. Grazers: Biocatalysts of terrestrial silica cycling. *Proc. R. Soc. B Biol. Sci.* **280**. doi:10.1098/rspb.2013.2083
- Vandevivere, P., S. A. Welch, W. J. Ullman, and D. L. Kirchman. 1994. Enhanced dissolution of silicate minerals by bacteria at near-neutral pH. *Microb. Ecol.* **27**: 241–251. doi:10.1007/BF00182408
- Vrieling, E. G., W. W. C. Gieskes, and T. P. M. Beelen. 1999. Silicon Deposition in Diatoms: Control by the pH inside the Silicon Deposition Vesicle. *J. Phycol.* **35**: 548–559. doi:10.1046/j.1529-8817.1999.3530548.x
- Wetzel, R. G. 2001. Iron, Sulfur, and Silica cycles, p. 289–330. *In* *Limnology*. Academic Press.
- Whallon, J. H., S. L. Flegler, and K. L. Klomparens. 1989. Energy-Dispersive X-Ray Microanalysis. *Bioscience* **39**: 256–259. doi:10.2307/1311163

- Wilken, S., B. Hoffmann, N. Hersch, and others. 2011. Diatom frustules show increased mechanical strength and altered valve morphology under iron limitation. *Limnol. Ocean.* **56**: 1399–1410. doi:10.4319/lo.2011.56.4.1399
- Young, E. B., R. C. Tucker, and L. A. Pansch. 2010. Alkaline phosphatase in freshwater *Cladophora*-epiphyte assemblages: Regulation in response to phosphorus supply and localization. *J. Phycol.* **46**: 93–101. doi:10.1111/j.1529-8817.2009.00782.x
- Znachor, P., K. Šimek, and J. Nedoma. 2012. Bacterial colonization of the freshwater planktonic diatom *Fragilaria crotonensis*. *Aquat. Microb. Ecol.* **66**: 87–94. doi:10.3354/ame01560

APPENDIX A:

ROLE OF NEARSHORE BENTHIC ALGAE IN LAKE MICHIGAN

RESEARCH ARTICLE

Role of nearshore benthic algae in
the Lake Michigan silica cycle

John A. Berges^{1,2*}, Allison M. Driskill¹, Emily J. Guinn^{1^{¶a}}, Kaytee Pokrzywinski^{1^{¶b}}, Jessica Quinlan^{1^{¶c}}, Benjamin von Korff^{1^{¶d}}, Erica B. Young^{1,2}

1 Department of Biological Sciences, University of Wisconsin-Milwaukee, Milwaukee, Wisconsin, United States of America, **2** School of Freshwater Sciences, University of Wisconsin-Milwaukee, Milwaukee, Wisconsin, United States of America

^{¶a} Current address: Department of Chemistry and Biochemistry, DePauw University, Greencastle, Indiana, United States of America

^{¶b} Current address: National Oceanic and Atmospheric Administration, National Centers for Coastal Ocean Science, Beaufort, North Carolina, United States of America

^{¶c} Current address: Environmental Compliance and Sustainability, Kohl's Incorporated, Menomonee Falls, Wisconsin, United States of America

^{¶d} Current address: Minnesota State University Mankato, Water Resources Center, South Mankato, Minnesota, United States of America

* berges@uwm.edu

OPEN ACCESS

Citation: Berges JA, Driskill AM, Guinn EJ, Pokrzywinski K, Quinlan J, von Korff B, et al. (2021) Role of nearshore benthic algae in the Lake Michigan silica cycle. PLoS ONE 16(8): e0256838. <https://doi.org/10.1371/journal.pone.0256838>

Editor: Douglas A. Campbell, Mount Allison University, CANADA

Received: May 14, 2021

Accepted: August 16, 2021

Published: August 26, 2021

Copyright: This is an open access article, free of all copyright, and may be freely reproduced, distributed, transmitted, modified, built upon, or otherwise used by anyone for any lawful purpose. The work is made available under the [Creative Commons CC0](https://creativecommons.org/licenses/by/4.0/) public domain dedication.

Data Availability Statement: Data presented in this paper are available in Microsoft Excel spreadsheet format from doi: [10.6084/m9.figshare.13369034.v1](https://doi.org/10.6084/m9.figshare.13369034.v1).

Funding: Research was supported by grant R/HCE-33 to JAB and EB from Wisconsin Sea Grant Institute (seagrant.wisc.edu). EJG and BvK were supported by grant OCE 0354031 (to R. Cuhel and

C. Aguilar) from the National Science Foundation Research Experience for Undergraduates ([nsf.gov](https://www.nsf.gov)). KP and JQ received support from University of Wisconsin's Summer Undergraduate Research

Abstract

Si cycling is linked with processes from global carbon sequestration to community composition and is especially important in aquatic ecosystems. Lake Michigan has seen dramatic fluctuations in dissolved silica (dSi) over several decades, which have been examined in the context of planktonic processes (diatom blooms), but the role of benthic organisms (macroalgae and their epiphytes) in Si cycling have not been explored. To assess significance of nearshore benthic algae in Si dynamics, we assembled dSi data from an offshore site sampled since the late 1980's, and sampled off three Milwaukee beaches during 2005–19.

Using colorimetric assays and alkaline digestion, we measured dSi, biogenic silica in particulate suspended material (pSi) and biogenic silica in benthic macroalgae (*Cladophora*) and epiphytic diatoms (bSi). Offshore, dSi increased about 1 μM per year from 25 μM in the late 1980's to nearly 40 μM in 2019. Nearshore dSi fluctuated dramatically annually, from near zero to concentrations similar to offshore. Both *Cladophora* and its epiphytes contained significant bSi, reaching up to 30% of dry mass ($300 \text{ mg Si g dry mass}^{-1}$) of the assemblage in summer. Microscopic analyses including localization with a Si-specific-stain and X-ray microanalysis showed bSi in epiphytic diatom cells walls, but the nature and localization of Si in macroalgae remained unclear. A simple model was developed estimating Si demand of algae using the areal macroalgal biomass, growth rates inferred from P-content, and bSi content, and comparing Si demand with dSi available in the water column. This indicated that 7–70% of the dSi in water overlying nearshore benthic algal beds could be removed per day. Key elements of the Si cycle, including which organisms sequester bSi and how rapidly Si is recycled, remain unclear. This work has implications for coastal marine waters where large macroalgal biomass accumulates but bSi content is virtually unknown.

Awards (uwm.edu/our/programs/support-for-undergraduate-research-fellows-surf/). The funders had no role in study design, data collection and analysis, decision to publish, or preparation of the manuscript.

Competing interests: The authors have declared that no competing interests exist.

INTRODUCTION

The global Si cycle profoundly affects the earth, from the draw-down of atmospheric CO₂ due to chemical weathering of silicate minerals to driving changes in groups of silica-requiring organisms such as radiolarians, sponges and diatoms (one of the most productive groups of phytoplankton) over geological time [1]. In aquatic ecosystems, Si has been strongly linked to global carbon cycling, limitations of diatom primary production, and the efficiency of trophic transfer in freshwater lakes, streams and wetlands [2–4]. The short-term biogeochemical cycling of Si in aquatic ecosystems involves bioavailable dissolved silicate (dSi, usually considered as Si(OH)₄ and SiO(OH)⁻) and Si incorporated into organisms as biogenic silicate (bSi, hydrated polymeric silica). Modification of the biogeochemical cycle of Si by eutrophication is now clear in many aquatic ecosystems, but was first noted in the Laurentian Great Lakes [5].

There have been major changes in Si in the Laurentian Great Lakes, driven by anthropogenic nutrient inputs, invasive species and climate change [5–7]. Eutrophication from ~1954 to 1977 led to declines in dSi in the Laurentian Great Lakes and a build-up of bSi in sediments [6]. In the open waters of the lake, invasive Dreissenid mussels have depleted phytoplankton biomass and changed species composition [8], potentially changing water column dSi. In particular, declining spring diatom blooms have been associated with rising spring dSi concentrations [9–12]. At the same time, Dreissenid mussels have concentrated limiting phosphorus (P) in the nearshore benthos, described as a ‘nearshore shunt’ [13]. Mussel grazing removes water column particles, which both decreases light attenuation, and releases nutrients (especially P), for benthic filamentous algae (chiefly *Cladophora*), and dense epiphytic assemblages of silica-requiring diatoms [14, 15].

While changes to Si cycling in the open waters of the Great Lakes have been relatively well-appreciated, elements of benthic silica cycling have not been as well examined. Budgets for Si sources, sinks and regeneration in Lake Michigan are incomplete and based on the open lake

[16] with little consideration for Si recycling in nearshore sediments [17], or the influence of Dreissenid mussels and benthic algal growth. To address this problem and assess the significance of benthic algal assemblages in nearshore silica dynamics, we measured water column dSi and bSi in algal assemblages at several nearshore sites over a 15-year period, and used a simple model to explore the potential Si demand of these assemblages in nearshore Lake Michigan. Our results demonstrate dynamic dSi in the nearshore, high bSi in benthic algae and the potential for benthic algae to have significant local effects on Si cycling in Lake Michigan and, by extension, other freshwater bodies.

MATERIALS AND METHODS

Field collections

In order to provide a baseline comparison for the nearshore, dSi data for the water column at the Fox Point station in the open waters of Lake Michigan (43.16 N, 87.67 W, 100 m depth) was assembled from seasonal data sets in the periods 1988–1991 and 2007–2009, which were described and published as averages by Engevoold et al. [12]. In 2018 and 2019, additional dSi data was collected from Fox Point on vertical profiles collected from the RV *Neeskay*, essentially as previously described [12].

Three nearshore sites close to Milwaukee, Wisconsin (Atwater Beach 43.09 N, 87.87 W, Bradford Beach 43.06 N 87.87 W, and Linwood Beach 43.07 N 87.87 W) were sampled at intervals during February–December over several years between 2005 and 2019. In 2005, 2006, 2008 and 2018 sampling was conducted in the summer–fall period, in 2010 sampling focused on winter–spring, and in 2009 and 2019 sampling was conducted through all seasons. The sites are readily accessible, heavily influenced by riverine inputs, upwelling and nearshore beds of benthic algae. Samples were collected from surface water at 1 m depth by wading from shore and water used for dSi (filtrate) and suspended, particulate biogenic silicate (pSi, material captured on filters). In addition, detached and floating benthic algae at 1 m depth was collected for determination of biogenic Si (bSi). In 2006, attached benthic algae were sampled from the substratum by SCUBA diving at 10 m depth off all three beaches, using quadruplicate 20 x 20 cm quadrats. Areal benthic algal biomass (dry mass) was determined after samples were cleaned of invertebrates, sediment and stones, dried (65°C for 24 h) and weighed.

Si analyses

Water samples were filtered (25 mm, 0.2 µm polycarbonate, Whatman Nucleopore), the filtrate used for dSi measurement [18] and filters with particulate material were stored frozen for later analysis of bSi. Benthic algal biomass was dried overnight at 65°C and both algal biomass and filters used for bSi analysis using high-temperature carbonate digestion (0.5% Na₂CO₃, 2 h extraction at 85°C, [19]). Carbonate digestion gave nearly identical results to hydroxide methods (using a shorter extraction at 100°C in 0.2 N NaOH, [20]), except that NaOH extracts of *Cladophora* samples were highly colored and bSi values more variable (cf. Krause et al. [21], who noted the two methods compared favorably for freshwater diatoms). Particulate P content was measured on ashed algal biomass followed by acid digestion [15].

Imaging of *Cladophora*-epiphyte assemblages

Cladophora-epiphyte assemblages were examined using light microscopy (Olympus BX-41) and scanning electron microscopy (SEM) in combination with elemental mapping (Hitachi S-4800 SEM with Bruker Quantax EDS system). In 2006 samples, Si incorporation into algal assemblages was examined by incubating algae for 2–4 days at 18 °C, with $\sim 30 \mu\text{mol photons m}^{-2} \text{s}^{-1}$ irradiance and 100 μM of the bSi incorporation label [2-(4-pyridyl)-5-[[4-dimethylaminoethylamino-carbamoyl)-methoxy]phenyl]oxazole] (PDMPO, Lysosensor™ Invitrogen, Carlsbad, CA) and samples examined using epifluorescence microscopy [22].

Modeling

To assess potential significance of benthic algae in nearshore Si cycling, the Si demand represented by the biomass was estimated with a simple model based on data collected in 2005–6. First, we estimated benthic algal Si demand. The average *Cladophora*-epiphyte biomass (g m^{-2}) and P content ($\text{mg P g dry mass}^{-1}$) were measured from field samples at the three sites as described above. The *in situ* growth rate of benthic algal assemblages (d^{-1}) was calculated using the measured P content of samples using a Droop-type relationship between growth rate and P content published for Lake Huron *Cladophora* by Auer and Canale ([23], Fig 7). We used average bSi contents determined from nearshore sampling to estimate algal Si content, as described above. Estimates of benthic algal areal coverage (m^2) were derived from aerial photographs (from summer 2005, Source: SSEC RealEarth, UW-Madison, <http://re.ssec.wisc.edu/?products=WICoast.100¢er=43.086,-87.864&zoom=13>), with nearshore area constrained by the 10 m depth contour, above which *Cladophora* growth is most abundant [24, 25]. The daily Si demand was calculated as the product of the measured average biomass and algal bSi content, the estimated daily growth rate, and areal coverage. Next, we calculated the dSi available in the water overlying the areas of each of the nearshore regions. The area (m^2) was broken into depth contours 0–5 m and 5–10 m, by the mean depth in each area (i.e. 2.5 m or 7.5 m) and this was multiplied by the average dSi (10 μM) over the summer 2006 period. By dividing the dSi available by the daily Si demand, we calculated the potential proportion of dSi that could be used by the benthic algal assemblages and expressed this as a percentage.

Statistical analyses

Data were analyzed using General Linear Model procedures, typically linear regression and Analysis of Variance, using logarithmic transformations when necessary to meet assumption of normality and homoscedasticity ([26], IBM SPSS Statistics version 26.0). Seasonal Mann- Kendall analyses [27] were used for offshore water-column dSi data, but uneven replication across season prevented this technique from being used for nearshore data.

RESULTS AND DISCUSSION

Rising offshore dSi over 20 years

Pelagic dSi in Lake Michigan has dramatically increased over recent decades. At the open water Lake Michigan station (Fox Point), dSi within the upper 60 m has increased from the period 1988–91, when typical dSi was on the order of 10 μM and maximum values were 20–25 μM , to during 2007–9 and 2018–9 when dSi averages close to 30 μM and values up to 40 μM have been recorded (Fig 1, [12]). A Seasonal Mann-Kendall analysis [27] demonstrated a highly significant increase in dSi over the period ($P < 0.001$), averaging about 1 μM per year (Sen's slope 0.87 μM per year). Eutrophication from ~1954 to 1977 reportedly led to a 33 μM decline in dSi in the Laurentian Great Lakes and a build-up of sediment bSi [5]. But from a low of ~5 μM in 1988–90, the declining trend was reversed, a change attributed to phosphorus reduction efforts and invasive Dreissenid mussels which depleted phytoplankton biomass and changed phytoplankton species composition (especially decreased diatom abundance), resulting in declines in water column Si demand [8]. In Lake Michigan, declining spring diatom blooms have been associated with rising dSi in spring and a loss of seasonal variation in pelagic dSi. For example, at Fox Point Station Lake Michigan during 1986–1988 there were predictable seasonal dSi decreases from 20–25 μM in March to close to 0 in surface waters by July, while dSi remained at about 15 μM below the thermocline [12, 28]. Records from 2000 to 2006 show that surface dSi concentrations increased to close to those of deep water, and also that the seasonal oscillations in dSi were lost [11].

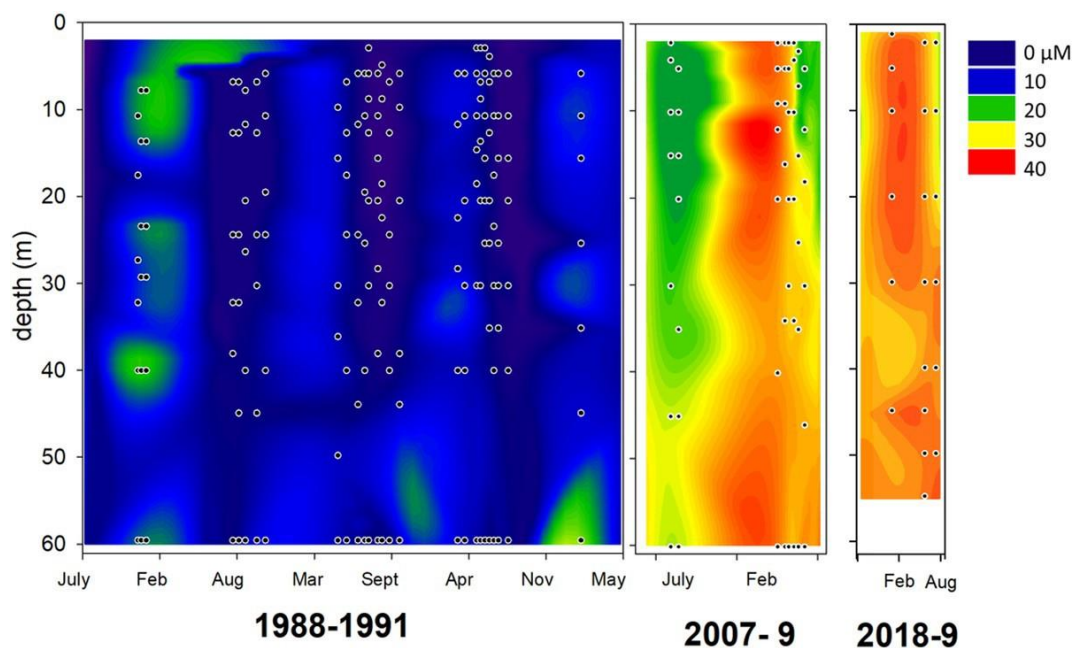


Fig 1. Dissolved silica concentrations (dSi) at Fox Point, Lake Michigan during the periods 1988–1991, 2007–2009 and 2018–9 through the top 60 m of the 100 m water column. Dots indicate sampling points.

<https://doi.org/10.1371/journal.pone.0256838.g001>

The observed changes in dSi are typically attributed to changes in diatom abundance, but such explanations are not completely satisfactory. Long-term dSi data from Environmental Protection Agency sampling between 1983 and 2008 do show dSi increases and slower seasonal draw-downs of dSi that can be attributed to reduced diatom blooms [10]. Finer scale sampling and primary production estimates provide evidence that the key changes in diatoms have occurred in the spring isothermal mixing period (April–May) when, until the late 1990’s, a diatom-dominated spring bloom occurred, but has subsequently been less dominant [9].

However, it might be expected that changes in spring diatoms blooms would be reflected in biomass or diatom species abundances later in the year, however few such differences are apparent during summer stratified period between the late 1980’s and the late 2000’s (see [12], S1 Fig). Moreover, declines in diatom blooms do not explain the water-column wide increases in dSi that have been observed. Missing from more recent analyses of the silica cycle has been consideration of pelagic or benthic bSi pools. Conley and Scavia [29] showed that at the 100 m deep Grand Haven Lake Michigan station during the April–May spring diatom bloom, a major pool (8–11 μM) of bSi developed in the $>20 \mu\text{m}$ size fraction, which corresponded well with a draw-down in dSi from about 13 to 3 μM . The bloom rapidly died, fragmented and the bSi returned to dSi almost quantitatively [29].

Increasing dSi in deep water of Lake Michigan suggests additional changes, for example, in regeneration of bSi from sediments. Schelske et al. [30] noted that dSi remineralization depends heavily on the flux of material to the benthos and is very sensitive to regional differences in deposition; silica deposition has not been examined in Lake Michigan in some time [31] and an understanding of current diatom bloom dynamics at this level in Lake Michigan is lacking. However, very recent analysis of sediment cores taken at three stations in Lake Michigan found that bSi in cores (as a proportion of dry mass) was similar or increased from 1960 to 2009, while there was a shift from larger to smaller-sized diatoms preserved in cores [32]. Increases in sediment bSi are difficult to reconcile with either declines in diatom blooms or increased regeneration from sediments, and underline gaps in our understanding of the Lake Michigan silica cycle. Rising dSi represents a major biogeochemical shift in Lake Michigan, but such shifts are not unprecedented. Rising nitrate in Lake Superior is also occurring, hypothesized to be caused by alterations in nitrification [33].

Nearshore Si dynamics

In the western nearshore region of Lake Michigan, there were significant seasonal variations in Si pools. dSi varied widely, fluctuating between deep-lake values of over 30 μM to less than 1 μM within a space of days, in some years (Fig 2). Nearshore dSi fluctuations were examined by clustering values into seasons (spring, summer, fall and winter) and analyzing using a three-way ANOVA with location, year and season as factors. There was a significant interaction between year and season ($P < 0.05$), thus data were compared by year using Tukey post-hoc comparisons. No significant differences were found among the three locations (Atwater, Bradford and Linnwood, $P > 0.05$), however, while in 2005–2011, dSi in spring and summer were significantly lower than in fall and winter ($P < 0.05$), no significant seasonal differences were detected in 2018 or 2019 ($P > 0.05$). Particulate biogenic Si suspended in nearshore water (pSi) examined using a three-way ANOVA (location, season, year) showed no significant differences ($P > 0.05$), though highest values tended to occur in fall and winter (Fig 2). The bSi content in macroalgal biomass collected from the three locations ranged from a few $\text{mg Si (g dry mass)}^{-1}$ in June when macroalgal biomass is just starting to appear in the water, to over 300 $\text{mg Si (g dry mass)}^{-1}$ (i.e. over 30% of dry mass) in late July–August at Atwater Beach (Fig 2). Analysis by three-way ANOVA (location, year, season), showed significant

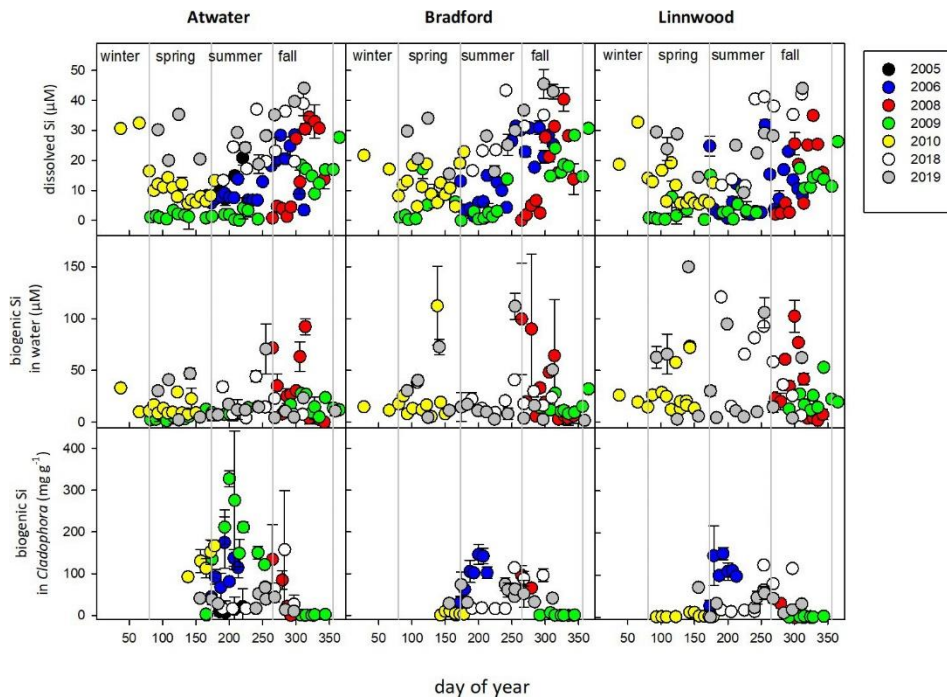


Fig 2. Dissolved silicate, suspended biogenic silica and biogenic silica in *Cladophora* assemblages in samples collected at 1 m depth at three Milwaukee-area beaches during 2005–2019.

<https://doi.org/10.1371/journal.pone.0256838.g002>

interactions between location and year, and season and year ($P < 0.001$ in both cases), requiring separate Tukey post-hoc comparisons by year and location. *Cladophora* bSi values were significantly higher in 2005 and 2006 than in other years ($P < 0.05$). In the years 2005–2011, bSi values were higher in summer than other seasons ($P < 0.05$), but not significantly different among winter, spring and fall, and also significantly higher at the Atwater site versus the Linnwood or Bradford Beach sites ($P < 0.05$). These differences observed in bSi among seasons and sites in 2005–11, did not hold in 2018 and 2019 ($P > 0.05$ in both cases). Although we have no objective measures of changing *Cladophora* growth or appearance on beaches over the course of this study, subjectively, beach accumulation was considerably worse in the earlier years, and this is reflected in declining frequency of Google searches by the public for information on “*Cladophora*” over the period (S2 Fig), suggesting that the algal biomass may have been more obvious to the public in the earlier period. In contrast, Kuczynski et al. [34], were able to use closures of a Lake Ontario beach as an index of *Cladophora* blooms because a County Health Department had defined “excessive *Cladophora* on the beach” as a criterion. It is also worth noting that Lake Michigan water levels have fairly consistently increased over the same time period (S2 Fig).

Increases in nearshore dSi are most likely driven by upwelling from deep lake waters; the frequency and magnitude appear to be consistent with patterns of measured and modelled upwelling [35]. River inputs are an alternative source of dSi, but US Geological Survey records for the common inflow of the Milwaukee, Menomonee and Kinnickinnic Rivers to Lake Michigan (Station 4087000, waterdata.usgs.gov) show modest average dSi concentrations of 245.1 (\pm 143.1) μ M over the period 1980 to 2009, with no clear evidence of temporal trends, and no correlation between river discharge volume and dSi measured at nearshore sites. However, we have not adequately assessed bSi in river inputs because such measurements have rarely been taken. Riverine bSi is dominantly from terrestrial vegetation, and there is evidence that this plays a role in global silica cycling equivalent to that of oceanic diatoms [36]; river bSi as a component of the “terrestrial silica pump” also needs to be considered.

Si in benthic algal biomass

Cladophora typically showed dense epiphyte loads, dominated by diatoms (Fig 3). Species composition was similar to that described by Young et al. [15]: the most common species were *Cocconeis* sp., *Gomphonema* sp., *Tabellaria flocculosa*, *Rhoicosphenia curvata*, and *Cymbella* sp. along with *Dinobryon* sp., with filamentous cyanobacteria (including *Fischerella* sp. and *Pleurocladia lacustris*) present (Fig 3A and 3C). Elemental mapping over SEM surfaces showed highest Si localization within these epiphytic diatoms (Fig 3D), and epifluorescence microscopy of samples labelled with PDMPO showed Si incorporation in epiphytic diatoms, but only red chlorophyll fluorescence in *Cladophora* filaments (Fig 3B). PDMPO staining mechanism is not entirely clear but the basis of this oxazole dye (originally developed for studying intracellular pH) is strongly pH-dependent and depends strongly on surface chemistry and concentration [37], so labelling of algal bSi may be challenging in multicellular algae like *Cladophora*.

Nevertheless, it seems likely that significant bSi in benthic algal assemblages is contributed by the epiphytic diatoms. However, in 2005, we were able to obtain relatively epiphyte-free “green” *Cladophora*. In July samples, *Cladophora* with typical epiphyte loads averaged 166 ± 68.4 mg Si (g dry mass)⁻¹, while *Cladophora* with low epiphyte load had just 9.61 ± 1.79 mg Si (g dry mass)⁻¹. Malkin et al. [14] published the only other comparable data set on benthic algal Si from a 2 m deep station in Lake Ontario in 2005 from spring through autumn, using hot NaOH extraction for bSi. While water column dSi was much lower (2.7–8.3 μ M), bSi for the *Cladophora*-epiphyte assemblages was similar to the present study: 56–224 mg Si (g dry mass)⁻¹, they also reported cultured *Cladophora* (without epiphytes) had only 4 mg Si (g dry

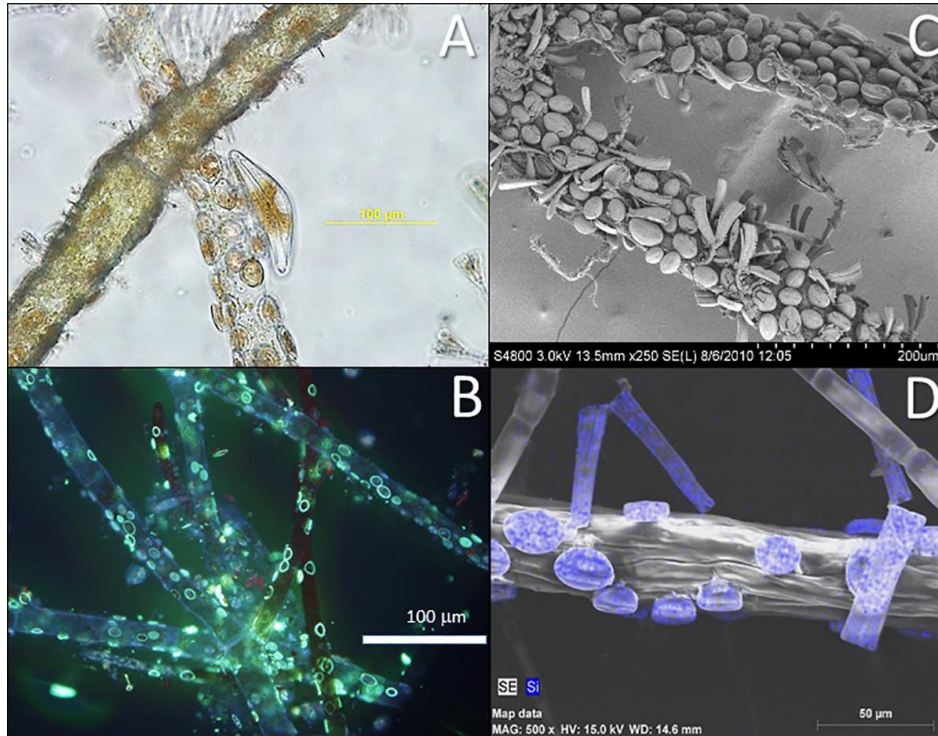


Fig 3. **A.** Light microscopy image of *Cladophora* filament with encrusting diatom epiphytes. **B.** Epifluorescence microscopy image of PDMPO-labeling of bSi (pale green) accumulation in epiphytic diatoms on surfaces of *Cladophora* filaments. **C.** Scanning electron microscope (SEM) images of *Cladophora* filaments with typical dense late-summer diatom epiphyte load. **D.** SEM elemental mapping of Si (blue dots) on *Cladophora* and epiphytes—elemental spot analysis over *Cocconeis* diatom cells yielded signals for C ~0.6 cps(eV) and Si >7.5 cps(eV) compared to *Cladophora*, C ~0.6 cps(eV), Si <0.1 cps(eV). Scale bars are as marked.

<https://doi.org/10.1371/journal.pone.0256838.g003>

mass)⁻¹. Combining our summer estimates of bSi in the *Cladophora*-epiphyte assemblage, our P content measured in benthic samples in 2006 (see above), and average C and N contents determined on *Cladophora* samples collected in 2005–6, we can approximate the molar C:N:P:Si stoichiometry of the assemblage as 331:21:1:62. Previous Lake Michigan Si budgets have not included these benthic algal assemblages [38] and they clearly could represent significant local Si pools, though their impact on the overall lake budget is more limited because of the relatively small area of the nearshore region relative to the open waters of the lake.

Cladophora itself clearly contains some bSi, though its structural or physiological roles are unclear. Moore and Traquair [39] showed that growth of *Cladophora* was promoted by Si and inhibited by the silicate analog GeO₂ and they speculated that electron dense areas in *Cladophora* cell walls might be sites of Si deposition. It is not especially surprising that *Cladophora* might contain bSi because it is in the evolutionary lineage leading to higher plants and many angiosperms, including freshwater macrophytes, take up dSi [2]; *Elodea*, *Potamogeton* and *Myriophyllum* species use bSi structurally and contain

Site	μ (d^{-1})	Cover ($\times 10^6 m^2$)	Biomass ($g m^{-2}$)	bSi Content ($mg g^{-1}$)	Si demand (tonnes d^{-1}) ^a	Available Si (tonnes) ^b	% Si used (d^{-1})
Atwater	0.48	3.10	70.3	111.2	11.6	16.4	71.0
Bradford	0.58	3.14	10.8	109.9	2.15	9.45	22.7
Linnwood	0.58	1.75	10.8	113.7	1.26	16.7	7.5

Table 1. Modelled effects of the *Cladophora*-epiphyte assemblages on dSi at three Lake Michigan nearshore sites.

Growth rates (μ) were estimated from *Cladophora* P-content, cover determined using aerial photographs, biomass from measurements of samples collected *in situ*, and bSi content determined in samples collected from the nearshore. The % Si used (d^{-1}) represents the maximum daily Si demand of benthic *Cladophora*-epiphyte assemblages relative to that available in the overlying water column.

^aBased on modeled growth rate (from P content), biomass and bSi content

^bBased on an average dSi of 10 μM and volume of overlying water.

<https://doi.org/10.1371/journal.pone.0256838.t001>

Modelling of nearshore Si demand

We used some simple calculations to contextualize nearshore Si cycling by benthic algal bio-mass. Using data collected in 2005–6, we calculated dSi demand of the *Cladophora*-epiphyte assemblages in nearshore waters off the three beach sites, using a combination of aerial photos (S3 Fig) for areal coverage, *in situ* sampling for areal biomass, and growth rates derived from an established relationship with internal P-content [23]. Areal benthic algal bSi were calculated by multiplying biomass by bSi content to yield 43.7–279 $mmol m^{-2}$ across the three sites (Table 1). These values are quite comparable to areal benthic algal bSi in Lake Ontario at a 2 m deep station: 22.7 $mmol m^{-2}$ in spring, rising to 490 $mmol m^{-2}$ at peak *Cladophora* biomass in summer [14]. P content of *Cladophora*-epiphyte assemblages ranged from 0.6 to 3 $mg P g drymass^{-1}$, very

2–70 $mg Si (g dry mass)^{-1}$ ([40–42], Jack, Young and Berges unpublished). Freshwater phytoplankton groups contain bSi including some chrysophytes and even certain chlorophytes [43], but Si in diverse groups has not been incorporated into budgets or models; the current Lake Michigan Eutrophication Model (LM3-Eutro) only associates dSi uptake with planktonic diatoms [44]. Marine cyanobacteria in the genus *Synechococcus* from the Eastern equatorial Pacific Ocean accumulated Si and exhibited Si:P ratios approaching that of diatoms, and in fact the water column inventory of Si associated with cyanobacteria exceeded that in diatoms [45]. Potential Si pools in freshwater cyanobacteria, which are increasing in abundance in the Great Lakes [11], is unknown. In marine macroalgae, Markham and Hagmeier [46] showed negative growth effects of GeO_2 in several species, suggesting requirements for Si uptake, bSi deposition has been associated with wound healing in *Saccharina japonica* kelp sporophytes [47], and a red seaweed showed evidence of increased temperature and irradiance stress when Si was less than 50 μM [48]. There is clearly a need to re-evaluate the pools and role of silica in broader taxonomic groups within aquatic ecosystems.

comparable to those found in Lake Huron [23], and mean values for samples from the three nearshore sites resulted in growth rates estimates between 0.4 to 0.6 d⁻¹, based on Auer and Canale's [23] data which found nutrient-replete net growth rates of 0.714 d⁻¹.

Determining the overlying water volume from depth intervals, and assuming an average 10 μM dissolved silicate (based on summer 2005–2006 values, Fig 2), we calculated that Si demand by the benthic *Cladophora*-epiphyte assemblages could account for 7 to 70% of dSi in the overlying water each day (Table 1). This substantial proportion of available dSi would easily explain the observed nearshore fluctuations in dSi (Fig 2) during the growing season. These calculations represent a theoretical maximum, and *Cladophora* cannot effectively access the whole overlying water column to deplete dSi, and *Cladophora* growth is unlikely to be maintained at consistently high rates and in step with epiphyte growth for many weeks. Nonetheless, the fluctuations in dSi in nearshore waters are demonstrated over several years of sampling, and the potential effects of the *Cladophora*-epiphyte assemblage on Si demand and cycling are evident.

Importantly, we currently have very little idea where the bSi that is taken up by the *Cladophora*-epiphyte assemblage is stored, how labile it is, or where it goes after the assemblages die and break down. Because *Cladophora* coverage and biomass can be extensive in the nearshore (exceeding 80% of the benthic surface area and reaching up to 260 g dry mass m⁻², [49]), the need to understand links to P cycling and model its growth dynamics have been appreciated [50]. However, while there is evidence of P-limitation in *Cladophora* (e.g. the presence of alkaline phosphatase activity [15], nutrient stoichiometry [25]), benthic algae in Lake Michigan also shows evidence of secondary limitation by dSi at concentrations below approximately

14 μM; nutrient enrichment with P + N + Si show greater effects than enrichment without Si [51]. Furthermore, if we consider the benthic diatoms in the assemblage, there is evidence that they may be capable of extraordinary dSi uptake and uptake kinetics may not show saturation at typical lake dSi [52]. The critical importance of attached algae (including diatoms) in lake and river ecosystems with respect to food web effects has been recognized [53], but the roles of these groups in biogeochemical nutrient cycling are also significant and need further consideration.

Critical gaps in understanding

In both the open lake and nearshore, recycling of bSi is a particularly critical component of Si budgets, yet our understanding is dated and fragmented. In open Lake Michigan waters, 80–100% of bSi may be recycled annually [5, 54, 55] and just 5% of bSi due to diatom production was estimated to be buried annually [56]. Schelske [38] completed a mass-balance and found that Lake Michigan

contrasted sharply with Lake Superior in that Si demand by diatoms after the winter dSi maximum was 71% in Michigan vs. only 8% in Superior, a difference attributed to the eutrophication and P additions to Michigan. Nearshore Lake Michigan has received less attention than the open lake, but although we have now demonstrated seasonal depletion of dSi (Fig 2) we still know little about nearshore bSi recycling. In another deep lake system, Lake Malawi, riverine inputs were more significant as ~25% of Si input to the epilimnion (mostly as bSi within phytoliths from maize and grasses), but 75% Si still came from vertical exchange of Si-rich water from depth, and only 7 to 11% of diatom production becomes permanently buried [57]. In the shallower Lough Neagh, Northern Ireland, seasonal recycling of Si in the sediments is the major source of dSi to planktonic diatoms and benthic invertebrates play a major role in remineralization [58]. Indeed, Quigley and Vanderploeg [59] demonstrated the effectiveness of the benthic amphipod *Diporeia* in digesting diatom frustules, but it is also worth noting that *Diporeia* has significantly declined in Lake Michigan following the invasion by Dreissenid mussels [32, 60]. Alternatively, the activity of invertebrates such as amphipods may also suppress dSi regeneration from sediments by burying bSi deposits [17]. There is little doubt that the invasion of Dreissenid mussels into Lake Michigan and other lakes has radically changed food web dynamics, and the cycling of phosphorus [13]. Since the examination of Si in Lake Michigan in the 1980's [56], invasion and expansion of mussels and establishment of benthic algal blooms have quite likely altered Si cycling and pools, and a re-evaluation of these is needed. There is no doubt that changes in silica recycling can have profound effects on aquatic ecosystem function. In eutrophic Lake Kasumigaura (Japan), a three-decade-long increase in dSi, driven by sediment release and resuspension, has resulted in increases in diatoms and decreases in cyanobacteria in the phytoplankton [61].

CONCLUSIONS

In conclusion, we have shown that benthic macroalgae and their epiphytes constitute a significant pool of bSi in nearshore Lake Michigan with potentially significant effects on dSi, but many key elements of the nearshore silica cycle such as rates of recycling of algal bSi pools remain poorly understood. Our work also has implications for coastal marine waters where large biomasses of macroalgae accumulate but bSi pools within this biomass, or contribution to Si cycling is virtually unknown.

SUPPORTING INFORMATION

S1 Fig. Comparison of diatom abundances at offshore Lake Michigan sites between the late 1980's and 2008. Average counts of diatoms in samples collected June through August at two Lake Michigan stations at 100 m depth. 1985–8 data from Sandgren and Lehman (Sandgren CD, Lehman JT. Response of chlorophyll a, phytoplankton and microzooplankton to invasion of Lake Michigan by *Bythotrephes*. *Verh. Int. Ver. Theor. Angew. Limnol.* 1991; 24:386–92), 2008 data from Simmons et al. (Simmons LJ, Sandgren CD, Berges JA. Problems and pitfalls in using HPLC pigment analysis to distinguish Lake Michigan phytoplankton taxa. *J. Great Lakes Res.* 2016; 42: 397–404). (PDF)

S2 Fig. Comparison of popularity of Google searches for “Cladophora” with mean Lake Michigan water levels. Relative popularity of Google searches for the term “Cladophora” in Wisconsin, 2004 through 2019 by month, assessed with Google Trends (trends.google.com). Mean water level in Lake Michigan from US Army Corp of Engineers (www.lre.usace.army.mil/Missions/Great-Lakes-Information/Great-Lakes-Information-2/Water-Level-Data/). (PDF)

S3 Fig. Images showing the nearshore regions of three Milwaukee areas beaches examined in *Cladophora* modeling. Aerial photographs (Source: SSEC RealEarth, UW-Madison, re.ssec.wisc.edu/?products=WICoast.100¢er=43.086,-87.864&zoom=13) and matching geo-referenced charts with depth contours (created by the authors in ESRI's ArcGIS v.10.6; nocopyrighted material was used) for three sites near Milwaukee, Wisconsin. Regions outlined in red represent the extent of benthic *Cladophora* distributions selected down to the 10 m depth contour. (PDF)

ACKNOWLEDGMENTS

We thank Paul Engevd for assistance with older datasets, Hunter Carrick and Art Brooks for valuable discussions, Harvey Bootsma for assistance and support in sampling and advice on analyses, John Janssen for providing digital copies of aerial photos, Heather Owen for help with SEM elemental analysis, and the captain and crew of the RV *Neeskay* for sampling support.

AUTHOR CONTRIBUTIONS

Conceptualization: John A. Berges, Erica B. Young.

Data curation: John A. Berges.

Formal analysis: John A. Berges, Allison M. Driskill, Kaytee Pokrzywinski, Jessica Quinlan, Benjamin von Korff, Erica B. Young.

Funding acquisition: John A. Berges, Erica B. Young.

Investigation: John A. Berges, Allison M. Driskill, Emily J. Guinn, Kaytee Pokrzywinski, Jessica Quinlan, Benjamin von Korff, Erica B. Young.

Methodology: John A. Berges, Emily J. Guinn, Kaytee Pokrzywinski, Benjamin von Korff, Erica B. Young.

Project administration: John A. Berges. **Resources:**

John A. Berges, Erica B. Young. **Supervision:** John A.

Berges, Erica B. Young.

Validation: John A. Berges, Emily J. Guinn, Erica B. Young.

Writing – original draft: John A. Berges, Erica B. Young.

Writing – review & editing: John A. Berges, Allison M. Driskill, Emily J. Guinn, Kaytee Pokrzywinski, Jessica Quinlan, Benjamin von Korff, Erica B. Young.

REFERENCES

1. Conley DJ, Frings PJ, Fontorbe G, Clymans W, Stadmark J, Hendry KR, et al. Biosilicification drives a decline of dissolved Si in the oceans through geologic time. *Front. Mar. Sci.* 2017; 4:397. <https://doi.org/10.3389/fmars.2017.00397>
2. Struyf E, Conley DJ. Silica: an essential nutrient in wetland biogeochemistry. *Front. Ecol. Environ.* 2009; 7:88–94. <https://doi.org/10.1890/070126>
3. Treguer PJ, De La Rocha CL. The world ocean silica cycle. *Ann. Rev. Mar. Sci.* 2013; 5: 477–501. <https://doi.org/10.1146/annurev-marine-121211-172346> PMID: 22809182
4. Wang B, Liu CQ, Maberly SC, Wang F, Hartmann J. Coupling of carbon and silicon geochemical cycles in rivers and lakes. *Sci. Rep.* 2016; 6:35832. <https://doi.org/10.1038/srep35832> PMID: 27775007
5. Conley DJ, Schelske CL, Stoermer EF. Modification of the biogeochemical cycle of silica with eutrophication. *Mar. Ecol. Prog. Ser.* 1993; 101:179–92. <https://doi.org/10.3354/meps101179>
6. Schelske CL, Stoermer EF. Eutrophication, silica depletion, and predicted changes in algal quality in Lake Michigan. *Science* 1971; 173:423–4. <https://doi.org/10.1126/science.173.3995.423> PMID: 17770443
7. Shapiro J, Swain EB. Lessons from the silica “decline” in Lake Michigan. *Science* 1983; 221:457–9. <https://doi.org/10.1126/science.221.4609.457> PMID: 17755481
8. Barbiero RP, Tuchman ML, Warren GJ, Rockwell DC. Evidence of recovery from phosphorus enrichment in Lake Michigan. *Can. J. Fish. Aquat. Sci.* 2002; 59:1639–47. <https://doi.org/10.1139/f02-132>

9. Fahnenstiel G, Pothoven S, Vanderploeg H, Klarer D, Nalepa T, Scavia D. Recent changes in primary production and phytoplankton in the offshore region of southeastern Lake Michigan. *J. Great Lakes Res.* 2010; 36:20–9. <https://doi.org/10.1016/j.jglr.2010.03.009>
10. Evans MA, Fahnenstiel G, Scavia D. Incidental Oligotrophication of North American Great Lakes. *Environ. Sci. Technol.* 2011; 45:3297–303. <https://doi.org/10.1021/es103892w> PMID: 21417221
11. Cuhel RL, Aguilar C. Ecosystem transformations of the Laurentian Great Lake Michigan by nonindigenous biological invaders. *Ann. Rev. Mar. Sci.* 2013; 5:289–320. <https://doi.org/10.1146/annurev-marine-120710-100952> PMID: 22809179
12. Engevoold PM, Young EB, Sandgren CD, Berges JA. Pressure from top and bottom: Lower food web responses to changes in nutrient cycling and invasive species in western Lake Michigan. *J. Great Lakes Res.* 2015; 41:86–94. <https://doi.org/10.1016/j.jglr.2015.04.015>
13. Hecky RE, Smith RE, Barton DR, Guildford SJ, Taylor WD, Charlton MN, et al. The nearshore phosphorus shunt: a consequence of ecosystem engineering by dreissenids in the Laurentian Great Lakes. *Can. J. Fish. Aquat. Sci.* 2004; 61:1285–93. <https://doi.org/10.1139/f04-065>
14. Malkin SY, Sorichetti RJ, Wiklund JA, Hecky RE. Seasonal abundance, community composition, and silica content of diatoms epiphytic on *Cladophora glomerata*. *J. Great Lakes Res.* 2009; 35:199–205. <https://doi.org/10.1016/j.jglr.2008.12.008>
15. Young EB, Tucker RC, Pansch LA. Alkaline phosphatase in freshwater *Cladophora*-epiphyte assemblages: regulation in response to phosphorus supply and localization. *J. Phycol.* 2010; 46:93–101. <https://doi.org/10.1111/j.1529-8817.2009.00782.x>
16. Schelske CL. Diatoms as mediators of biogeochemical silica depletion in the Laurentian Great Lakes. In: Stoermer EF, Smol JP, editors. *The Diatoms: Applications for the Environmental and Earth Sciences*. Cambridge: Cambridge University Press; 1999. p. 73–84.
17. Quigley MA, Robbins JA. Silica regeneration processes in nearshore southern Lake Michigan. *J. Great Lakes Res.* 1984; 10:383–92. [https://doi.org/10.1016/S0380-1330\(84\)71854-5](https://doi.org/10.1016/S0380-1330(84)71854-5)
18. Parsons T, Maita M, Lalli C. *A manual of chemical and biological methods for seawater analysis*. Oxford: Pergamon Press; 1984. 173 p.
19. Paasche E. Silicon content of five marine plankton diatom species measured with a rapid filter method. *Limnol. Oceanogr.* 1980; 25:474–80. <https://doi.org/10.4319/lo.1980.25.3.0474>
20. Brzezinski MA, Nelson DM. Seasonal changes in the silicon cycle within a Gulf Stream warm-core ring. *Deep Sea Research.* 1989; 36:1009–30. [https://doi.org/10.1016/0198-0149\(89\)90075-7](https://doi.org/10.1016/0198-0149(89)90075-7)
21. Krause GL, Schelske CL, Davis CO. Comparison of three wet-alkaline methods of digestion of biogenic silica in water. *Freshw. Biol.* 1983; 13:73–81. <https://doi.org/10.1111/j.1365-2427.1983.tb00658>
22. Leblanc K, Hutchins DA. New applications of a biogenic silica deposition fluorophore in the study of oceanic diatoms. *Limnol. Oceanogr. Meth.* 2005; 3:462–76. <https://doi.org/10.4319/lom.2005.3.462>
23. Auer MT, Canale RP. Ecological studies and mathematical modeling of *Cladophora* in Lake Huron: 3. The dependence of growth rates on internal phosphorus pool size. *J. Great Lakes Res.* 1982; 8:93–99. [https://doi.org/10.1016/S0380-1330\(82\)71947-1](https://doi.org/10.1016/S0380-1330(82)71947-1)
24. Tomlinson LM, Auer MT, Bootsma HA, Owens EM. The Great Lakes *Cladophora* Model: development, testing, and application to Lake Michigan. *J. Great Lakes Res.* 2010; 36:287–97. <https://doi.org/10.1016/j.jglr.2010.03.005>
25. Bootsma HA, Young EB, Berges JA. Temporal and spatial patterns of *Cladophora* biomass and nutrient stoichiometry in Lake Michigan. In: Bootsma HA, T. JE, Young EB, Berges JA, editors. *Cladophora Research and Management in the Great Lakes: Proceedings of a Workshop; December 8, 2004; Great Lakes WATER Institute: University of Wisconsin-Milwaukee; 2004. p. 81–8.*
26. Zar JH. *Biostatistical Analysis*. Second Edition ed. Englewood Cliffs: Prentice-Hall, Inc.; 1984. <https://doi.org/10.1093/infdis/150.5.778> PMID: 6436396

27. Hirsch RM, Slack JR. A nonparametric trend test for seasonal data with serial dependence. *Water Resources Res.* 1984; 20:727–32. <https://doi.org/10.1029/WR020i006p00727>
28. Brooks AS, Edgington DN. Biogeochemical control of phosphorus cycling and primary production in Lake Michigan. *Limnol. Oceanogr.* 1994; 39:961–8. <https://doi.org/10.4319/lo.1994.39.4.0961>
29. Conley DJ, Scavia D. Size structure of particulate biogenic silica in Lake Michigan. *J. Great Lakes Res.* 1991; 17:18–24. [https://doi.org/10.1016/S0380-1330\(91\)71338-5](https://doi.org/10.1016/S0380-1330(91)71338-5)
30. Schelske CL, Stoermer EF, Kenney WF. Historic low-level phosphorus enrichment in the Great Lakes inferred from biogenic silica accumulation in sediments. *Limnol. Oceanogr.* 2006; 51:728–48. https://doi.org/10.4319/lo.2006.51.1_part_2.0728
31. Conley DJ. Mechanisms controlling silica flux from sediments and implications for the biogeochemical cycling of silica in Lake Michigan. PhD Thesis. Ann Arbor: University of Michigan; 1987.
32. Edlund MB, Jude DJ, Nalepa TF. Diets of the benthic amphipod *Diporeia* in southern Lake Michigan before and after the dreissenid invasion. *J. Great Lakes Res.* 2021; 47:447–62. <https://doi.org/10.1016/j.jglr.2021.01.018>
33. Sterner RW, Anagnostou E, Brovold S, Bullerjahn GS, Finlay JC, Kumar S, et al. Increasing stoichiometric imbalance in North America's largest lake: nitrification in Lake Superior. *Geophys. Res. Lett.* 2007; 34: L10406. <https://doi.org/10.1029/2006GL028861>
34. Kuczynski A, Auer MT, Brooks CN, Grimm AG. The *Cladophora* resurgence in Lake Ontario: characterization and implications for management. *Can. J. Fish. Aquat. Sci.* 2016; 73(6):999–1013. <https://doi.org/10.1139/cjfas-2015-0460>
35. Plattner S, Mason DM, Leshkevich GA, Schwab DJ, Rutherford ES. Classifying and forecasting coastal upwellings in Lake Michigan using satellite derived temperature images and buoy data. *J. Great Lakes Res.* 2006; 32:63–76. [https://doi.org/10.3394/0380-1330\(2006\)32\[63:CAFCUJ\]2.0.CO;2](https://doi.org/10.3394/0380-1330(2006)32[63:CAFCUJ]2.0.CO;2)
36. Carey JC, Fulweiler RW. The terrestrial silica pump. *PLoS One.* 2012; 7(12):e52932. <https://doi.org/10.1371/journal.pone.0052932> PMID: 23300825
37. Parambath M, Hanley QS, M-MF J., Giesa T, Buehler MJ, Perry CC. The nature of the silicophilic fluorescence of PDMPO. *Phys. Chem. Chem. Phys.* 2016; 18: 5938–48. <https://doi.org/10.1039/c5cp05105c> PMID: 26685751
38. Schelske CL. Biogeochemical silica mass balances in Lake Michigan and Lake Superior. *Biogeochemistry.* 1985; 1:197–218. <https://doi.org/10.1007/BF02187199>
39. Moore LF, Traquair JA. Silicon, a required nutrient for *Cladophora glomerata* (L) Kütz. (Chlorophyta) *Planta.* 1976; 128:179–82. <https://doi.org/10.1007/BF00390321> PMID: 24430695
40. Rawlence DJ, Whitton JS. Elements in aquatic macrophytes, water, plankton, and sediments surveyed in three North Island lakes. *New Zealand J. Mar. Freshw. Res.* 1977; 11:73–93. <https://doi.org/10.1080/00288330.1977.9515662>
41. Struyf E, Van Damme S, Gribsholt B, Middelburg JJ, Meire P. Biogenic silica in tidal freshwater marsh sediments and vegetation (Schelde estuary, Belgium). *Mar. Ecol. Prog. Ser.* 2005; 303:51–60. <https://doi.org/10.3354/meps303051>
42. Schoelynck J, Bal K, Backx H, Okruszko T, Meire P, Struyf E. Silica uptake in aquatic and wetland macrophytes: a strategic choice between silica, lignin and cellulose? *New Phytol.* 2010; 186:385–91. <https://doi.org/10.1111/j.1469-8137.2009.03176.x> PMID: 20136720
43. Preisig HR. Siliceous structures and silicification in flagellated protists. *Protoplasma.* 1994; 181:29–42. https://doi.org/10.1007/978-3-7091-9378-5_2
44. Pauer JJ, Anstead AM, Melendez W, Rossmann R, Taunt KW, Kreis RG Jr. The Lake Michigan eutrophication model, LM3-Eutro: model development and calibration. *Water Env. Res.* 2008; 80:853–61. <https://doi.org/10.2175/106143008x304686> PMID: 18939608

45. Baines SB, Twining BS, Brzezinski MA, Krause J, Vogt S, Assael D, et al. Significant silicon accumulation by marine picocyanobacteria. *Nat. Geosci.* 2012; 5:886–91. <https://doi.org/10.1038/ngeo1641>
46. Markham JW, Hagmeier E. Observations on the effects of germanium dioxide on the growth of macroalgae and diatoms. *Phycologia* 1982; 21:125–30. <https://doi.org/10.2216/i0031-8884-21-2-125.1>
47. Mizuta H, Yasui H. Protective function of silicon deposition in *Saccharina japonica* sporophytes (Phaeophyceae). *J. Appl. Phycol.* 2012; 24:1177–82. <https://doi.org/10.1007/s10811-011-9750-8> PMID: 23002326
48. Le B, Nadeem M, Yang S-H, Shin J-A, Kang M-G, Chung G, et al. Effect of silicon in *Pyropia yezoensis* under temperature and irradiance stresses through antioxidant gene expression. *J. Appl. Phycol.* 2018;31:1297–302. <https://doi.org/10.1007/s10811-018-1605-0>
49. Auer MT, Tomlinson LM, Higgins SN, Malkin SY, Howell ET, Bootsma HA. Great Lakes *Cladophora* in the 21st century: same algae-different ecosystem. *J. Great Lakes Res.* 2010; 36:248–55. <https://doi.org/10.1016/j.jglr.2010.03.001>
50. Bootsma HA, Rowe MD, Brooks CN, Vanderploeg HA. Commentary: The need for model development related to *Cladophora* and nutrient management in Lake Michigan. *J Great Lakes Res.* 2015; 41:7–15. <https://doi.org/10.1016/j.jglr.2015.03.023>
51. Carrick HJ, Lowe RL. Nutrient limitation of benthic algae in Lake Michigan: The role of silica. *J. Phycol.* 2007; 43:228–34. <https://doi.org/10.1111/j.1529-8817.2007.00326.x>
52. Leynaert A, Longphuir SN, Claquin P, Chauvaud L, Ragueneau O. No limit? The multiphasic uptake of silicic acid by benthic diatoms. *Limnol. Oceanogr.* 2009; 54:571–6. <https://doi.org/10.4319/lo.2009.54.2.0571>
53. Vadeboncoeur Y, Power ME. Attached algae: the cryptic base of inverted trophic pyramids in freshwaters. *Ann. Rev. Ecol. Evol. Syst.* 2017; 48:255–79. <https://doi.org/10.1146/annurev-ecolsys-121415-032340>
54. Conway HL, Parker JI, Yaguchi EM, Mellinger DL. Biological utilization and regeneration of silicon in Lake Michigan. *J. Fish. Res. Board Can.* 1977; 34:537–44. <https://doi.org/10.1139/f77-085>
55. Parker JI, Conway HL, Yaguchi EM. Dissolution of diatom frustules and recycling of amorphous silicon in Lake Michigan. *J. Fish. Res. Board Can.* 1977; 34:545–51. <https://doi.org/10.1139/f77-086>
56. Schelske CL, Conley DJ, Stoermer EF, Newberry TL, Campbell CD. Biogenic silica and phosphorus accumulation in sediments as indices of eutrophication in the Laurentian Great Lakes. *Hydrobiologia* 1986; 143:79–86. <https://doi.org/10.1007/BF00026648>
57. Bootsma HA, Hecky RE, Johnson TC, Kling HJ, Mwita J. Inputs, outputs, and internal cycling of silica in a large, tropical lake. *J. Great Lakes Res.* 2003; 29:121–38. [https://doi.org/10.1016/S0380-1330\(03\)70543-7](https://doi.org/10.1016/S0380-1330(03)70543-7)
58. Gibson CE, Wang G, Foy RH. Silica and diatom growth in Lough Neagh: the importance of internal recycling. *Freshw. Biol.* 2000; 45:285–93. <https://doi.org/10.1111/j.1365-2427.2000.00624.x>
59. Quigley MA, Vanderploeg HA. Ingestion of live filamentous diatoms by the Great Lakes amphipod, *Diporeia* sp.: a case study of the limited value of gut contents analysis. *Hydrobiologia* 1991; 223:141–8. <https://doi.org/10.1007/BF00047635>
60. Nalepa TF, Fanslow DL, Iii AJF, Lang GA, Eadie BJ, Quigley MA. Continued disappearance of the benthic amphipod *Diporeia* spp. in Lake Michigan: is there evidence for food limitation? *Can. J. Fish. Aquat. Sci.* 2006; 63:872–90. <https://doi.org/10.1139/f05-262>
61. Arai H, Fukushima T. Impacts of long-term increase in silicon concentration on diatom blooms in Lake Kasumigaura, Japan. *Annales de Limnologie* 2014; 50:335–46. <https://doi.org/10.1051/limn/2014027>

APPENDIX B:
RIVERINE AND NEARSHORE LAKE MICHIGAN

Introduction

Nearshore Si cycling can be greatly affected by riverine inputs. Land use highly affects nutrient loading to Lake Michigan from rivers, which has been well documented for P and N (Robertson and Saad 2011). Some plants, like grasses, contain bSi deposits in the form of phytoliths (Street-Perrott and Barker 2008), which can be more soluble than frustules in freshwater (Loucaides et al. 2008). Land use can be a good predictor of riverine bSi inputs (Struyf et al. 2010) and large portions of riverine Si can be attributed to plants (Bootsma et al. 2003), with bSi inputs typically increasing after precipitation events (Smis et al. 2011).

Grazers can accelerate the dissolution of

phytoliths through their fecal matter (Vandevenne et al. 2013; Schoelynck et al. 2019).

Agricultural areas in Wisconsin are usually a mix of cows and crops (Fig. 1a, (von

Keyserlingk et al. 2013)), which could mean high Si inputs from rivers that run through

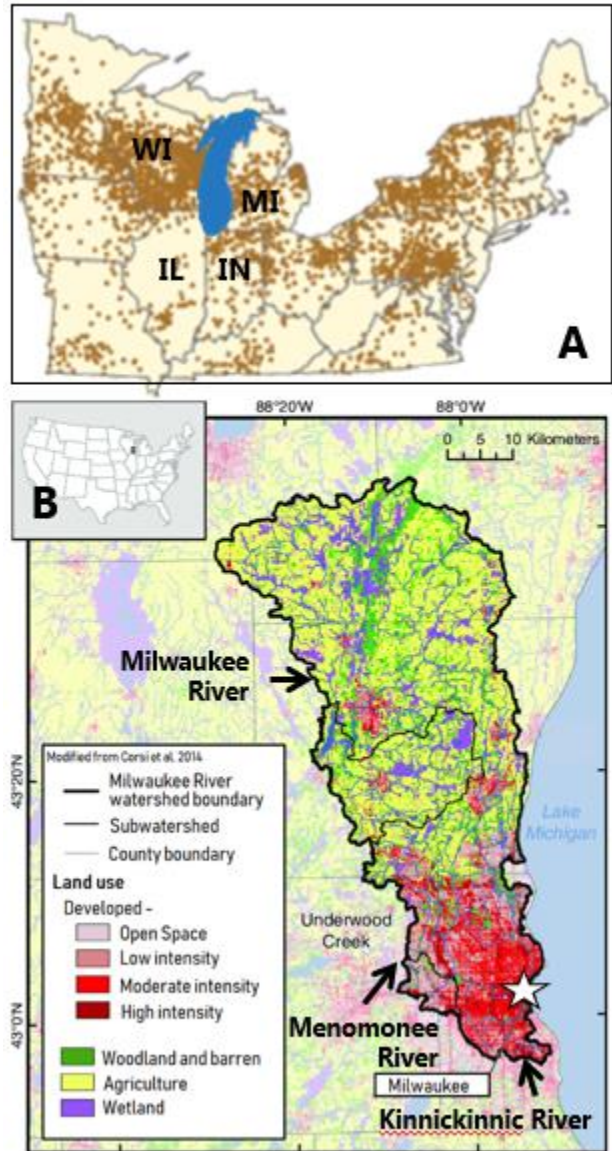


Figure 1. Dots representing 1,500 cows according to 2007 dairy census (A) with states surrounding Lake Michigan labelled (modified from Keyserlingk et al. 2013). Land use within the drainage basins of 3 Milwaukee area rivers (B) that feed into Lake Michigan under the Hoan Bridge (star): the Milwaukee River, Menomonee river, and Kinnickinnic river (modified from Corsi et al. 2014).

agricultural regions. We chose 2 sampling sites, one representing the Milwaukee River only (Pleasant St. Bridge) and one where the Milwaukee river, Kinnickinnic River (KK), and Menomonee River combine to flow into Lake Michigan (Hoan Bridge). The Milwaukee River runs through mainly agricultural areas, while the KK and Menomonee river are mostly urban (Fig. 1b, Corsi et al. 2014).

Methodology (brief)

- Sampling for nearshore dSi, bSi, and drift *Cladophora* (Fig. 2)
 - o Beaches by wading
 - o Rivers by tossing a bucket on a string from over a bridge (repeated each time per replicate)
- Filter through 0.8 μm PC filter
 - o Filter processed for bSi (0.5% Na_2CO_3 method, see previous chapters)
 - o Filtrate processed for dSi



Figure 2. Green squares (1-3) represent beach sampling sites Atwater (1), Linnwood (2), Bradford (3). Purple squares (4 & 5) represent river sampling sites Pleasant St. Bridge (Milwaukee river only, 4) and Hoan Bridge (Milwaukee, KK, Menomonee rivers)

Results

Rivers

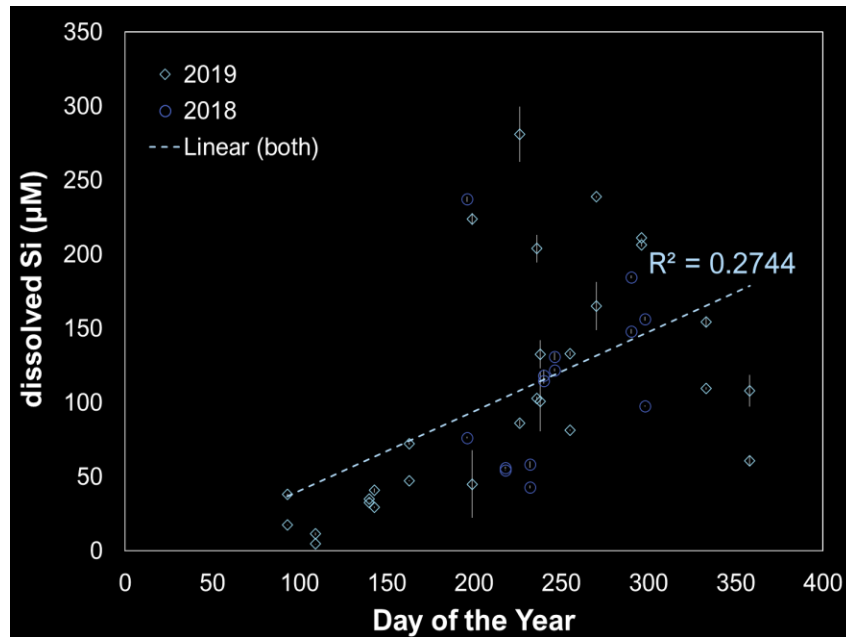


Figure 3. Mean riverine dSi concentrations for 2018 & 2019 show significant positive correlation with day of the year ($p < 0.01$) but not with daily discharge. Error bars indicate SD ($n = 6$).

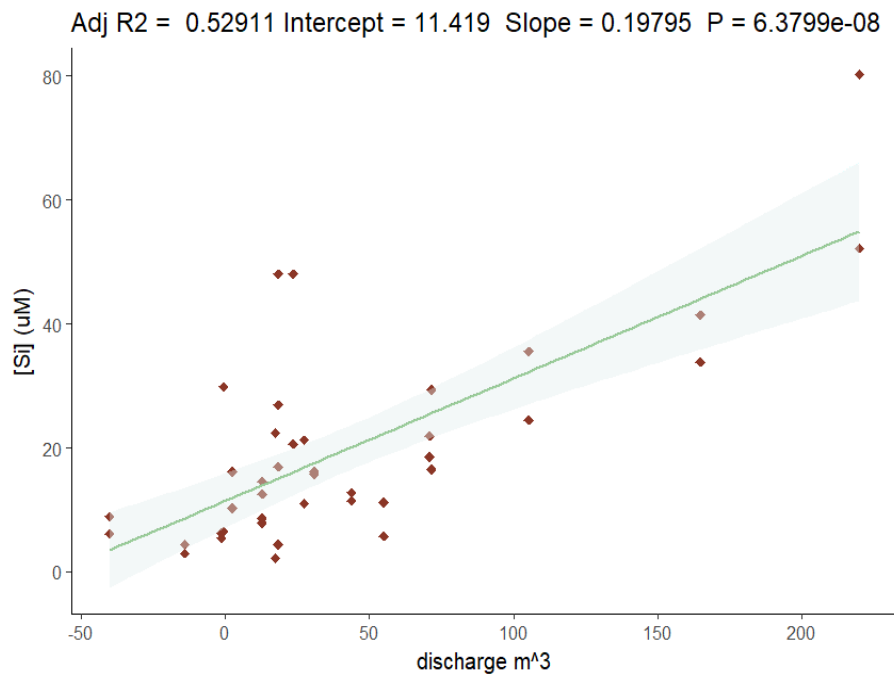


Figure 4. Mean riverine particulate Si is positively correlated with mean daily discharge rates ($p < 0.01$), shading indicates 95% CI. There was no strong correlation with day of the year for riverine bSi

Nearshore (Beaches and Cladophora)

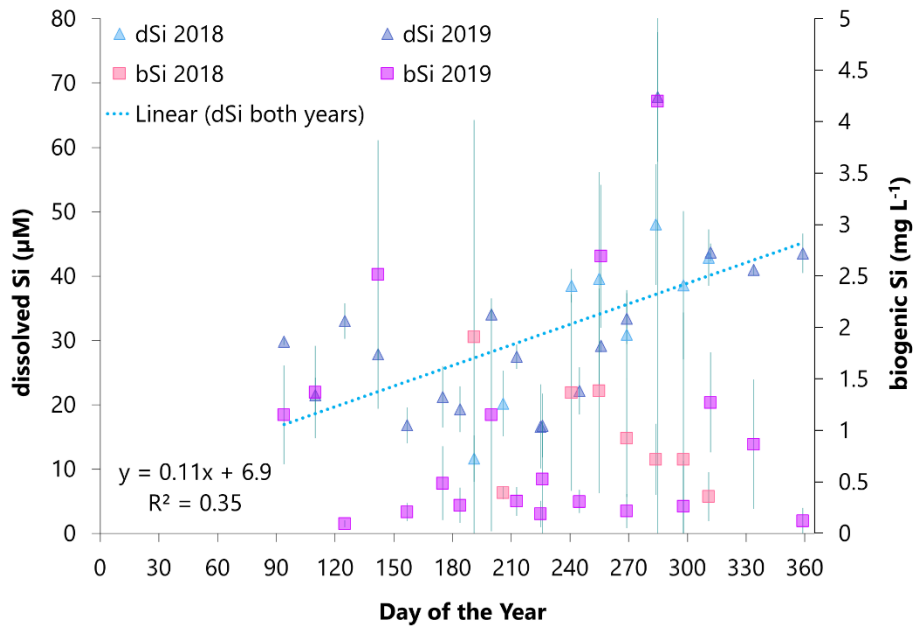


Figure 5. Mean nearshore WI dSi concentrations (triangles) increased from April to December in 2018-2019 ($p < 0.01$, $R^2 = 0.35$). Particulate concentrations (squares) were extremely variable and had no seasonal correlation. Error bars indicate SD ($n = 9$).

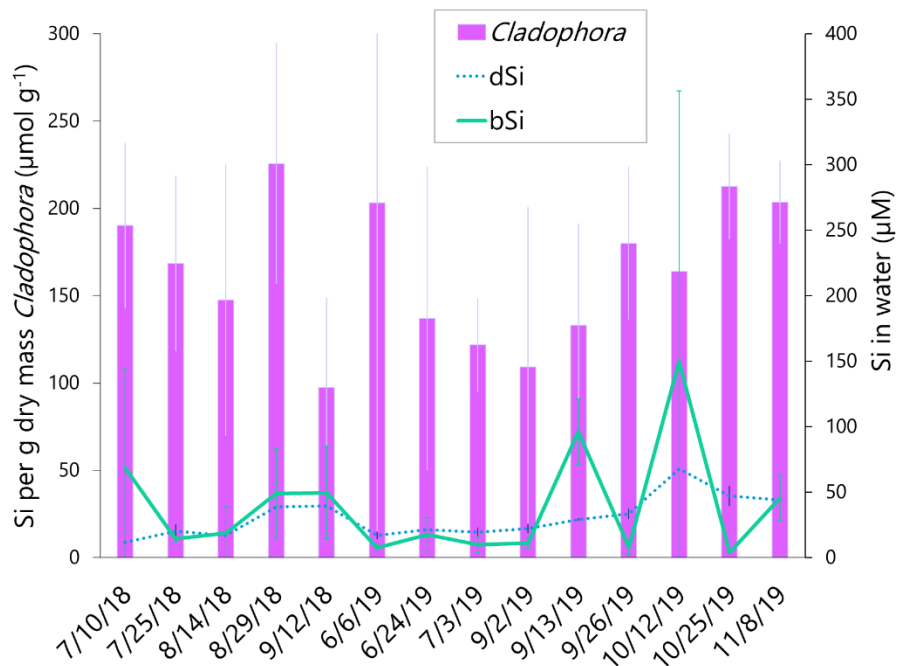


Figure 6: Mean Si in *Cladophora* + epiphyte assemblages (purple bars, error bars = SD, $n = 6$) plotted with mean dSi (blue dash line, error bars = SD, $n = 9$) and bSi (green solid line, error = SD, $n = 9$). There was no significant difference between 2018 and 2019 Si in *Cladophora* assemblages.

Comparisons to East Lake Michigan

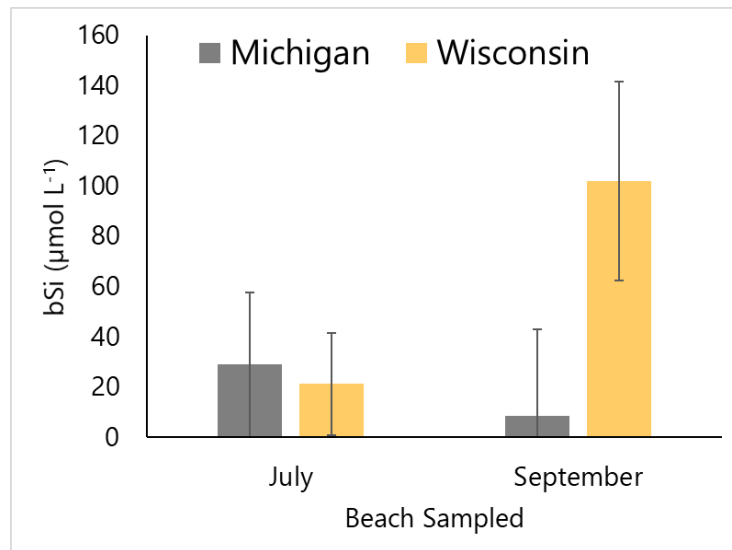


Figure 7. Particulate Si concentrations (bSi) were higher in Wisconsin than Michigan nearshore in September 2018 ($p < 0.01$). Error bars represent WI has prominent *Cladophora* blooms, which are not found along MI coast, so higher particulate Si in WI could relate to this difference, especially late in the season when filaments slough off and degrade nearshore. The highest dSi value in 2019 (Fig. 6, 10/12/19) corresponded to a large sloughing event of *Cladophora*.

SUMMARY AND DISCUSSION

- Riverine bSi concentrations are highly correlated with rainfall events which can wash particulate Si into the river, especially from plants
- Riverine dSi increases throughout the year, likely from the degradation of plant material washing in during the winter.
 - o Preliminary data with undergraduate researcher Steven Girard showed the potential for labile Si in riparian vegetation
- dSi in both rivers and nearshore is more strongly correlated to date than bSi data
- The bSi in *Cladophora* assemblages is high

- Both bSi and dSi in the water increase as *Cladophora* senesces
- *Cladophora* communities may host bacteria which accelerate dissolution, allowing for tight recycling of Si within the community

APPENDIX C:

DY-V RECIPE

DY-V recipe

Compound	Molar mass (g)	g in stock (1 L)	Stock concentration (mM)	In 1L media	Final concentration in DYV
CaCl · 2H₂O	147.01	75	510.17	1 mL	510.17 μM
MgSO₄ · 7H₂O	246.47	50.99	206.8812	1 mL	206.88 μM
MES	195.2	Add directly to media		0.2 g	1.02 mM
KCl	74.55	3	40.24145	1 mL	40.24 μM
H₃BO₃	61.83	0.8	12.9387	1 mL	12.94 μM
NaNO₃	84.9947	46.7	549.446	0.5 mL	274.72 μM
Na₂SiO₃ · 9H₂O	284.2	15	52.77973	1 mL	52.78 μM
NaH₂PO₄	119.98	3.094	25.78763	0.5 mL	12.89 μM
Trace Metals mix					
ZnSO₄ · 7H₂O	287.56	0.073	0.25386	1 mL	253.86 nM
CoSO₄ · 7H₂O	281.1	0.016	0.056919		56.92 nM
MnSO₄ · 4H₂O	223.05	0.54	2.420982		2.42 μM
Na₂MoO₄ · 2H₂O	241.94	0.00148	0.006117		6.12 nM
Na₂SeO₃	172.94	0.000173	0.001		1.00 nM
NiCl₂ · 6H₂O	237.69	0.00149	0.006269		6.27 nM
Na₂EDTA · 2H₂O	372.24	3.086	8.29035		8.29 μM
Fe Metal mix					
FeCl₃ · 6H₂O	270.3	1.77	6.54828	0.5 mL	3.27 μM
Na₂EDTA · 2H₂O	372.24	2.44	6.554911		3.28 μM
Vitamin Stock					
Thiamine-HCl	337.26	0.1	0.296507	0.5 mL	148.25 nM
Biotin	244.31	0.002	0.008186		4.09 nM
B12	1355.37	0.001	0.000738		0.37 nM

To make 1L of media:

- Combine stock solutions using volumes for 1 L of media
- Bring final volume to 1 L with Milli-Q H₂O
- Adjust pH to 6.8 with NaOH or HCl
- Autoclave on liquid setting 30 min (55 min for volumes > 2L)

For volumes over 1 L, bubble CO₂ through a GF/F filter overnight.

Double N/P/Si recipes add 1 mL L⁻¹ NaNO₃ and NaH₂PO₄, add 2 mL L⁻¹ Na₂SiO₃ · 9H₂O